# Dissertation

Submitted to the
Combined Faculties for the Natural Sciences
and
for Mathematics
of the Ruperto-Carola University of Heidelberg, Germany
for the degree of
Doctor of Natural Sciences

Presented by

Simon Jungbauer
Born in Heilbronn, Germany

Oral examination: 02.06.2008

# Mechanical stimulation of cells:
# Dynamic behavior of cells on cyclical stretched substrates

Referees:
Prof. Dr. G. Elisabeth Pollerberg
Prof. Dr. Joachim P. Spatz

# Table of Contents

# SUMMARY

Besides the biochemical factors in the environment, physical factors can also influence biological processes in tissues or in single cells. For, example the mechanical stimulation of cells can regulate their proliferation, apoptosis or the expression of genes within them. Previous studies concerning the influence of cyclical strain on cells adhering to flexible substrates showed that the cells attempt to reorient themselves to be perpendicular to the stretch direction. This behavior has been described qualitatively, but no systematic, quantitative studies of this phenomenon have yet been undertaken. Furthermore, the cells were only observed prior to and following stretch. Studies of cellular dynamics during the cyclical stretch are lacking.

In the present study, our aim was to both observe and quantitatively describe the dynamics of the cellular reaction by means of a biophysical model. We therefore developed a new stretching system which allows live-cell observations during the stretching experiments.

The behavior of different cell types was investigated, according to a variety of different parameters such as stretching frequency, stretching amplitude, or cell density. As a model system, we used two types of fibroblasts: rat embryonic fibroblasts (REF52) and primary human fibroblasts (HDF) taken from donors of various ages.

We observed that the perpendicular reorientation of the cells occurs at an exponential rate over time. Accordingly, we employed a simple mathematical model to determine how long it characteristically took for the cells to reorient themselves in response to the various mechanical parameters.

Our results demonstrated a previously unknown characteristic biphasic cellular behavior which depended on the stretching frequency. Both REF52 and HDF fibroblasts were found to reorient faster, until a certain threshold frequency was reached. In this regime the characteristic reorientation time decreased by a power law, as the frequency increased (characteristic time ~ $f^n$). Above this threshold frequency, the characteristic time ceased to decrease. When the cells were stretched with higher frequencies than this threshold frequency, a saturation of the characteristic time was reached. All tested cell types displayed this biphasic behavior. Cell-specific differences, however, were observed in the reaction kinetics and in the threshold frequencies. The REF52 cells already began to react at a frequency which is approximately 10 times lower compared to the HDF1 cells, in general they reoriented themselves faster than the HDF1 cells at all frequencies. Furthermore, we demonstrated that older HDF cells reoriented themselves faster than young HDF cells.

When we increased the cell density to a confluent cell layer, we also observed a power law dependent decrease in the characteristic reorientation time, when the frequency increased. Compared with the single cells, however, a plateau of saturation of the characteristic reorientation time could not be observed. Furthermore, the confluent cells reacted approximately twice as fast as the single cells. Activation of cell-cell contacts involved in mechanotransduction in addition to focal contacts may constitute one possible explanation for this observation.

When the stretching amplitude was varied, the characteristic reorientation time was found to decrease, along with an increase in amplitude. However, in contrast to the frequency variation, in this case we observed a linear decrease.

The different reaction characteristics resulting from variations in the stretch frequency and the stretch amplitude (power law-dependent and linear) suggested that the inserted energy, the reorientation process depends on can not be described as a simple product of frequency and amplitude.

Fluorescence microscopy was used to observe the dynamics of focal adhesion contacts during cyclical stretch. We determined that focal adhesions reoriented themselves faster, compared to the entire cell.
Our investigations showed for the first time the reaction dynamics of cells during cyclical mechanical stretch. We thereby determined an interesting general reaction characteristic which was found to be dependent on the stretch frequency, and involved cell-specific thresholds. The molecular mechanisms underlying these observations will be further investigated in future studies.

# ZUSAMMENFASSUNG

Neben biochemischen Faktoren in der Zellumgebung, können insbesondere auch physikalische Signale, biologische Prozesse in Geweben und einzelnen Zellen beeinflussen und regulieren. So kann zum Beispiel die mechanische Stimulierung von Zellen, deren Proliferation, Apoptose oder das Anschalten von bestimmten genetischen Programmen steuern. Es wurden schon Studien über den Einfluss von zyklischem Dehnen auf Zellen gemacht. Hierzu wurden Zellen auf eine flexible Kunststoffmembranen gesetzt und beobachtet, dass die Zellen versuchen sich, senkrecht zur Zugrichtung anzuordnen. Da dieses Verhalten bisher nur qualitativ beschrieben wurde, gibt es noch keine quantitativen und systematischen Untersuchungen zu diesem Verhalten. Des Weiteren wurden die Zellen nur vor und nach einer bestimmten Zugzeit beobachtet. Die Dynamik der zellulären Reaktion auf das zyklische Dehnen wurde noch nicht untersucht.
In dieser Arbeit soll eben diese Dynamik der Zellen beobachtet und anhand von biophysikalischen Modellen quantitativ untersucht werden. Dafür musste ein neues Zugsystem entwickelt werden, das es ermöglicht die Zellen lebendig, während des Zugvorgangs zu beobachten.
Das Verhalten verschiedener Zelltypen wurde dann unter Veränderung verschiedener Parametern wie Zugfrequenz, Zugamplitude oder Zelldichte beobachtet. Als Modellsystem wurden verschiedene Fibroblastentypen gewählt, embryonale Fibroblasten von Ratten (REF52) und primäre Fibroblasten (HDF) von jungen und alten menschlichen Spendern.
Wir konnten feststellen, dass sich die Zellen im zeitlichen Verlauf exponentiell senkrecht zur Zugrichtung orientieren. Mit Hilfe eines einfachen mathematischen Modells konnten wir die charakteristischen Zeiten für die Umorientierung der Zellen bestimmen und vergleichen.
Die Frequenzabhängikeitsstudien zeigten ein bisher unbekanntes biphasisches Reaktionsverhalten. Sowohl REF52 als auch menschliche Fibroblasten orientieren sich bis zu einer gewissen Grenzfrequenz schneller mit einer Zunahme der Zugfrequenz. In dieser Phase nimmt die Zeit für die Umorganisation der Zellen bei steigender Zugfrequenz mit einem Potenzgesetz ab.
Überschreitet man die Grenzfrequenz bleibt die Umorientierungszeit nahezu konstant. In dieser Phase tritt eine Sättigung der Zellreaktion ein. Alle getesteten Zelltypen zeigten das gleiche charakteristische, biphasische Verhalten. Unterschiede zeigten sich jedoch in der Reaktionskinetik und der Grenzfrequenz der Zellen. So zeigten die REF52-Zellen schon bei einer etwa 10-fach niedrigeren Frequenz eine Reaktion und generell konnten wir eine schnellere Umorientierung der REF52 Zellen bei allen Frequenzen beobachten, verglichen mit den HDF1 Zellen. Außerdem organisierten sich Zellen von älteren Spendern schneller um als von jungen Spendern.
Eine Erhöhung der Zelldichte, so dass anstatt Einzel-Zellen eine konfluente Zellschicht zu beobachten ist, hat gezeigt, dass die charakteristischen Zeiten für die Umorientierung mit Zunahme der Frequenz mit einem Potenzgesetzt abnehmen, jedoch im Gegensatz zu den Einzel-Zell-Beobachtungen kein Sättigungsplateau annehmen. Außerdem reagieren die konfluenten Zellen ungefähr um einen Faktor zwei schneller als einzelne Zellen. Hierbei kann die Aktivierung von Zell-Zell Kontakten, zusätzlich zu den fokalen Kontakten, in der Mechanotransduktion eine Rolle spielen.
Bei Veränderung der Zug-Amplitude orientieren sich die Zellen mit Erhöhung der Amplitude schneller um. Allerdings konnten wir hierbei eine lineare Abhängigkeit und keine Potentzgesetz-Abhängigkeit beobachten.
Die bei Frequenz- und Amplitudenänderung unterschiedliche Reaktionscharakteristiken (mit einem Potenzgesetz, sowie linear), deuten darauf hin, dass die Energie, von der der

Umorientierung abhängt, nicht einfach als Produkt aus Geschwindigkeit des mechanischen Reizes (Frequenz) und der Zugamplitude beschrieben werden kann.
Mit Hilfe der Fluoreszenzmikroskopie konnten Fokale Adhäsionskontakte während des Ziehens verfolgt werden und die Dynamik der mechanisch induzierten Umorganisation untersucht werden. Wir haben festgestellt, dass der Umorientierung der Zelle ein Umorientieren der Fokalen Adhäsionskontakte voraus geht.
Zusammenfassend konnte mit den Untersuchungen erstmals die Reaktionsdynamik der Zellen auf zyklisches mechanisches Stimulieren bestimmt werden. Dabei wurden interessante allgemeine Reaktionscharakteristiken und spezifische Schwellenwerte festgestellt, deren molekularen Ursachen durch weitere Arbeiten bestimmt werden müssen.

# 1. Introduction

In the biological world, a wide variety of different shapes and body profiles can be found. These natural phenomena have long been the focus of physical biologists (Thompson 1992). The intriguing question of how cells of only 10-40 µm in diameter can assemble and reproduce the shape of an organism that is meters in size has still not been answered. It is also not understood how cells can recognize their spatial position within such multicellular systems, even less is known about how they arrive at their destination within an organism.
It is, however, known that cellular assemblies design and create the complex structure and morphology of different tissues during development. Moreover, extracellular matrices and neighboring cells play an essential role in generating the major signals used by single cells to establish and maintain their shape and function (Fig.1.1). On the one hand, single cells have to communicate with the biochemistry of their environment, such as the chemical nature of the extracellular matrix. On the other hand, they are also capable of sensing physical signals in their surroundings, such as forces. After sensing the signals, cells must respond appropriately to them, over time, in order to function properly.

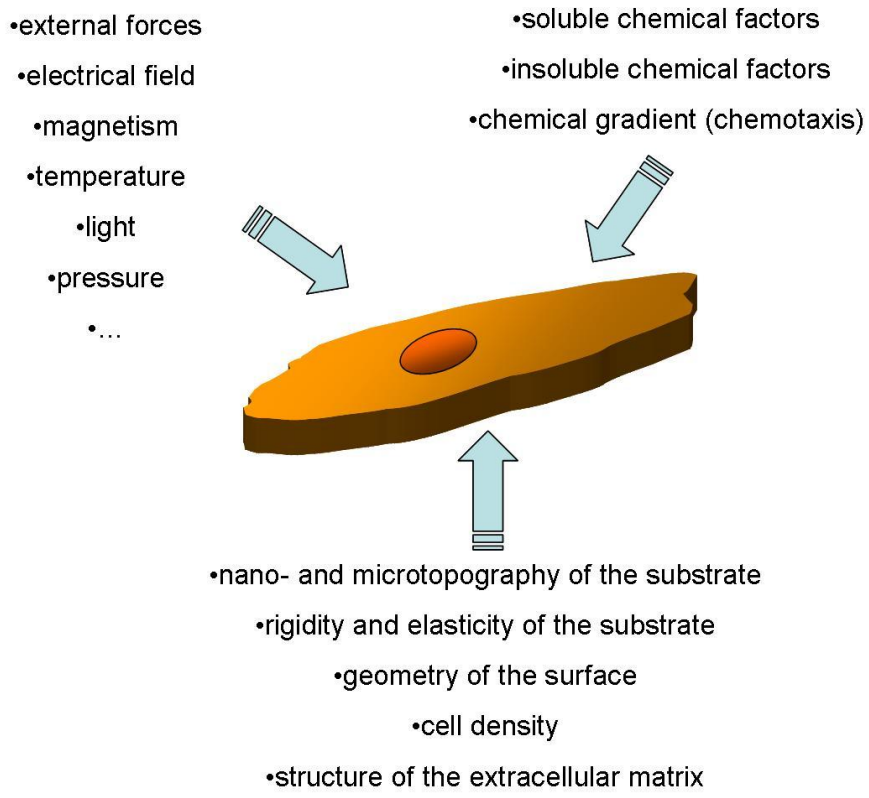


**Fig. 1.1: External influence on cells**

## 1.1 Influence of forces on tissue engineering and disease

It has long been known that mechanical forces were critical regulators of growth and form in biology (Thompson 1992). For example Wolff's law, stating that bone in a healthy person or animal will adapt to mechanical load by remodeling the bone structure, was published in 1892 (Wolff 1892). However, during the molecular biology revolution, a greater understanding of disease and cellular behavior led to a loss of interest in mechanics.

Many tissues in the body are subjected to internal and external mechanical stimuli and researchers now discovered the last years the importance of forces in various biological processes, particularly in tissue engineering or disease. For example, patterns of cellular growth can generate forces that help to bring tissue into their specific forms (Nelson *et al.* 2005). It was shown that forces generated by tissue itself play a major role as a possible feedback regulator of tissue growth (Shraiman 2005). Furthermore, for the success of fracture repair, forces are of immense importance (Augat *et al.* 2005). Mechanical load is an important signal which serves to regulate the growth of bones. Early studies in the 1970 showed that disuse of the multiskeletal system influences the growth and stability of bones. In that connection, Uthoff *et al.* performed experiments, comparing normally used and disused bones of young and old dogs (Fig1.2). They found that a disuse of bone destabilize it, and changes the morphology, resulting in a loss of bone mass (Uhthoff and Jaworski 1978).

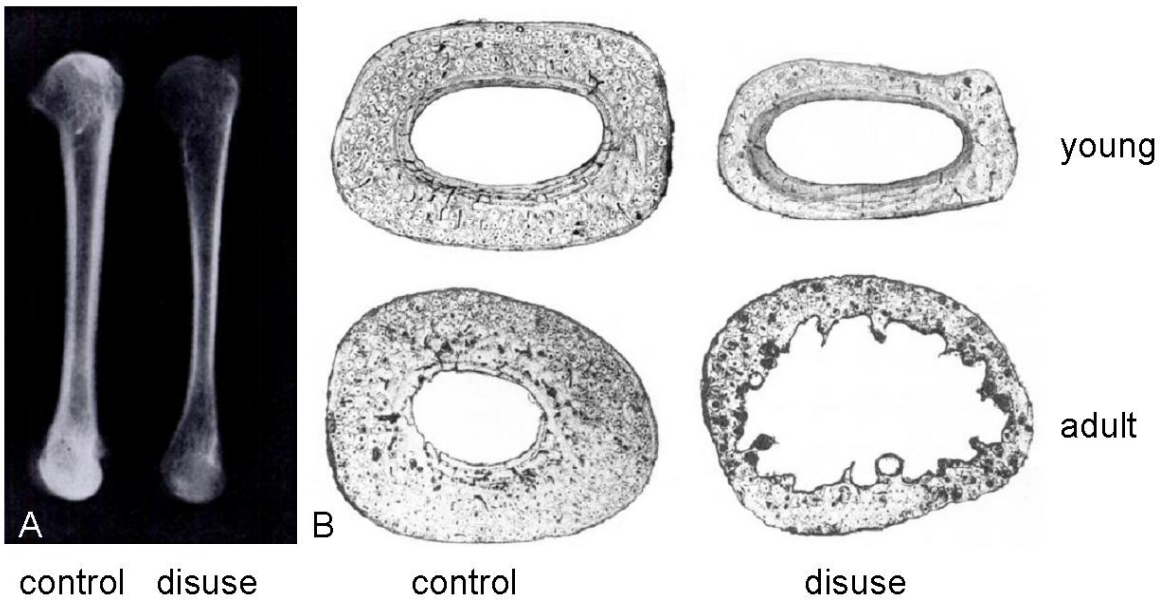


**Fig. 1.2: A: Radiograph of a metacarpal bone of a dog. Left: Control. Right: After 40 weeks of disuse. B: Cross-sections of metacarpal bone of young and adult dogs. Left: Control. Right: after 40 weeks of disuse. (Uhthoff and Jaworski 1978).**

Similar effects can be seen in the engineering and development of tissue-engineered tendons. In studies of Calve *et al.*, the stress-strain curve of the natural tendon from a chick embryo

and a tissue-engineered tendon which was not subjected to mechanical load were compared. They showed that both tendons displayed the same characteristic; however, the mechanical properties of the constructed tendon were significantly lower, in an order of a magnitude, than those of natural tendon. (Calve *et al.* 2004). This means that when designing artificial tissues, we should keep clearly in mind that mechanical aspects, like external or internal forces, play a critical role in their proper functioning (Curtis and Riehle 2001; Ignatius *et al.* 2005).

Furthermore, new studies showed that the age of cells influences mechanical properties and signaling of cells. Studies of Blough *et al.* displayed that rat aortic tissues becomes stiffer with age (Blough *et al.* 2007) and studies of Berdyyeva where they measured the stiffness of endothelia cells by means of atomic force microscopy corroborate theses results (Berdyyeva *et al.* 2005). Together with studies showing that changes in the extracellular matrix as well as in the cell itself as it ages influence the complex mechanism of mechanotransduction and mechanophysiology (Silver *et al.* 2003), we can expect, that the cellular reaction on mechanical signals differs with age.

In addition, mechanics can play decisive role in variety of different diseases. Table 1.1 presents a brief overview of some diseases known to be related to abnormalities in mechanotransduction. These abnormalities may occur at a number of different levels. The disease may be caused by changes in the mechanical properties of the cells, by alteration of the tissue structure, or by deregulation of the mechanochemical conversion (Ingber 2003)

For a better understanding of the effects of mechanics on the biology of an organism, it is necessary to explore the fundamental structural “building blocks” which make up the organism: a single cell.

| Medical field | Disease | Character of mechanical deregulation |
|---|---|---|
| Cardiology | Angina (vasospasm) | C,T |
| | Atherosclerosis | T,M |
| | Arterial fibrillation | M |
| | Heart failure | C,T,M? |
| | Hypertension | C,T,M? |
| | Intimal hyperplasia | C,T,M? |
| | Valve disease | T |
| Dermatology | Scleroderma | T |
| Gastroenterology | Achalasia | C |
| | Irritable bowel syndrome | C,M? |
| | Volvulus | C,T |
| Nephrology | Diabetic nephropathy | C,T,M? |
| | Glomerulsclerosis | C,T,M? |
| Neurology | Cerebral edema | T |
| | Facial tics | C |
| | Hydrocephalus | T,C? |
| | Migraine | C,M? |
| | Stroke | C,T |
| | Stuttering | C |
| Oncology | Cancer | C,T,M? |
| | Metastasis | C |
| Ophthalmology | Glaucoma | C,T,M? |
| Orthopedics | Ankylosing spondylitis | C,T |
| | Carpal tunnel syndrome | C,T |
| | Chronic back pain | C,T |
| | Osteoporosis | T,M |
| | Osteoarthritis | T |
| | Rheumatoid arthritis | T |
| Pediatrics | Collagenopathies | T |
| | Congenital deafness | C,T,M |
| | Mucopolysaccharidoses | T |
| | Musculodystrophies | C,T,M |
| | Osteochondroplasias | C,T |
| | Polycystic kidney disease | T,M |
| | Pulmonary hypertension of the newborn | C,T,M? |
| Pulmonary medicine | ARDS | C,T,M |
| | Asthma | C,T,M? |
| | Emphysema | T |
| | Pulmonary fibrosis | T |
| | Pulmonary hypertension | C,T,M |
| | Ventilator injury | C,M |
| Reproductive medicine | Pre-eclampsia | C,T,M |
| | Sexual dysfunction ( male & female) | C,M? |
| Urology | Urinary frequency/incontinence | C,M? |

**Table 1.1: A partial list of diseases resulting from abnormal mechanotransduction. C: Changes in cell mechanics. T: Alteration in tissue structure. M: Deregulation of mechanochemical conversion ? indicates situations where deregulation of mechanochemical conversion is likely, but remains to be demonstrated). From (Ingber 2003).**

## 1.2 Mechanical forces in cell biology

In biology and medicine, researchers tend to focus on the importance of genes and chemical factors in controlling cellular functions, whereas they totally ignore the importance of the physical factors which influence cellular behavior and cellular reactions (Chen and Ingber 1999; Ingber 2003; Janmey and McCulloch 2007; Kemkemer *et al.* 1999).

Although the physical influence on cell functions has received much less attention than genomic information, there has been a renaissance in the field of cellular mechanobiology during the last decade. The molecular biology revolution led to many new "genome–age" technologies, such as, gene and protein profiling techniques, powerful bioinformatics, new possibilities in micro- and nanotechnology, and new visualization methods. These new possibilities provide us with tools to unravel the molecular basics and the principles underlying the mechanosensing and mechanoregulation of cells.

As previously mentioned, mechanical effects can influence several biological processes (Ingber 2003). At the single cell level, force can influence cellular functions such as gene expression, proliferation, apoptosis, differentiation, reorganization of internal cell structures, or the reorganization of the entire cell (Fig. 1.3). Force can initiate cell protrusion, alter motility, and affect the metabolic reactions that regulate cell function, cell division or cell death. Examples are: (i) dysfunction of lymphocytes at near-zero gravity (Cogoli *et al.* 1984); (ii) force-dependent acceleration of axonal elongation in neurons (Heidemann and Buxbaum 1994; Smith *et al.* 2001); (iii) force-dependent changes in the transcription of cytoskeletal proteins in osteoblasts and other cell types (Wang J. *et al.* 2002); (iv) altered transcription in endothelial cells subjected to flow (Passerini *et al.* 2004); and (v) force-dependent changes in the morphology and orientation of cells and their cytoskeletons (Kaunas *et al.* 2005; Neidlinger-Wilke *et al.* 2001; Wang *et al.* 2001).

In addition to externally imposed forces, cells also exert internally generated forces on the matrix on which they adhere. Some types of cells can behave as a kind of detector of material stiffness, changing their structure, motility and growth as they sense the mechanical properties of their surroundings (Balaban *et al.* 2001; Pelham and Wang 1997).

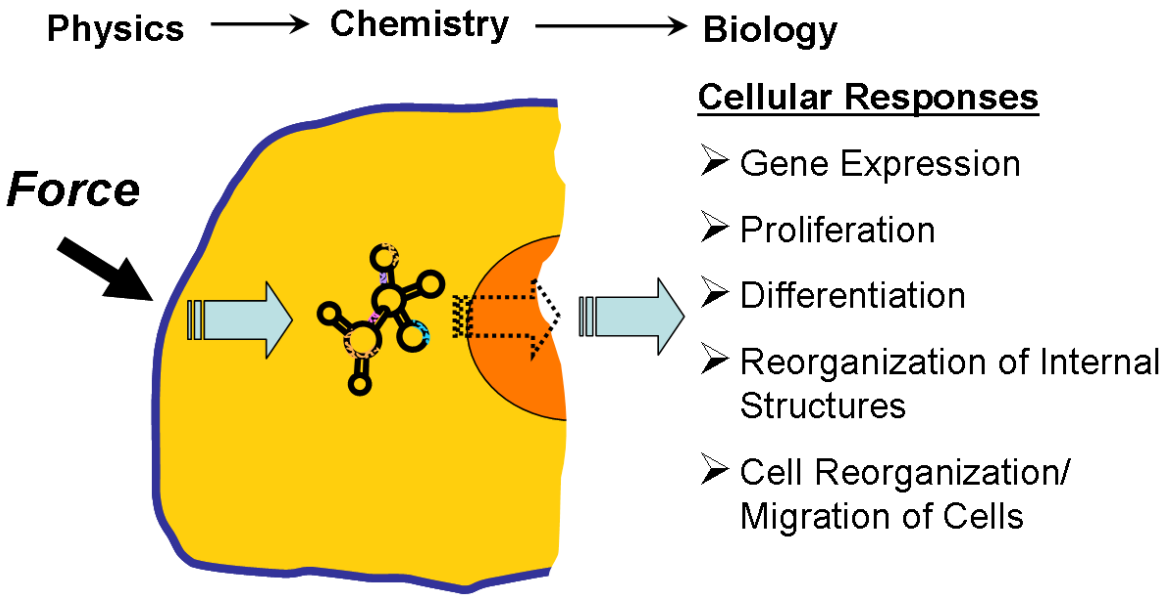


**Fig. 1.3: Mechanical forces in cell biology and their impact on cellular reactions. External forces must be translated via chemistry to a biological response.**

Cells from different tissues respond to varying types and levels of stress (force per unit area). For example, cartilage typically experiences stresses of 20 MPa. The chondrocytes within the chartilage can modify the expression of glycosaminoglycan or other constituents in response to these forces (Janmey and Weitz 2004). In a similar manner, osteocytes in bone respond to mechanical stress. Endothelial cells in contrast, respond to a shear stress of less than 1 Pa. (Dewey *et al.* 1981) and neutrophile granulocytes react to even lesser amounts of shear stress (Fukuda and Schmid-Schonbein 2003).

It is not only the strength of the applied forces, but also the time course or dynamic changes of the applied force that constitute crucial factors in the cellular response to stress. For example, endothelial cells in blood vessels respond to changes to turbulent stress, rather than to a specific magnitude of stress (Passerini *et al.* 2004).

Recent findings demonstrated, that the loading rate of the force onto the cell, and the matrix stiffening by the cellular activity can have a crucial impact on the cell itself (Vogel and Sheetz 2006; Yeung *et al.* 2005). Both mechanical sensing and the integration of different mechanical signals at different locations and times, occur through complex signaling pathways and target proteins that activate a programmed response to properly form, shape and influence cells and tissues (Vogel and Sheetz 2006).

## 1.3 How do cells sense force?

Cellular mechanosensing is a very complex process, involving a number of different cellular mechanisms. External force imposed on a cell must be transformed into a biochemical signal that can be processed by the cell. This can occur in different ways, such as

- Protein unfolding and stretch activated enzymes
- Stabilizing receptor-ligand bonds
- Opening of mechanosensitive ion channels
- Focal Adhesions as mechanosensors
- Transfer of the mechanical signal by the cytoskeleton (directly, or via biochemistry)
- Cell-cell contacts

The transduction of mechanical stimuli occurs through several signaling pathways. Many recent examples show that transduction takes place locally, at the cell periphery.
Figure 1.4 depicts various ways in which force is converted into biochemical signals (Vogel and Sheetz 2006). They include conformational changes in proteins [e.g. fibronectin in the extracellular matrix (ECM); (Gao *et al.* 2002)] due to stretching (Fig.1.4A) (Vogel 2006). The stretching of proteins induces exposure of cryptic peptide sequences which can result in the gain or loss of binding sites. Protein stretching can also entail increased separation between protein domains, or a gain or loss of enzyme function.
Application of external force can also influence receptor-ligand interactions. For example, weak non-covalent bonds between the ECM and the contractile cytoskeleton can be disrupted (slip bond) or they can be strengthened (catch bond; Fig. 1.4B) if a force is applied.
Another mechanism underlying the conversion of mechanical force into biochemical signals is the opening of membrane-embedded mechanosensitive ion channels (Fig 1.4C). These channels may be opened by membrane tension and bending, or by tethering to a stretched filamentous network such as the ECM (Sukharev and Anishkin 2004).

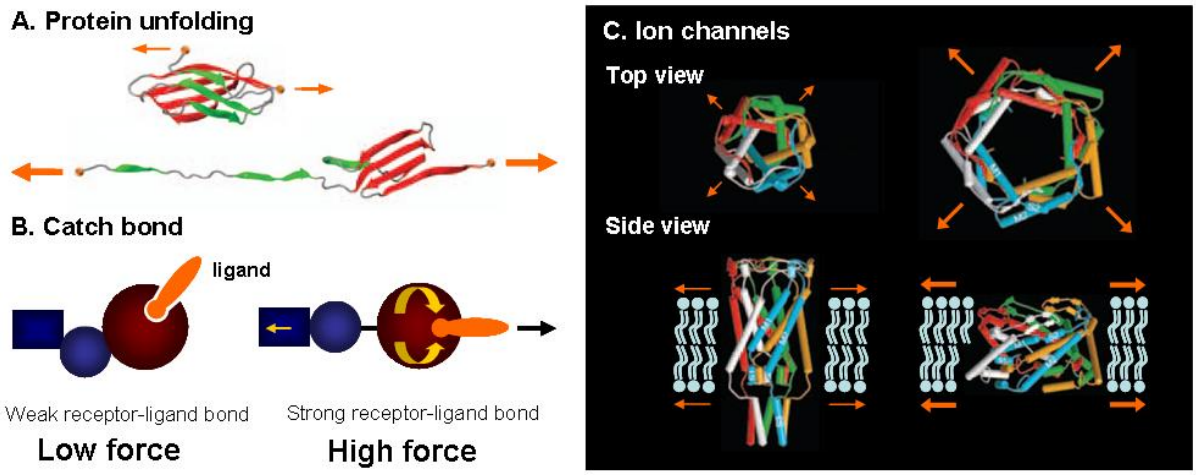


**Fig. 1.4: Three basic mechanisms of force sensing. A: Partial protein unfolding which causes a change in protein conformation. B: Stabilizing receptor-ligand bonds, by switching them into a long-lived state by means of force. C: Opening of mechanosensitve ion channels by membrane tension, or tethering to filamentous network. Orange arrows indicate force. Modified from (Vogel and Sheetz 2006).**

As mechanosensensors serves also a serial connection of three mechanically sensitive protein structures, the cytoskeleton, the extracellular matrix (ECM) and as linkage between them, the focal adhesions (Geiger *et al.* 2001; Janmey and Weitz 2004).

Any one of these proteins might respond to force by unfolding a part of their structure, and changing of the protein conformation. The unfolding process can open a binding site within the protein that initiates a signal in the cell interior as or the force is transmitted by the cytoskeleton itself. Figure 1.5 depicts how mechanotransduction can occur. In the resting state, a cell is attached to an ECM protein (fibronectin, vitronectin or collagen; Fig. 1.5Ac) by means of a bond to a transmembrane protein (integrin; Fig.1.5Ab). The transmembrane protein itself is also linked to the cytoskeleton via linkage to F-actin by talin or $\alpha$-actinin (Fig1.5Aa). A mechanical force can stimulate one of these three protein structures and a cellular response can be activated.

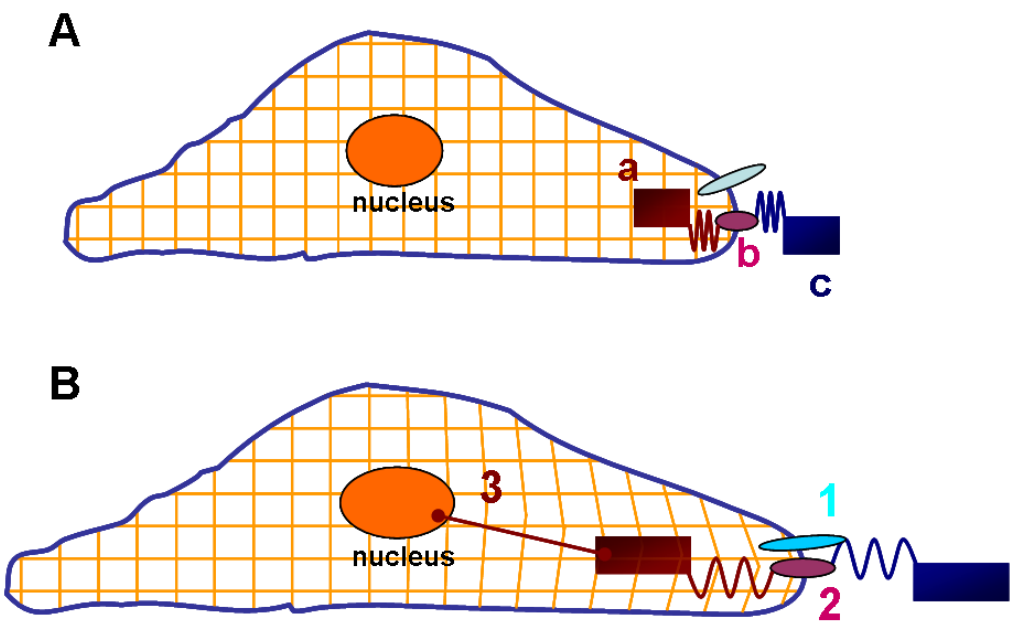


**Fig. 1.5: Schematic view of mechanotransduction at the membrane-cytoskeletal interface. A: Resting state of a cell; a: Linker protein to the cytoskeleton (talin, vinculin or α-actinin); b: Transmembrane protein (integrin); c: Extraecellular protein (fibronectin, vitronectin or collagen). B: Cell in a stretched state, with possible changes of proteins: 1: Extracellular matrix protein can activate transmembrane proteins by opening new binding sites; 2: Activation of a transmembrane linker protein by an extracellular matrix protein; 3: Stretching of intracellular proteins and transmission of force to the nucleus.**

For the activation of the cell, different scenarios are possible: First, a binding domain in an extracellular matrix protein might unfold (Gao *et al.* 2002; Oberhauser *et al.* 2002). This binding site can act as an activating ligand for an adjacent receptor (Fig1.5B1) (Galbraith *et al.* 2002). Secondly, the force might be transmitted by an extracellular protein to a transmembrane protein which undergoes an activating conformational change (Fig. 1.5B2) analogue to mechanosensitive channels (Riveline *et al.* 2001). Third, the extracellular and transmembrane proteins might remain unchanged but transmit the force to a protein bound to the receptor (fig. 1.5B3). This receptor (like α-actinin or vinculin) can act like the activated proteins in the first and second case (Yin and Janmey 2003). It is also known that a stretched cytoskeleton itself can transmit force. Proteins have a better binding affinity to a stretched cytoskeleton than to an unstretched cytoskeleton what cause an activation of local tyrosine phosphorylation which provides docking sites for cytosolic proteins and initiates signaling to activate Rap1 a small GTPase (Sawada and Sheetz 2002; Tamada *et al.* 2004).

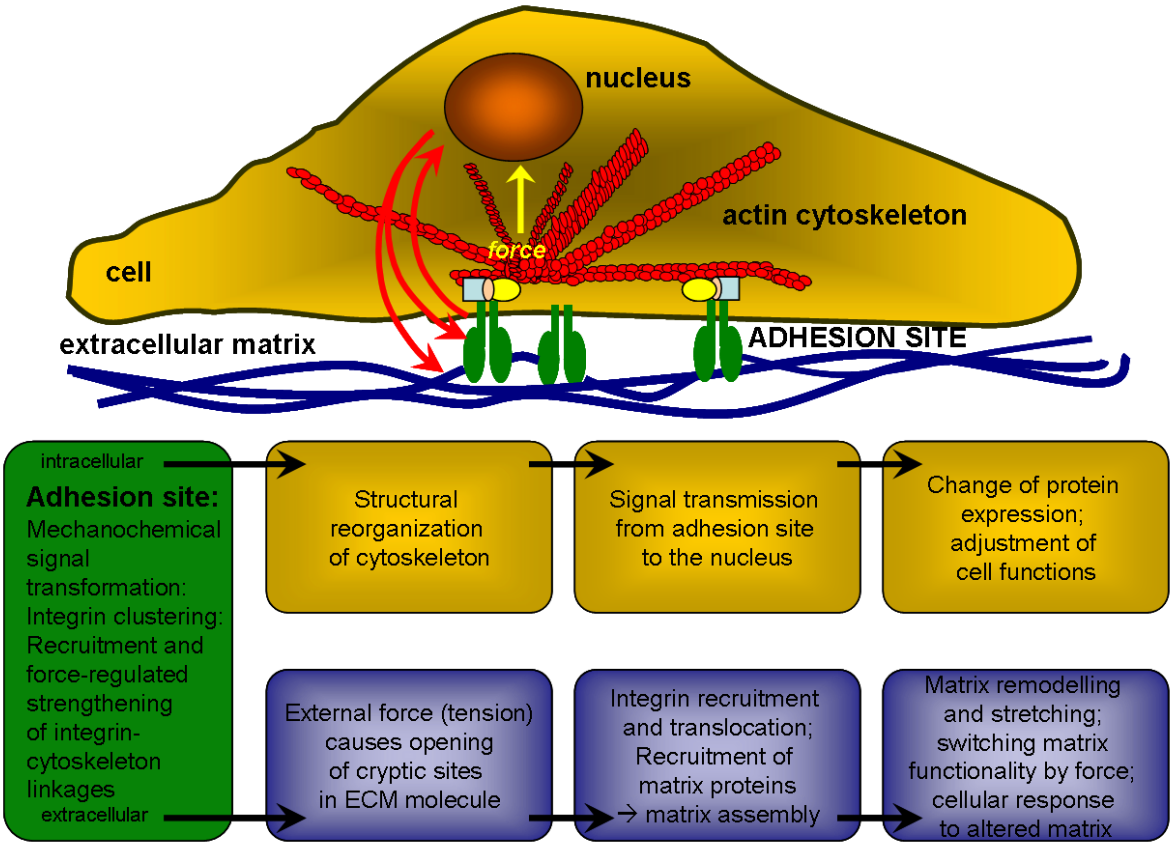


**Fig. 1.6: Schematic view of cellular processes involving mechanosensing and response. Intracellular (brown) and extracellular (blue) events. Modified from (Vogel and Sheetz 2006).**

Figure 1.6 provides a schematic view of the intracellular and extracellular events which occur during mechanosensation mediated by focal adhesion sites (Vogel and Sheetz 2006). At the adhesion site itself, the force is converted into a biochemical signal as described above. The cytoskeleton is then reorganized, and the biochemical signal or the force itself is transmitted to the nucleus. Within the nucleus, protein expression and cellular functions can be modified. Extracellular events include the opening of cryptic sites in ECM molecules and the recruitment of integrins and extracellular matrix proteins which lead to matrix remodeling, a change of matrix functions, and a cellular response to the altered matrix.

Mechanotransduction can not only occur via the connection of the cell's interior and the extracellular matrix with the focal adhesions as mechanosensors. A mechanical signal can also be propagated through the interconnected cell networks by cell-cell contacts. The transmission of the mechanical signal from a cell to the neighboring cell can take place by cell-extracellular matrix interactions, parcrine stimulation, gap junctions between the cells or cell-cell contacts, mediated by cadherins (Fig. 1.7; (Ko and McCulloch 2001).

Mechanical loading may induce the synthesis and release of cytokines which regulate cellular functions via paracrine mechanisms. Mechanical signals may also be transmitted through gap junctions as intercellular calcium waves. Another possibility to transmit forces between neighboring cells, are adherens junctions which are mediated by cadherins. Cadherins are

linked to the cytoskeleton and they are comparable in structure and function to the focal adhesions.

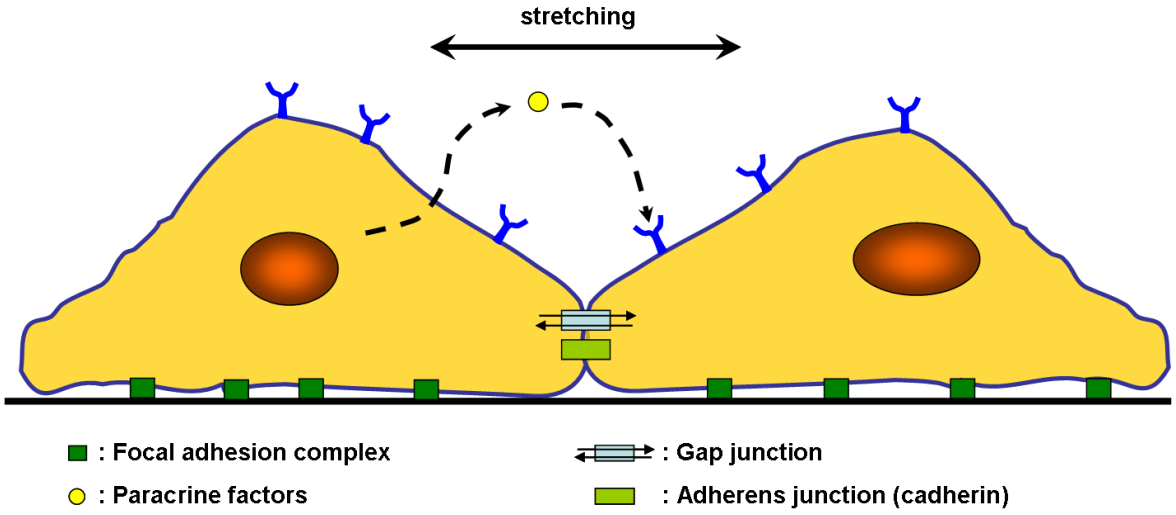


**Fig 1.7: Schematic view of intercellular mechanotransduction. Transmission of mechanical signals between neighboting cells may involve cell-extracellular matrix interactions, paracrine factors, gap junctions, and intercellular adhesive junctions, mediated by cadherins.**

Particularly in multicellular systems, the cell's response to mechanical stimulation, (e.g. deformation) does not necessarily depend on a change in protein structure, or a change in the membrane tension that causes the opening of an ion channel. The cellular response can also result from spatial redistribution of the signaling centers or enzymes and their substrates (Chen *et al.* 1997).

A recent study, in which compressive stresses deformed a monolayer of epithelial cells, found that signaling by autocrine factors was altered because the intercellular space between cell membranes containing epidermal growth factor (EGF) receptors decreased, to enable greater receptor occupancy by EGF at the receptors of the entire membrane of a cell (Tschumperlin *et al.* 2004)

Mechanosensing does not only involve a response to external forces. Cells also use internally generated stresses to probe the mechanical properties of their environment and respond to extracellular stiffness in a variety of different ways. For example, cells can stretch and wrinkle the substrates to which they adhere (Galbraith and Sheetz 1998; Pelham and Wang 1997; Schwarz *et al.* 2002; Tan *et al.* 2003). Researchers discovered that cells pull harder on stiffer surfaces, resulting in changes in cell morphology, motility, growth rate and intercellular signaling. The mechanism by which cells can measure the stiffness of their surroundings is still unknown, but it seems that an intact cytoskeleton is a critical factor; furthermore, the corresponding cell membrane complexes, such as focal adhesions, involved might be identical to those used for sensing external force (Discher *et al.* 2005).

## 1.4 Experimental methods for mechanical stimulation of cells

To investigate the cellular response to mechanical forces, as well as the mechanical properties of cells, various experimental set-ups may be employed. Cell deformation, viscoelastic, or other mechanical properties can be studied under conditions of uniaxial and biaxial tension or compression, pure shear, hydrostatic pressure, bending, twisting, or combinations of these methods. Studying the basic behavior of single cells can contribute to our understanding of the mechanical behavior of multicellular layers, or organisms, such as measurements of stress-strain data by stretching a single cell (Micoulet *et al.* 2005). It would be also interesting to investigate cellular behavior under conditions involving a combination of mechanical stimuli with biochemical or electrical stimuli (Bao and Suresh 2003).

One can broadly classify the experimental techniques developed thus far to study the mechanical impact of forces on cells and the mechanical properties of cells, into three different types (Fig.1.7): first, local probing of small parts of a single cell (type 1); secondly, mechanical loading of an entire cell (type 2); and thirdly, simultaneous mechanical stressing of a population of cells (type 3).

Examples of type 1 techniques include atomic force microscopy (AFM) (Mathur *et al.* 2001) and magnetic twisting cytometry (MTC) (Puig-De-Morales *et al.* 2001). With an atomic force microscope, it is possible to cause a local deformation in the cell with a sharp tip at the free end of a flexible cantilever. The deflection of a laser beam at the top of the calibrated cantilever tip can be measured, and the applied force then estimated. In the case of MTC, magnetic beads with functionalized surfaces are attached to a cell. An applied magnetic field creates a twisting moment on the beads, thereby deforming parts of the cell. With this method, one can estimate the elastic or viscoelastic properties of the deformed cellular part (Chen *et al.* 2001).

In the case of type 2 techniques, a cell can be aspirated into a micropipette. The cell is deformed by applying suction, through the micropipette, on the surface of a cell. It is possible to derive the mechanical response of the cell by recording the geometric changes of the cell during the experiment (Evans and Yeung 1989). For type 2 experiments, optical tweezers or a laser trap can also be used. In these cases, an attractive force is created between a dielectric bead of high refractive index and a laser beam, pulling the bead toward the focal point of the trap. Two microbeads in such a laser trap can operate as a tweezers, and deform a cell (Svoboda and Block 1994). This method produces only small forces in the range of pico Newton, and is therefore more often used for studies of molecule mechanics than for cells.

Shear-flow devices and stretching devices are typical methods used in type 3 experiments. They are applied to the study of mechanical responses involving an entire cell population of $10^2$ – $10^4$ cells. There are two different shear flow methods with a quantified flow which can be employed. Either a cone-and-plate viscometer, consisting of a stationary flat plate and a

rotating, inverted cone where laminar and turbulent flows can be applied, or a parallel-plate flow chamber, in which cells are subjected to laminar flow, are used (Usami *et al.* 1993). Different uniaxial, biaxial and pressure-controlled elastic-membrane stretching devices can also be used to deform cells (Banes *et al.* 1985; Neidlinger-Wilke *et al.* 1994; Wang *et al.* 1995b). In brief, cells are cultured on a thin, transparent polymer substrate such as an elastic silicone which is coated with an ECM protein to make the surface adhesive for cells. The substrate can be mechanically deformed while the cells are cultured on the substrate, and the effects of mechanical load on cell morphology and phenotype can be examined by means of standard microscopy.

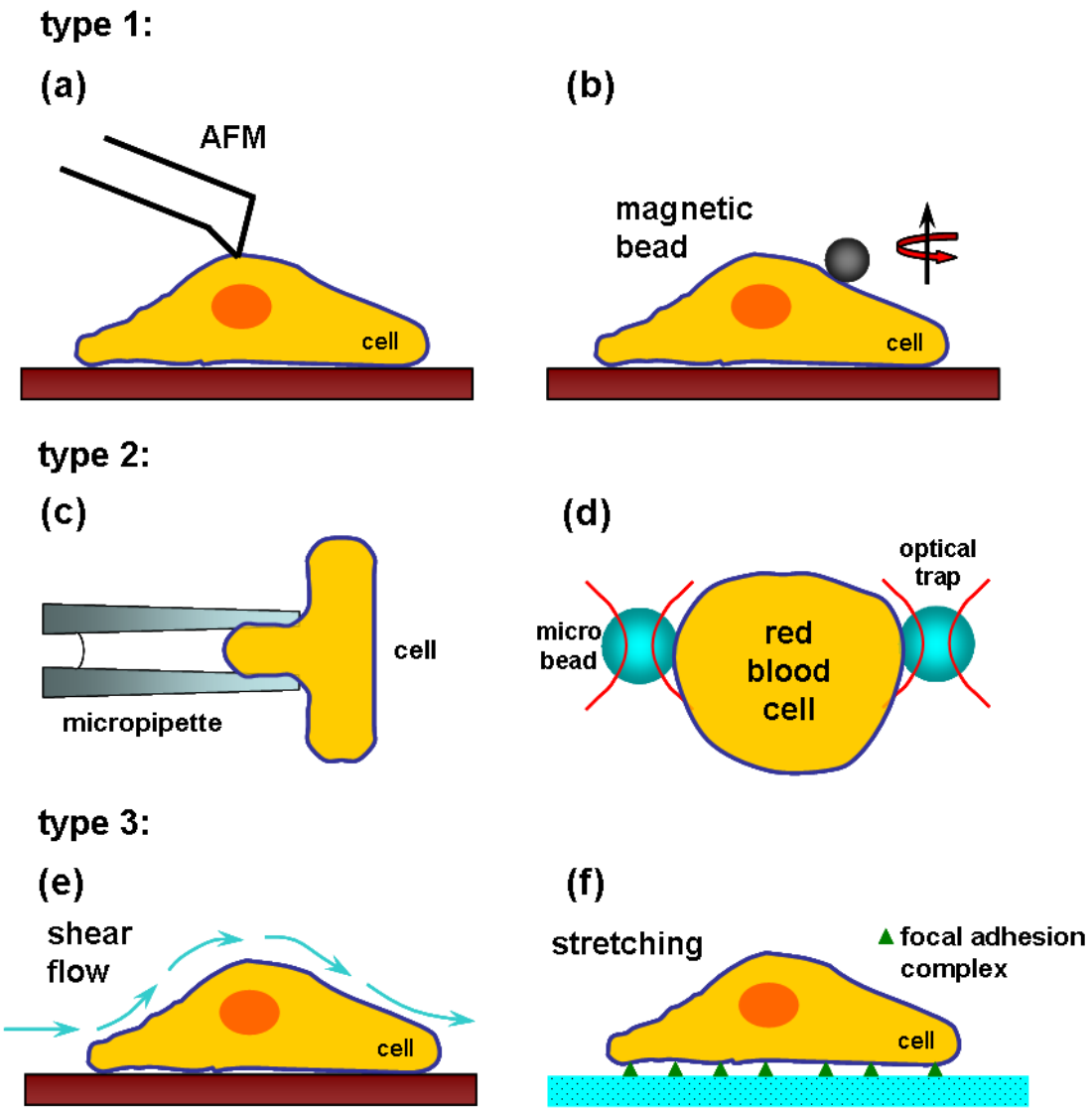


**Fig. 1.7: Schematic illustration of experimental methods used to probe the mechanical properties of living cells. Type 1: Probing of cell components with AFM (a) or magnetic beads (b). Type 2: Deformation of the entire cell by aspiration with a micropipette (c) or deforming with optical tweezers (d). Type 3: Determination of mechanical properties of cell populations by shear flow or by the stretching of cells adhering to elastic substrates. Modified from (Bao and Suresh 2003).**

Furthermore, the composition of the silicon substrates can be changed, by changing the ratio of the cross linker in the polymer gel. This change alters the mechanical properties of the substrates; the influence of substrate stiffness on the cellular response can then be investigated (Dembo and Wang 1999; Wang and Pelham 1998). In such studies, the focal adhesion contacts which serve as the link between the ECM and the cell, may be investigated by means of fluorescence microscopy of either antibody or fluorescent protein-labeled cells.

New techniques such as micropatterning have also been developed. The micropattering method enables the cells to adhere only to adhesive areas of the substrate (Lehnert *et al.* 2004). This method makes it possible to force the cells to adhere only to a certain part of the substrate and, for example, precondition them to lie in a certain orientation.

As already mentioned, the cells itself can produce forces. To observe and determine the strength of these internal forces, one used method involves the placement of cells on micropillar substrates (du Roure *et al.* 2005). Micropillar substrates are elastic substrates, usually made of an elastic silicone, with pillars in the micrometer range. With the elastic modulus, and the degree to which the cell deforms the pillars, one can calculate the force imposed by the cell on the substrate (du Roure *et al.* 2005; Tan *et al.* 2003).

In order to observe mechanical properties within the cell, microrheology methods may be employed (Bursac *et al.* 2005; Leung *et al.* 2007). In this case, polystyrene beads smaller than 1 µm are injected into the cell. The movement of the beads within the cell is observed and measured. These movement measurements provide information as to the internal viscoelastic properties of the cell.

In Table 1.2, various methods used to investigate the mechanical properties of cells are shown.

| Application | Technique | Example |
|---|---|---|
| **Cell population** | • Substrate deformation | • Effects of global stress on cell morphology (Geng *et al.* 2001) |
| **Cell population and single cell** | • Substrate composition<br>• Embedded particle tracking<br>• Microfabricated pillar array detector<br>• Magnetic twisting cytometry | • Effects of substrate stiffness on cell motility (Pelham and Wang 1997)<br>• Measuring cell migrating forces (Beningo and Wang 2002)<br>• Measuring inter/intracellular traction (Tan *et al.* 2003)(4)<br>• Characterizing frequency dependence of cellular components (Puig-De-Morales *et al.* 2001) |
| **Single cell** | • Cytodetacher<br>• Micropipette aspiration<br>• Optical stretcher<br>• Cantilever single cell stretcher | • Measure cell-substrate adhesion forces (Athanasiou *et al.* 1999)<br>• Viscoelastic properties of erythrocyte cortex (Evans and Yeung 1989)<br>• Noncontact, large deformation of cells (Guck *et al.* 2000)<br>• Measuring the mechanical properties of single cells (Micoulet *et al.* 2005) |
| **Single cell and single molecule** | • Atomic force microscopy<br>• High resolution force spectroscopy<br>• Microneedle<br>• Optical tweezers<br>• Magnetic tweezers<br>• Biomembrane force probe | • Cell/cytoskeletal protein stiffness (Radmacher 2002)<br>• Measure ligand-receptor unbinding forces (Benoit 2002)<br>• Qualitative cell stiffness during migration (Felder and Elson 1990)<br>• Effect of disease state on erythrocyte elasticity (Sleep *et al.* 1999)<br>• Viscoelastic deformation of cells and membranes (Bausch *et al.* 1998)<br>• Ligand-receptor unbinding (Yeung and Evans 1989) |

**Table 1.2: Different experimental methods used to observe mechanical influence on cells including examples. Modified from (K.J. Van Vliet 2003).**

## 1.5 Stretching of cells on elastic substrates

In this study, the active stretching of cells on deformable substrates was used to investigate the cellular response to mechanical stimulation. This method has been chosen by many different groups. Already in the 1980s, researchers used this method to study the response of cells subjected to mechanical stretch compared to unstimulated cells. Both Somjen (Somjen *et al.* 1980) and Hasegawa (Hasegawa *et al.* 1985), for example, developed a very simple experimental set-up to apply a constant stimulus to cells adhering to a silicone substrate. But in the real biological world, cells are also objected to periodically changed as well as to constant stimuli.

To investigate cells subjected to a dynamic, changed stimulation, such as cells in the connective tissue of the heart muscle, or in the lung various methods for dynamic stimulation of cells on elastic membranes were developed (Fig 1.8).

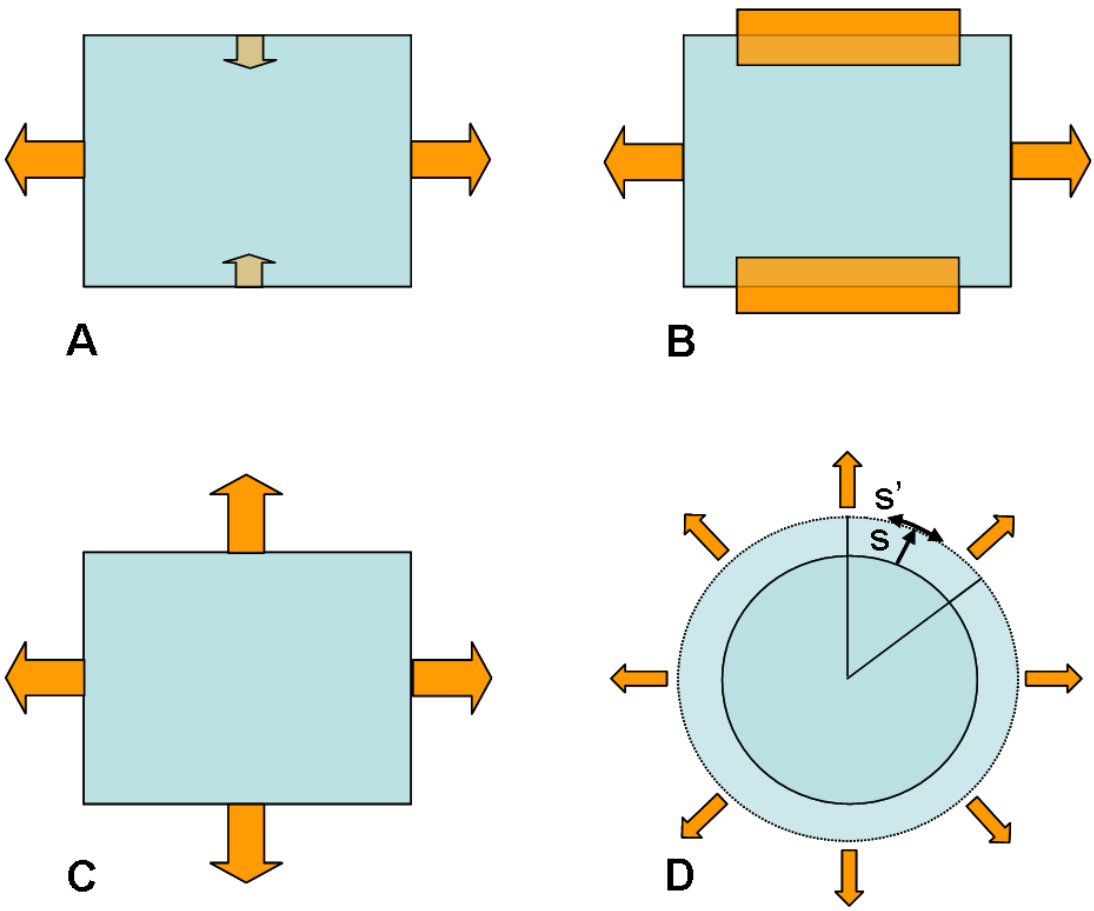


**Fig. 1.8: Scheme of different stretching variations. (A) Simple elongation strain (stretch in one direction; longitudinal elongation; free in orthogonal direction; transverse compression). (B) Pure uniaxial strain (stretch in one direction; longitudinal elongation; clamped in orthogonal direction; no transverse compression). (C) Biaxial strain (stretched in both directions), and (D) Multiaxial strain: the strain (S and S') is dependent on the radial position of the cells (realized with the Flexercell system).**

To realize the multiaxial strain (Fig. 1.8 D; multiaxial strain), researchers put a round, flexible rubber membrane on a loading post which is smaller in diameter than the membrane. Between a gasket and the loading post it is possible to apply a vacuum what causes a stretch of the membrane. By variation of the vacuum it is possible to vary the stretch (Banes *et al.* 1985; now commercially available as the Flexercell system) or Pender and McCulloch (Pender and McCulloch 1991) for the cyclical stimulation of fibroblasts. However, a major disadvantage of stretching methods with round substrates is that the strain amplitude is position-dependent and the cells are stretched in radial and circumferential direction (heterogeneous strain). The strain S and S' depends on the radial position of the cells on the substrate, and the amplitude of stretch occurs in all directions (Fig. 1.8 D).

For systematical analyses and quantitative experiments of the cellular response to mechanical stretch, it is necessary to apply a homogeneous strain field. This obtains a defined cell response to a defined external force. There are different ways to realize this requirement, as shown in Figure 1.8:

(A) Simple elongation, in which the membrane is stretched in one direction, and is allowed to compress in its orthogonal direction; (B) pure uniaxial stretching, in which the membrane is stretched in one direction, but the orthogonal edges are clamped, so that there is no deformation in the orthogonal direction; and (C) equi-biaxial stretching, in which the membrane is stretched equally in both orthogonal directions.

The method of stretching cells on a deformable substrate enables observations of the reaction of the entire cell or, rather, the surface of the cell, by means of phase-contrast microscopy. Fluorescence microscopy may be used to obtain a view of the inside of the cell. Furthermore, both single-cell behavior, as well as the behavior of a population of cells, may be observed in this manner. This method allows also a biochemical treatment of an entire cell population during mechanical stimulation.

A disadvantage of the realized experimental set-ups is the fact that they provide results for cellular reactions either without mechanical strain, or following a certain period of stretching. This means that no time-dependent observations of the cellular response during cyclic stretch are possible. Furthermore, the cells have to be fixed before investigating them under the microscope: an observation of living cells is not possible. Thus far, the only investigations of the dynamics of the cellular response were undertaken by Hayakawa (Hayakawa *et al.* 2001). They tracked cellular reorganization during six time points over a 90-minute period which provides only a limited temporal resolution of the cellular dynamics.

The method of stretching cells adhering on a flexible substrate was used by many research groups. In the 1980s Dartsch and colleagues investigated for example the behavior of arterial smooth muscle cells adhering to a silicone membrane which is subjected to uniaxial cyclical stretch (Fig. 1.8 B) (Dartsch and Betz 1989; Dartsch *et al.* 1986). These experiments were performed at a frequency of 50 $min^{-1}$ with three different amplitudes: 2%, 5%, and 10%. They observed that the cells change from an initial, random orientation, to an orientation that is perpendicular with respect to the stretch direction after subjected to cyclical stretch for 14

days. After applying a cyclical stretch, with an amplitude of 2%, the cells maintained their random orientation, as they did in the control experiments without applying cyclical stretch. However, when the cells are subjected to a strain of 5%, Dartsch and coworkers observed a perpendicular alignment to the stretch direction of the cells, up to a maximum angle of 61 (±9) degrees. When subjected to an amplitude of 10%, the maximum angle increased to 76(±5) degrees.

The method was further improved and advanced by Neidlinger-Wilke (Neidlinger-Wilke *et al.* 1994) and Wang (Campbell *et al.* 2003). Both groups investigated the behavior of fibroblasts and osteoblasts under cyclical stretch, in greater detail. They carried out phase contrast studies and fluorescent studies by taking pictures before stretching, and by taking pictures of fixed cells after they had been exposed to stretching for a certain period of time.

Neidlinger -Wilke and colleagues observed, for example, that an increase or decrease in cell proliferation was dependent on the frequency or the loading cycles of the applied cyclic stretch (Kaspar *et al.* 2002). They also found an increase of cell proliferation for stretching amplitudes of 1 %, while the cell proliferation decreased for stretch amplitudes of 2.4 % and higher (Neidlinger-Wilke *et al.* 1994). Moreover, they determined that the axial strain on cells causes the cellular reorientation process (Neidlinger-Wilke *et al.* 2001). Another result of their studies was that the perpendicular orientation of fibroblasts occurs within the first three hours of the applied stretch (Neidlinger-Wilke *et al.* 2002).

The Wang group used a similar experimental set-up. They hypothesized that the preferred direction of minimal substrate deformation is correlated with the preferred direction in which melanocytes align after 24 hours of cyclical stretching (Wang *et al.* 1995b). In a later work, they showed that reorientation of human aortic endothelial cells and stress fiber reorganization occur specifically in the direction of the minimum substrate deformation (Wang J. H.-C. 2000). In further studies they reported for the cellular response after three hours cyclical stretch, that the rate and extent of cell reorientation are primarily dependent on the stretching magnitude, not the stretching rate. Furthermore, microtubules are not essential to cell reorientation and stress fiber formation (Wang *et al.* 2001). Wang *et al.* also investigated human patellar tendon fibroblasts which are forced to be parallel or perpendicular to the stretch direction by means of microgrooved substrates, in order to determine if the fibroblast reorientation is dependent on the initial orientation of the fibroblast. Therefore, they preoriented the fibroblast by means of microgrooves parallel and perpendicular to the stretch direction and after four hours of cyclical stretch, determined the amount of $\alpha$-smooth muscle actin and other cellular proteins. These studies showed that the fibroblasts produce more $\alpha$-smooth muscle actin, if they are orientated parallel to the stretch direction (Wang *et al.* 2004). The same researchers also examined the cytoskeletal reorientation after cyclical stretch is applied to the cells. They stained actin filaments of cells which are not subjected to cyclical stretch and of cells which were subjected to cyclical stretch for three hours an compared them. They found that the cytoskeleton also orients perpendicular to the stretch direction (Wang *et*

*al.* 2001). Studies by Sumpio (Iba and Sumpio 1991) and other groups (Kakisis *et al.* 2004; Na *et al.* 2007; Yoshigi *et al.* 2005) corroborate theses findings, they could also observe a perpendicular reorientation to the stretch directon of the actin filaments.

Takemasa and colleagues developed yet another experimental set-up, in order to obtain a greater variation in stretching amplitude (Shirinsky *et al.* 1989; Takemasa *et al.* 1997). They observed a greater perpendicular alignment of the actin fibers at higher stretching amplitudes (Takemasa *et al.* 1998).

Other groups employed the method of stretching cells on elastic substrates to examine the molecular details in greater depth. In studies undertaken by Kaunas *et al*., for example, they were interested in the mechanism underlying the reorientation of the stress fibers. Kaunas and coworkers were focused on the influence of small GTPases such as Rho which regulates the formation of the actin stress fibers (Hall 1998; Ridley and Hall 1992; Yano *et al.* 1996). Inhibition of Rho, Rhokinase and myosin-light chain kinase (MLCK) causes, in contrast to untreated cells, a parallel alignment of actin stress fibers in cells subjected to cyclical stretch. This finding demonstrates that the Rho/Rho-kinase/MLCK pathway plays an important role in the cellular response to cyclical stretching. They also determined that expression of an active Rho V14 plasmid leads to enhanced stress-induced perpendicular stress fiber orientation, comparable to an increase of the stretching amplitude of 3 %. This augmentation of the perpendicular orientation could be blocked by blocking RhoV14. These findings demonstrated that the Rho pathway plays a crucial role in determining both the direction and extent of stretch-induced actin stress fiber orientation (Kaunas *et al.* 2005; Kaunas *et al.* 2006).

In contrast to perpendicular orientation of cells during cyclical stretch, Eastwood *et al*. found, that cells which were exposed to static or quasi-static strain, meaning strain with very low frequencies (15 $min^{-1}$), for 16 hours, were aligned parallel to the stretch direction (Eastwood *et al.* 1998). The finding of parallel alignment during quasi-static stretch of the cells by Eastwood and coworkers showed that there must be frequency dependence for the alignment of cells subjected to mechanical stretch. A quantitative study including experiments with different stretch frequencies over a wide range from quasi static to high frequencies could provide a frequency dependence of the reorientation process.

Very recent studies with a small variation of the stretch frequency carried out by Liu *et al*. explored the role of the stretch frequency, and showed that aortic smooth muscle cells align more perpendicular at different frequencies. (Liu *et al.* 2007).

# 1.6 Models describing cells subjected to cyclical stretch

If cells are stimulated by mechanical stretch, they reorient themselves perpendicular to the stretch direction. Such cellular behavior has been described by a number of theoretical models.

## 1.6.1 Cells as a mechanical dipole

Safran *et al.* established a model in which cells were described as mechanically active force dipoles (Fig. 1.9(Bischofs *et al.* 2004; De Rumi *et al.* 2007). To simplify the model they assume needle-like cells with a bipolar character, such as fibroblasts, for example. This simple theoretical model includes the contractile force due to the mechanosensitivity of cells, and the elasticity of the matrix. The model idealizes a stationary adhering cell as being exposed to a pair of equal and opposing contraction forces; one might also speak of "tensional homeostasis". This force pattern is generated by active myosin II molecular motors and the actin stress fibers that connect focal adhesions on the opposite sides of the cell. Based on such an idea, the model describes the cell as an elastic dipole interacting with a periodic external strain field.

Cells can change their contractile activity and orientation by reorganization of focal adhesions and stress fibers in response to external forces. This reorganization can only occur if the temporal change in the force is slower than the time required for the focal adhesions and stress fibers to remodel. This relaxation time is of unknown magnitude, and represents the reorganization of actin stress fibers and focal adhesions. If the inverse frequency of the applied strain is much slower than this relaxation time, the mean orientation of the cell is perpendicular to the strain, and fairly independent of frequency. If the inverse frequency is much faster than the relaxation time, then the model of Safran *et al.* predicts that cells align themselves nearly parallel to the strain, independent of the frequency. They predict a change from a parallel orientation at low frequencies, to a perpendicular orientation at high frequencies.

Cells which begin to adhere to a gel establish an increasing contractile force until reaching a steady state value over time. Further application of external strain results in a decrease in the average contractile force exerted by the cells (Brown *et al.* 1998). Safran and colleagues make the key assumption that cells regulate their contractile activity to maintain an optimal local force ($\boldsymbol{T}^*$) in the presence of external stress.

Fig. 1.9 shows a needle like cell with focal adhesions and actin stress fibers. The contractile forces generate the elastic dipole $\boldsymbol{P}$, while $\boldsymbol{T}$ represents the external force applied at the angle $\theta$ with respect to the direction of the cell axis **z**.

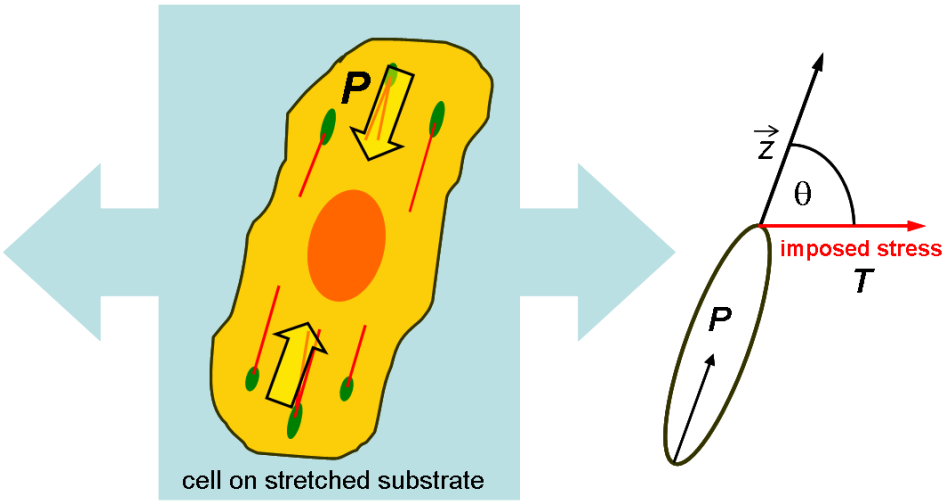


**Fig. 1.9: Cells as mechanical dipoles. Internal forces created by actin fibers linked to focal adhesions cause an elastic dipole, *P*. The cyclic stretch causes an external force, affecting the cell. The cells try to balance the internal and external forces to an optimum → cellular reorientation. θ = angle between the stretch direction and the main axis of the cell. (De *et al.* 2007).**

The cell measures local forces in the direction of the stress fibers, meaning in the z direction. The reaction force in the z direction to the focal adhesions is proportional to $-\boldsymbol{P}$, and the force of the external stress in the z-direction is proportional to $\boldsymbol{T}\cos^2\theta$. The cell attempts to optimize the inner stress by remodeling the stress fibers to the optimal local force which is proportional $\boldsymbol{T}^*$. $\boldsymbol{T}^*$ represents the optimal internal force for cell contraction; the cell attempts to maintain this optimal value. The cell also attempts to minimize the so called free energy (represented by $\boldsymbol{F}_{cell}$). The external force $\boldsymbol{T}$ and the optimal inner force $\boldsymbol{T}^*$ are constant, what means that the cell has to balance by the dipole moment $\boldsymbol{P}$ (De Rumi *et al.* 2007).

$$F_{cell} = \frac{1}{2}\chi\left(-P + T\cos^2\theta - T^*\right)^2$$

Where $\chi$ is a measure of cell activity, and depends on the ability of the cell to reorganize the cytoskeleton.

## 1.6.2 Interpretation of stress fiber organization under conditions of cyclic stretch

Wei *et al.* have another explanation for the perpendicular orientation of cells during uniaxial cyclic stretch (Wei *et al.*). They focus on the orientation of actin stress fibers which, like the cells, are also aligned perpendicular (Kaunas *et al.* 2005; Takemasa *et al.* 1998). They explain that the perpendicular alignment of the stress fibers is due to the stabilization and destabilization, respectively, of the stress fibers. In the loading half-cycle, the fibers aligned in the stretch direction have a maximum contraction strain rate, and hence dissociate during each

loading half cycle. But the fibers aligned in the perpendicular direction never contract, and do not dissociate (Fig 1.10).

This same theory also predicts a rise in bimodal stress fiber distribution upon transverse contraction, and a higher and greater perpendicular alignment of the actin stress fibers as the stretch frequency increases.

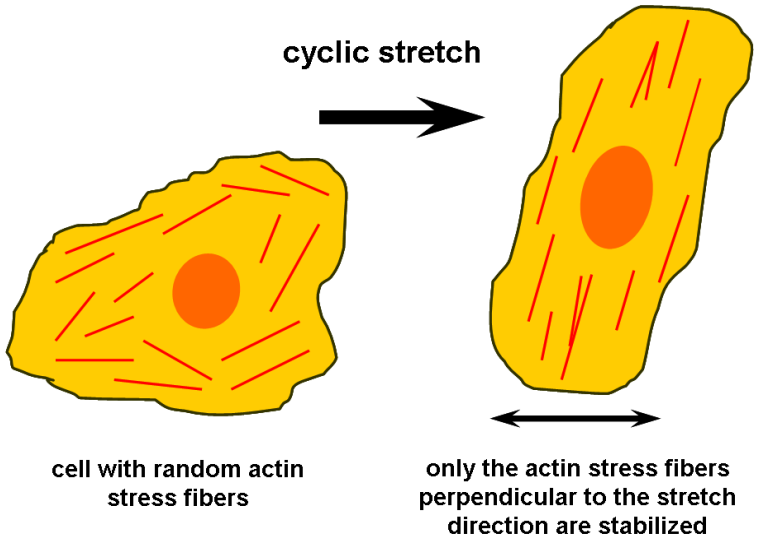


**Fig. 1.10: Actin stress fibers in the direction of the cyclic stretch are destabilized, while actin stress fibers perpendicular to the stretch direction are stabilized. This leads to a perpendicular orientation of the actin stress fibers and therefore, the entire cell. (Wei *et al.*)**

### 1.6.3 Other models

The groups of Gao (Chen 2006) and Garikipati (*personal communication*) attempt to describe a cell as a viscoelastic body, along the lines of the mechanical continuum theory. This body adheres to a flexible substrate, and modeling only passive mechanical properties are taken into account, excluding biological aspects such as the active cellular reaction. Under such circumstances, they predict a maximum rate of energy dissipation by the cell. In the case of a cell subjected to cyclical stretch, the energy dissipation would result in the perpendicular reorientation to the stretch direction of the cell.

In a series of studies, Stamenovic *et al.* (Lazopoulos and Stamenovic 2006; Stamenovic 2005; Stamenovic 2006) also attempt to describe cellular behavior during cyclic stretch as being dependent on the magnitude of the substrate strain, and the state of cell contractility. They base their theoretical framework on the theory of non-linear elasticity, and found a solution to predict cellular reorientation either global or Maxwell's criteria for stability. Their model predicts that cells would orient themselves away from the stretch direction during uniaxial stretch. Moreover, the orientation angle would increase as the magnitude of the strain increased.

## 1.7 Objectives of the study

The main aim of this study is to observe and investigate the cellular response to cyclical stretch in a detailed and quantitative manner. We are especially interested in the dynamics of the cellular response to cyclical stretch. Therefore, it was necessary to develop a totally new experimental set-up which would allow us to observe living cells under the influence of externally applied cyclical stretch. As model systems, we used common fibroblasts. After establishing and specifying the experimental set-up, the following questions were addressed:

- **What is the time course of the cellular response to cyclical stretch, and is there a general response characteristic?**
  Observation, determination, and quantification of different cellular parameters in dependence of frequency and stretching amplitude.

- **Are there cell type-specific and cell age-specific differences in the response kinetics and response characteristic?**
  Investigation and comparison of rat embryonic fibroblasts, human fibroblasts from donors of different ages, and human mesenchymal stem cells.

- **Does the cell density influence the cellular reaction?**

- **Is the cellular response dependent on the rate of substrate stretch or substrate relaxation?**

- **Can cyclical stretch influence cell division?**
  Observation of cell division during experiments with different stretch frequencies.

- **How do cells which cannot reorient themselves react?**
  Cells were forced into a certain orientation by micro-contact printing fibronectin lines on a non-adhesive surface.

- **How do focal adhesions as one important candidate for a cellular force sensor, react during cyclical stretch?**
  To obtain more information about the molecular processes underlying the cellular reorientation, the set-up was improved by the addition of fluorescence microscopy. Experiments with Paxillin YFP cells should serve as a bridge to observations at the molecular level.

A detailed, quantitative examination of the reorganization process is expected to provide important insights into the basic biological mechanisms underlying the reorientation process of cells during cyclical stretch. Knowledge of the characteristic time scales on the phenomenological levels must be mirrored by molecular processes, for example, the reorganization of the cytoskeleton.

# 2. Materials and Methods

## 2.1 Development of a stretching machine for live cell imaging

In this study, we employed a method involving the stretching of transparent expandable silicone substrates, as previously described (Brown 2000; Grabner 2000; Neidlinger-Wilke *et al.* 1994). This method enables observation of many single cells or cell populations during one experiment. This approach yield better statistics of the results and biochemical treatments of a cell population are possible. One disadvantage of this method is the difficulty in ascertaining if the cell strain conforms to the substrate strain; i.e., if the entire strain is transmitted to the cell (Fig.2.1). The applied force can be approximated. An applied strain of 10% would yield to force of approximately 50 nN, if we assume the Young modulus of a cell as 10 kPa and the average cell area of 20000 µm². Compared with Balaban's findings (Balaban *et al.* 2001), these forces are within the range of forces produced by the cell itself (contact stress when a cell is pulling on a substrate ~ 250 nN).

A new experimental set-up had to be developed, with specific requirements. For live cell experiments the set-up has to be surrounded by a climate chamber to perform special conditions such as a temperature of 37°C and a humid atmosphere of 5% $CO_2$. The set-up had to be mounted on a motorized microscope which enables us to synchronize the microscope and the stretching device. For the synchronization of the motor and the stretching device the software controlling of the stretching device had to be embedded into the microscope software.

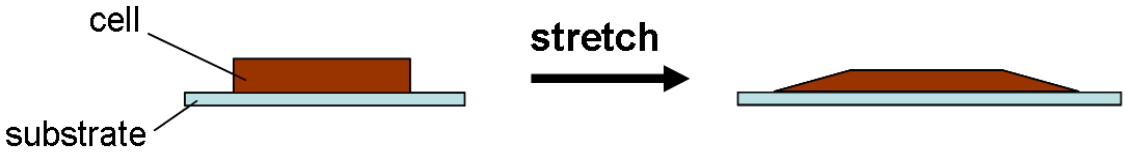


**Fig. 2.1: Scheme of stretching a cell on a substrate. How is the strain transferred to a cell?**

### 2.1.1 The experimental set-up

As shown in Fig. 1.8 (Section 1.5), there are different ways to create a stretching set-up. In this study the method of multiaxial strain was not used because of the mentioned disadvantages (Section 1.5). We developed a stretching device in our laboratory which allows us to apply both simple elongation strain and uniaxial strain (Fig. 2.2). For the uniaxial strain the stretched substrate was clamped from the orthogonal direction of the stretch direction. We could not apply pure uniaxial strain, because a small compression orthogonal to the stretch direction could be observed.

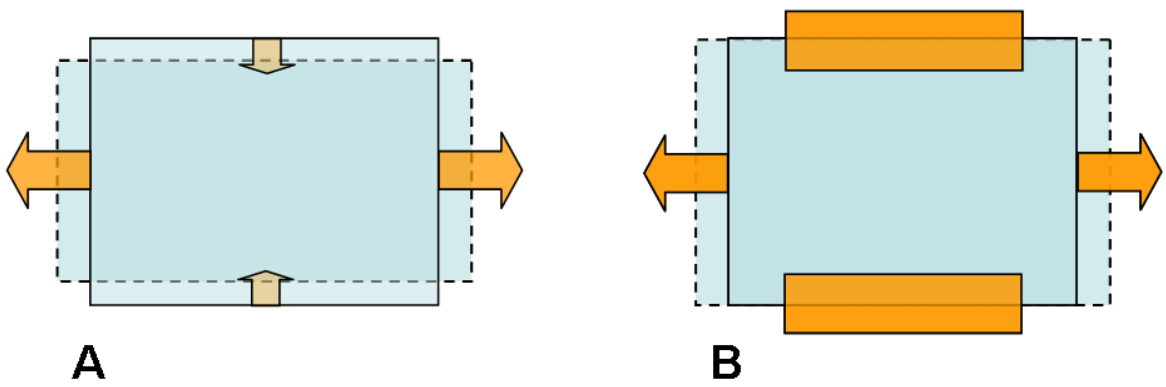


**Fig. 2.2: Scheme of the modes of the developed stretching set-up. (A) Simple elongation strain (stretch direction in one direction → longitudinal elongation; free in orthogonal direction; transverse compression). (B) Uniaxial strain (stretch in one direction; longitudinal elongation; clamped in orthogonal direction; almost no transverse compression). The dashed lines indicate the stretched substrate.**

The stretching system was developed in a manner which allows us to apply the cyclical stretch from two directions, meaning that the set-up had two motors, one for the stretch in x-direction and second one for the stretch in y-direction.

Fig. 2.3 shows a schematic view of the stretching device developed and built in-house. The device consists of two brushless DC-servomotors (3564K024CS; Faulhaber Group, Oberaich, Germany) which are placed in orthogonal positions. Alternatively, it is also possible to position them opposite one another. For the application of a wide range of different stretching frequencies, the motors can be supplied with different gears. Furthermore, it is also possible to mount the system with high-resolution micro-translation stages with a ballscrew drive (M111.1; Physik Instrumente PI, Karlsruhe, Germany), to perform stretch experiments where micro positioning is required.

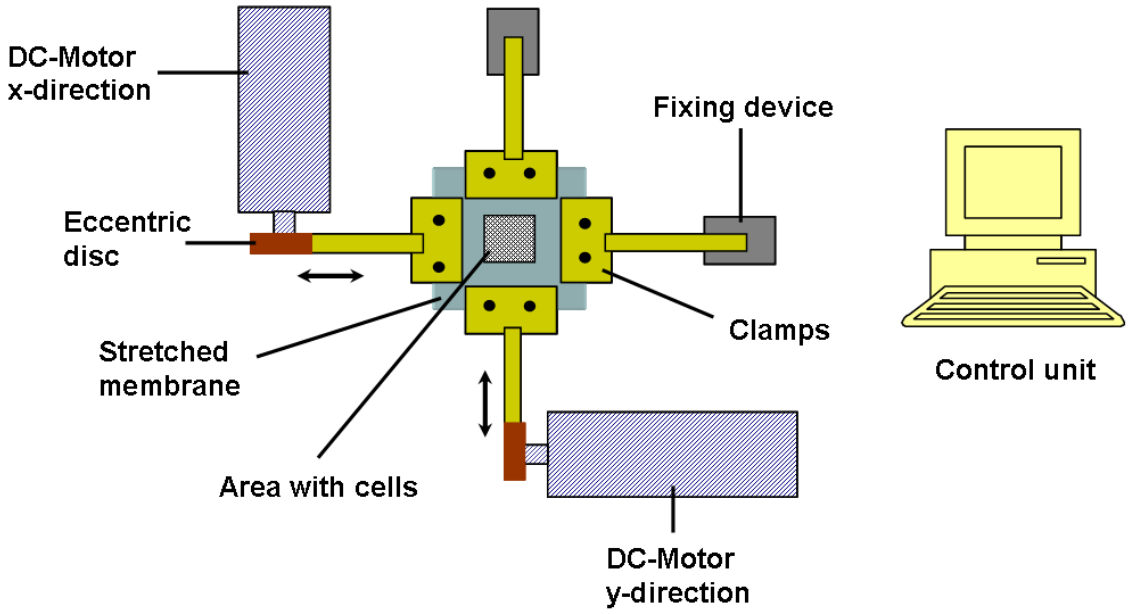


**Fig. 2.3: Schematic view of the stretching device developed in-house. A quadratic substrate can be clamped at all four edges. Two orthogonal positioned motors enable stretching in the x- and y- directions (the black double arrows indicate the stretch directions). The amplitude can be changed by changing the eccentric discs. The motors are controlled by a computer system. The substrate can be pre-stretched by means of the fixing devices.**

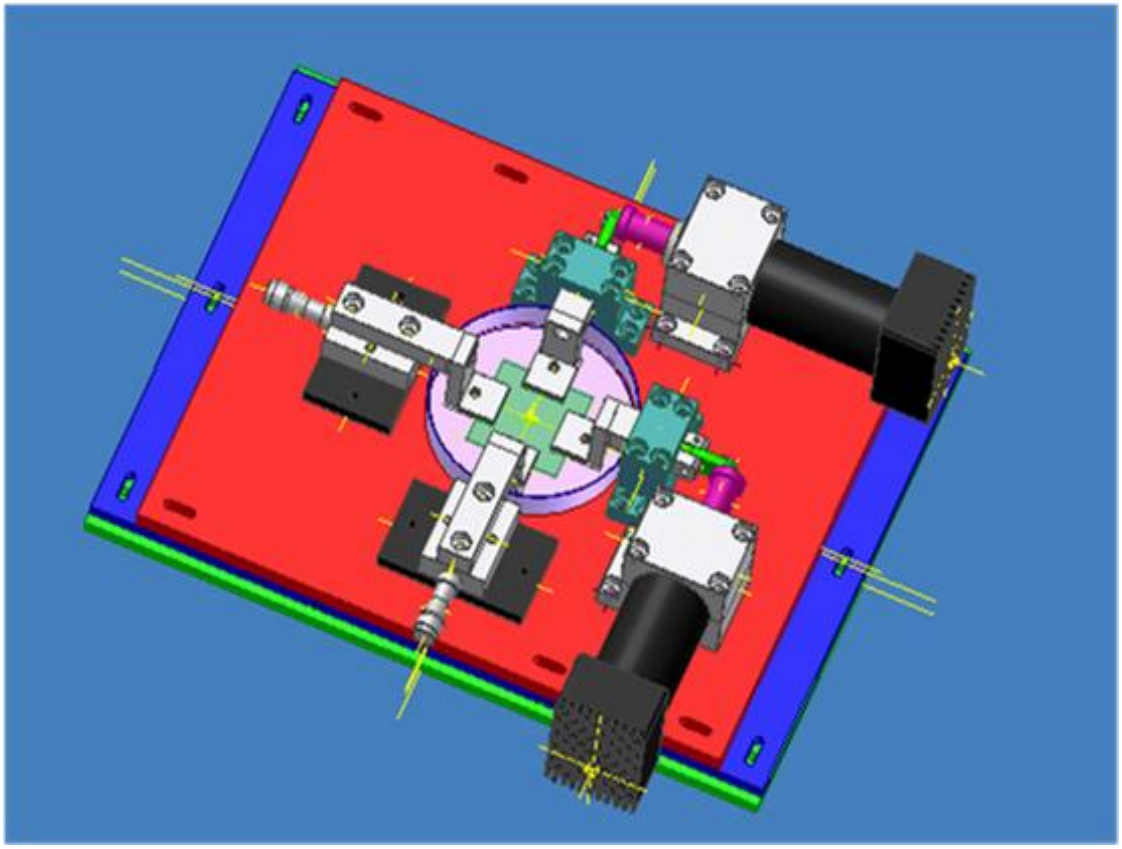

**Fig. 2.4: Technical drawing of the stretching device we developed. The device is built on three base plates (green, blue and red plate) so that it may be moved in the x- and y- directions. In the center is the clamped substrate.**

Each motor is responsible for the stretch in one direction, along the x- or y- axis. The motors can be controlled via the serial port by computer. As control software, the Faulhaber Motion Manager 3.3, or the microscope software can be used. With different gears, one is able to vary the frequency of the motors from 0.0001 $s^{-1}$ up to 20 $s^{-1}$. On the drive shaft of the motor is an eccentric disc which is connected to the connecting rod and the clamps. By changing the eccentric disc, one can vary the stretch amplitude from 1% up to 15 %. On the opposite site of the motor clamp is a fixing device. The fixing device is a manual linear stage (M460; Newport; France) which is connected to the opposite clamp. It is possible to move the fixing device between 0 and 5 mm which allows pre-stretching of the substrate, in order to avoid wrinkles on its surfaces. The base of the device consists of an x-y-stage, and enables the movement of the stretch system in both the x- and y- direction. The entire experimental set-up can be mounted on a inverse or upright microscope.

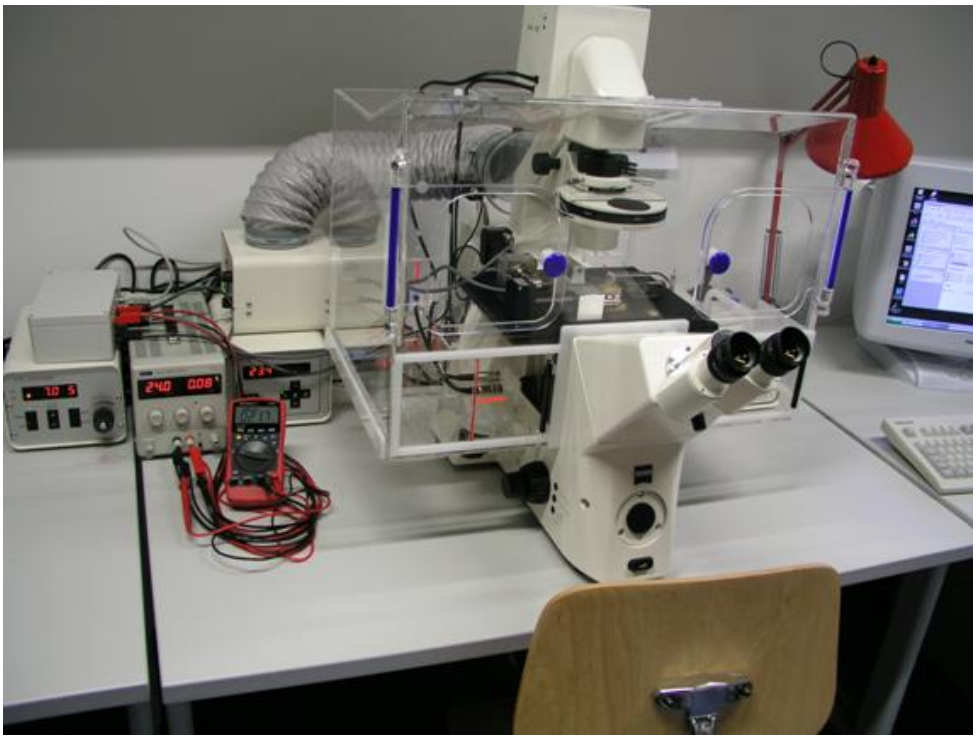

**Fig. 2.5: Experimental set-up: The stretching device is mounted on an inverse Zeiss Axiovert 200M microscope. The system is surrounded by a climate chamber for live cell imaging. The controllers on the left are responsible for regulating the temperature and amount of $CO_2$ within the climate chamber. Furthermore, one can see the motor controller and the motor power supply on the left. The entire system, including the microscope, is controlled by a computer (right side).**

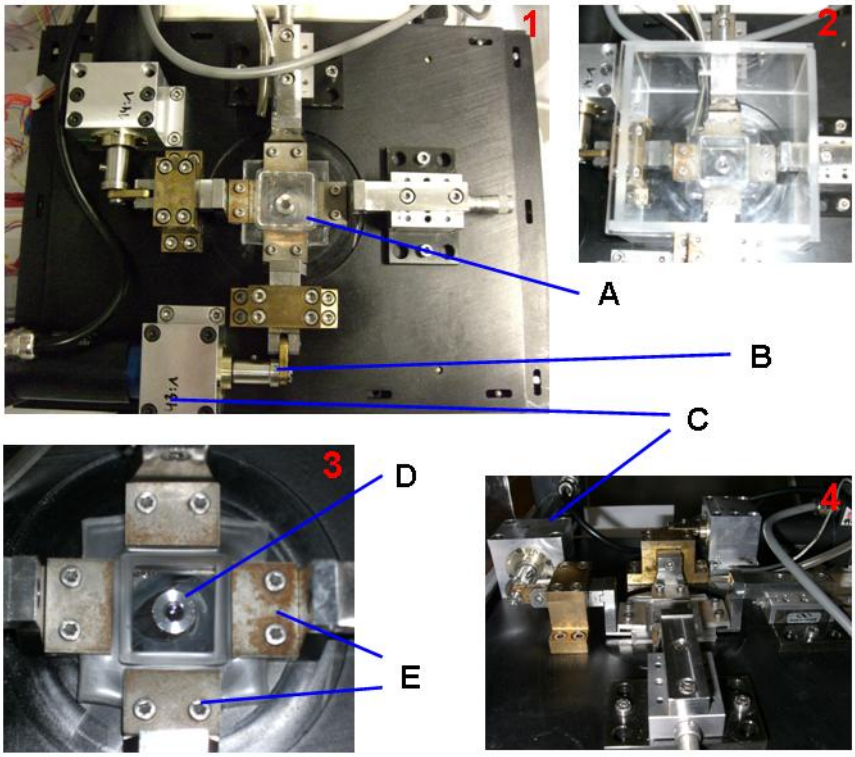


**Fig. 2.6: The stretching device. Panel 1: The entire device including the two motors. Panel 2: Small Plexiglass chamber to stabilize the $CO_2$ atmosphere. Panel 3: Close-up view of the clamped stretching chamber. Panel 4: Side view of the set-up. A: Clamped stretching chamber with cover. B: Eccentric disc. C: Motors with gear. D: 10x objective. E: Clamps.**

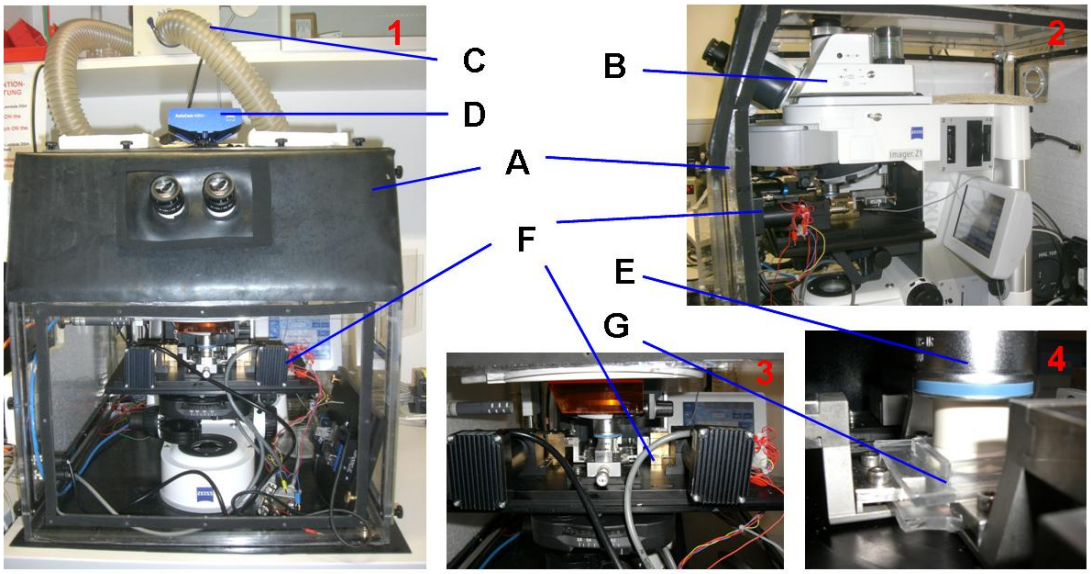


**Fig. 2.7: The stretching device mounted on an upright Zeiss Imager Z1 microscope: Panel 1: the entire device, enclosed in a climate chamber constructed in-house. Panel 2: Side view of the chamber, with the microscope and the experimental set-up. 3: Close-up view of the stretch device on the microscope stage. Panel 4: Close-up view of the stretching chamber with the 63x water immersion objective. A: Climate chamber. B: Upright microscope Imager Z1. C: Heating unit. D: Camera. E: Water immersion objective. F: Stretching device. G: Stretching chamber with cover.**

### 2.1.2 The stretching chamber

The stretching chamber consists of a quadratic (45mm x 45mm) elastic silicone substrate with an inserted chamber for culturing cells. The entire chamber is flexible and deformable (Fig. 2.9). The chamber for culturing cells is 20mm x 20mm in area, including the observation area, and may be filled with 2ml cell culture medium.

The stretching chambers were made by a Plexiglass mold constructed in-house (Fig. 2.8) and a silicone elastomer [Poly(di)methylsiloxan] PDMS ( Sylgard (184), Dow Corning, Midland, MI, USA). PDMS is a transparent, two-compound, nontoxic elastic silicone (its physical properties are described in Table 2.1). PDMS is commonly used for many cell culture applications (Lee *et al.* 2004; Neidlinger-Wilke *et al.* 1994).

To locate certain positions of the cell plating area under the microscope, markers were placed in the central region of the cell plating area. The markers consisted of small dots which delineate the center of the cell plating area. The stretching chambers must be covered, to avoid evaporation of the cell medium. Therefore, a cover designed in-house which enables $CO_2$ exchange, was used for experiments involving the inverted microscope. In the case of the upright microscope, a flexible PDMS membrane with a hole for the objective was used as a cover. Furthermore, the cover also protected against contamination with bacteria.

| | |
|---|---|
| **Young's modulus, E** | **1.2 – 2.0 MPa** |
| **Tensile strength, sm** | **6.2 MPa** |
| **Durometer hardness** | **50 Shore A** |
| **Viscosity, h** | **3900 mPa·s** |
| **Specific gravity, r** | **1.03 g/cm³** |
| **Thermal conductivity, k** | **0.18 W/(m·K)** |
| **Linear coefficient of thermal expansion, at** | **310·10-6 1/K** |
| **Dielectric constant, e** | **2.65** |
| **Refractive index, nr** | **1.430** |

**Table 2.1: Physical properties of Dow Corning Sylgard 184 PDMS.**

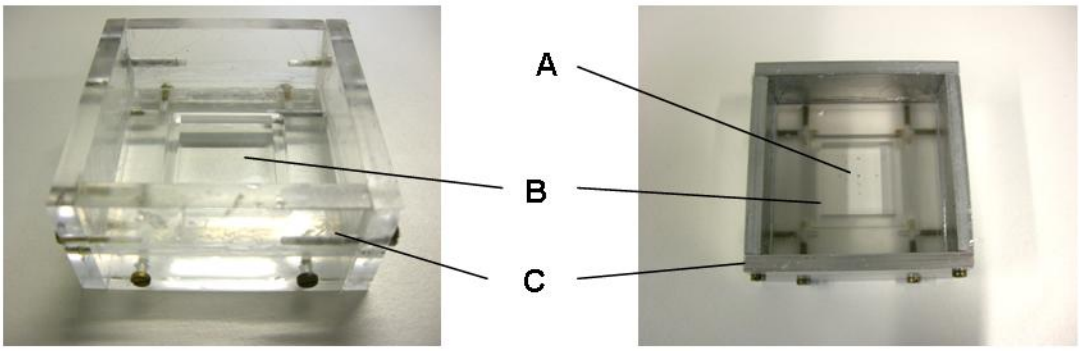


**Fig. 2.8: Molding chamber: The molding chambers are made of Plexiglass. The side part (C) is removable, to make the peeling-off of the PDMS chambers easier. The center (B) of the mold has to be clear and smooth in order to obtain a flat observation area. In the center are markers (A) which are later seen in the PDMS chamber. These markers make it easier to locate specific positions under the microscope.**

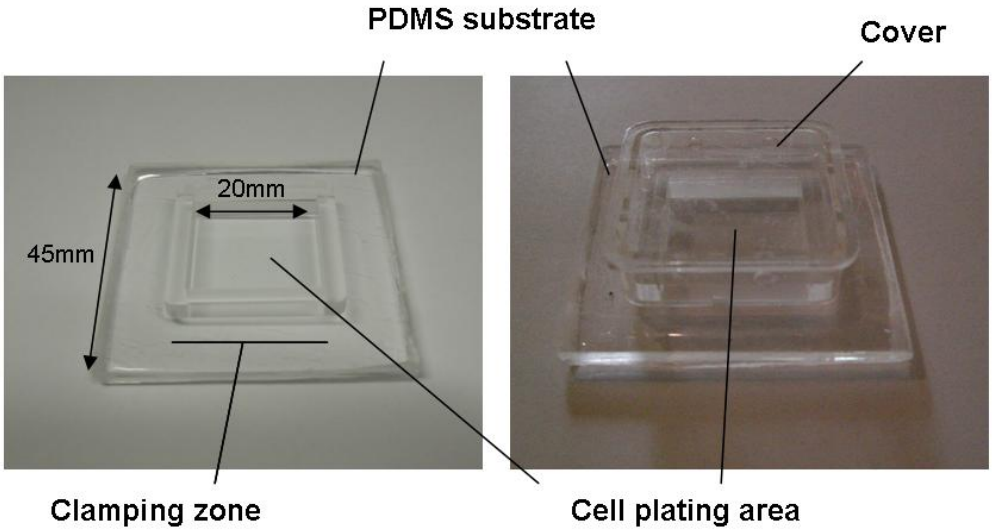


**Fig. 2.9: Stretching chamber: The entire chamber is made of PDMS. In the center of the chamber lies the cell culturing chamber and observation area. The chamber may be filled with 2ml cell culture medium. The chamber can be clamped at the edges to the stretching device. To avoid evaporation and contamination with bacteria, the chamber is covered.**

The suitability of PDMS for cell stretching experiments was already shown in studies by Neidlinger-Wilke (Neidlinger-Wilke *et al.* 1994). We mixed PDMS at a 10:1 ratio of the two compounds, the elastomer (basic compound) and the cross-linker. After mixing the two compounds and casting the PDMS, the molds were put into an exsiccator with a low-pressure atmosphere, to eliminate air bubbles. For the curing process, the mold was placed in an oven overnight (12 h) at 65°C. After the heating process, one can peel away the stretching chambers from the mold. To ensure that the chambers were of uniform thickness, each chamber was made from 3 g PDMS.

Before using the stretch chambers they must be sterilized. The chambers were sterilized by washing them for 60 s with 70% ethanol. Subsequently, the chambers were washed two times with PBS to make them usable for cell culture.

Cells do not adhere very well to PDMS surfaces. Therefore, before seeding the cells, the chambers were incubated with 1ml of 5 µg/ml fibronectin (see Section 2.2.1.1) solution overnight (12 h), to absorb the fibronectin on the surface of the stretching chambers. The minimum concentration of the fibronectin solution is cell type specific and has to be examined before the stretching studies (for cells in this study: 5 µg/ml).

### 2.1.3 Calibration and specification of the stretching system

Wrinkles on the PDMS surface can influence cellular behavior. To avoid these wrinkles, the chambers were pre-stretched with the fixing clamp. To proof that no wrinkles were produced, PDMS was cast into the stretching chambers in relaxed and stretched conditions. After the cross-linking process (overnight, at 40°C) a copy of the surface of the stretching chamber could be obtained. The topography of the copies of the stretching chamber surface could then be investigated by atomic force microscopy (AFM) and possible wrinkles in the center region of the substrate could be discovered.

The elasticity of PDMS was previously measured (Carrillo and L. & Puttlitz 2005), but the breaking elongation of the custom-made stretching chambers has still to be determined. Therefore, a stretching chamber was clamped from all sides, and stretched by increasing the stretch amplitude until it broke. The same experiments were carried out under cyclic strain conditions (frequency = 5 $s^{-1}$). The chambers were stretched for 24 hours to see if material fatigue occurred during this period. This time the period is three times longer than the stretching period during the experiments. Several calibration tests were made with different stretching amplitudes, until the stretching chamber broke.

Further mechanical characterization of the stretching chambers was undertaken by measuring the strain distribution in the chambers in both the relaxed and stretched states.

For this measurement, the displacement of dirt on the PDMS surface, or polystyrene beads which are molded together with the PDMS, were observed. Phase-contrast images of the surface in the relaxed and stretched states were taken and the displacement of the markers (dirt or polystyrene beads) were measured by an image analysis program (ImagePro Plus) in the relaxed and the stretched state. As markers, four points on the edges of the pictures (polystyrene bead or dirt, were marked (Fig. 2.10). The distances between all markers could be measured and compared with each others with and without stretch. In our case we only measured the diagonal points, meaning the distance between the point on the upper left side and on the lower right side, and the distance between the point on the lower left side and on the upper right side were then measured.

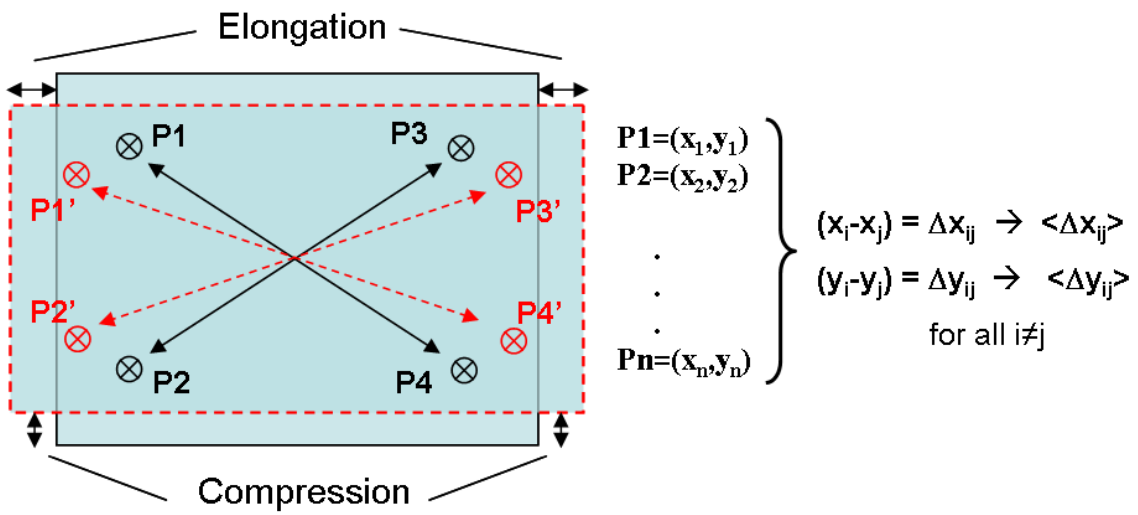


**Fig. 2.10: Schematic drawing of the measurement of the strain field. Points (P1-P4) at the edges of the observation area in the relaxed (black) and the maximum (dashed red) position of stretch were marked. Δx and Δy were measured and compared, both without and with stretch. The mean values were then determined.**

Fig. 2.11 gives phase-contrast images demonstrating schematically the measurements of elongation along the x-axis and compression along the y-axis. The distance between P1 and P4, and the distance between P2 and P3, were measured in the relaxed state and in the maximum stretched state (P1'-P4'), and compared, as shown in Fig. 2.10.

The percentage of change was evaluated by means of the definition of strain $\varepsilon = \Delta l / l_0$, where $l_0$ represents the length in the relaxed state, and $\Delta l$ represents the change in the length in the maximum stretch state. The mean value of the different measurements was caclulated, and listed for different stretch amplitudes (1%, 2%, 6%, 8%, 12.5%, and 15%; Tables 3.1.1 and 3.1.2).

Furthermore, it is not only necessary to know whether the strain field in the observed area is a homogenous distributed strain, it is also important to know if the applied strain is transferred to the cells. Therefore, the cells were marked and measured both prior to and at the maximum stretch (Fig. 2.11). The results were then compared to those of the measured strain field.

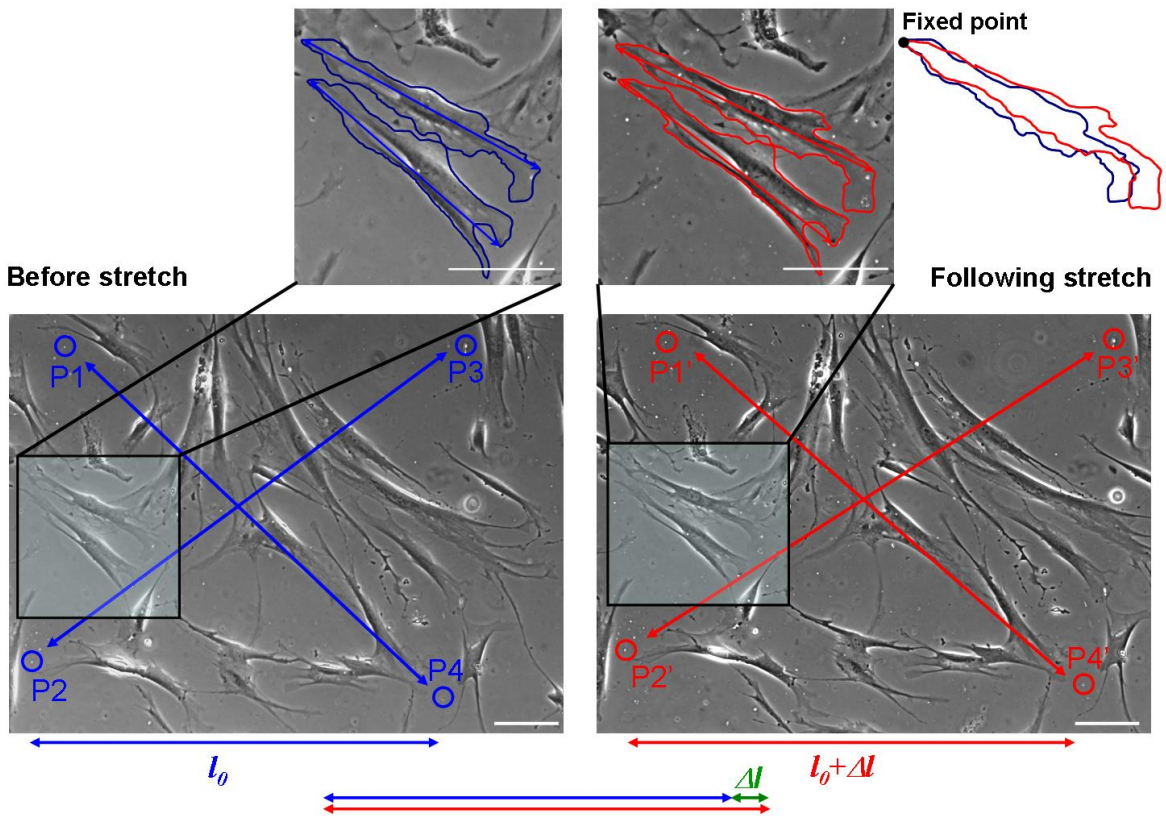


**Fig. 2.11: Measuring the strain field. Images were acquired both before and following stretch. Then polystyrene beads, or dirt on the substrate, were used as markers (P1 – P4). The distance between P1 and P4 and P2 and P3 was measured. The distances yield a component in both the x and y directions. The distances before (blue) and after (red) stretch were determined, and compared to the amount of theoretical expected strain. The strain was evaluated by measuring $l_0$ *and* $\Delta l$. Cells adhering to the substrate were also investigated. They were encircled before (blue) and following (red) stretch; differences along the x- and y- axes of the cells were compared, both before and following stretch. On the upper right side is a comparison of a cell before (blue) and following (red) stretch. At the top, images of a cell before (blue) and following (red) stretch, may be compared.**

## 2.1.4 Life-cell imaging during the stretching experiments

To observe cells by means of phase-contrast microscopy, the stretching device is mounted on a Zeiss Axiovert 200M microscope (Fig. 2.5). The microscope is motorized, and can be controlled by Zeiss AxioVision 4.6 software. The parts of the microscope is surrounded by a climate chamber (Zeiss) which allows control of both the temperature and the percentage of $CO_2$ in the atmosphere inside the chamber. In our experiments, the conditions used for live cell research within the chamber were 37°C and a 5% $CO_2$ humid atmosphere unless otherwise specified.

To observe cells with YFP-labeled paxillin, the device was mounted on an upright microscope (Zeiss Imager Z1; Fig 2.7). The upright microscope was surrounded by a climate chamber, as described.

We used several objectives. On the inverted microscope, either 10x, 20x or 40x long distance objectives were used. For the experiments with the upright microscope, 20x, 40x or 63x water immersion objectives were used.

During an experiment, the stretching chamber with adhering cells was clamped to the stretching machine in the relaxed state. This means that the cyclic strain was set to be always tensile with a magnitude equal to $(A/2(\sin(2\pi f t+\lambda)+1)$, thus causing no compression in the stretch direction. To avoid wrinkles on the substrate surface, the chambers were pre-stretched. The experiments began two hours after clamping and pre-stretching, so that the cells could accommodate to the pre-stretch and return to a relaxed state. In the next step of the experiment, the cyclical stretch was switched on and after a certain time, the stretching machine was stopped at the position (start position) at which the substrates are relaxed. An autofocus routine program was then commenced, and an image was acquired. The image was saved on the computer and the stretch began again until the next image was acquired. In most of the experiments, the time interval between two images 50 seconds. This interval varied, depending on the stretching frequency or the required time resolution of the experiment.

Various cameras were used for the different experiments. A PCO sensicam QE (Kelheim, Germany) was mounted to the Zeiss Axiovert 200M microscope. This camera could be controlled by ImageProPlus software. A Zeiss AxioCam MRm, or a Cascade II (Roper Scientific), could be used with the system on the upright Zeiss ImagerZ1 microscope. Both of these could be controlled by Zeiss AxioVision version 4.6 software. The highly sensitive EMCCD (electron multiplying charge-coupled device) Cascade camera was used for fluorescent microscopy with low light intensity samples.

In addition, our experimental set-up enables control of the rate of either the stretch or the relaxation turn. That means that we could employ a specific velocity $v_1$ from the zero position to maximum strain, and a different velocity $v_2$ when returning from maximum strain to zero.

### 2.1.5 Software used to control the system

To perform the experiments, different steps had to be controlled by software. Fig. 2.11 shows the flow chart of the software.

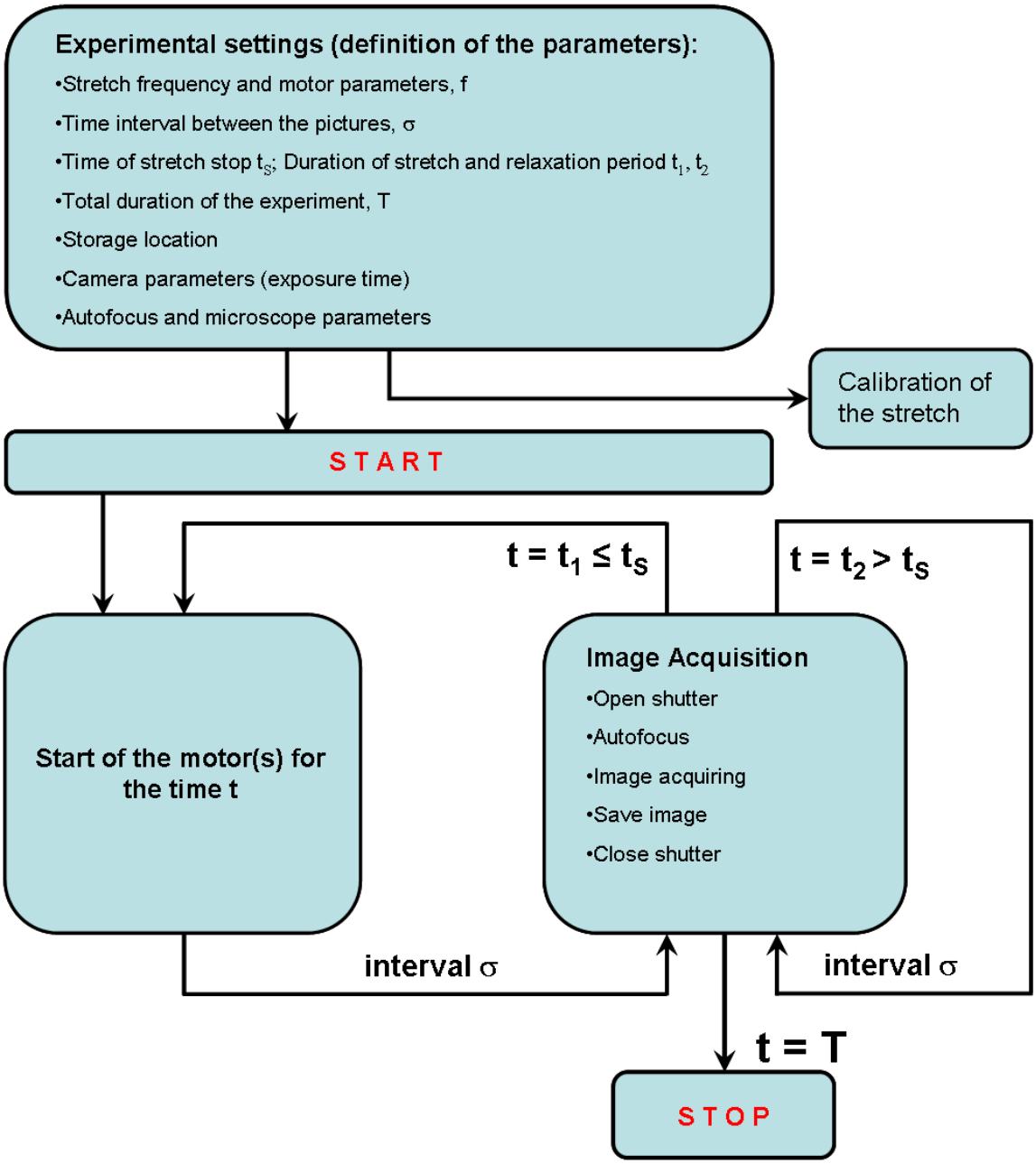


**Fig.2.11: Flow chart of the software developed inhouse to control the stretching device.**

In terms of the software, there were two different ways to control the experiments. For one type of experiments, ImageProPlus (Fig. 2.12) was used with a macro using the ImageProPlus macro language. This macro controls the experiment in a simple manner. The microscope and the stretching machine were controlled via the serial port of the computer. With this software,

it is possible to change the stretch frequency (f), the duration of the stretch ($t_1$), the duration of the experiment (T), including the observation time after stretch ($t_2$), and the time interval between the two images ($\sigma$). It is also possible to control and set the autofocus routine.

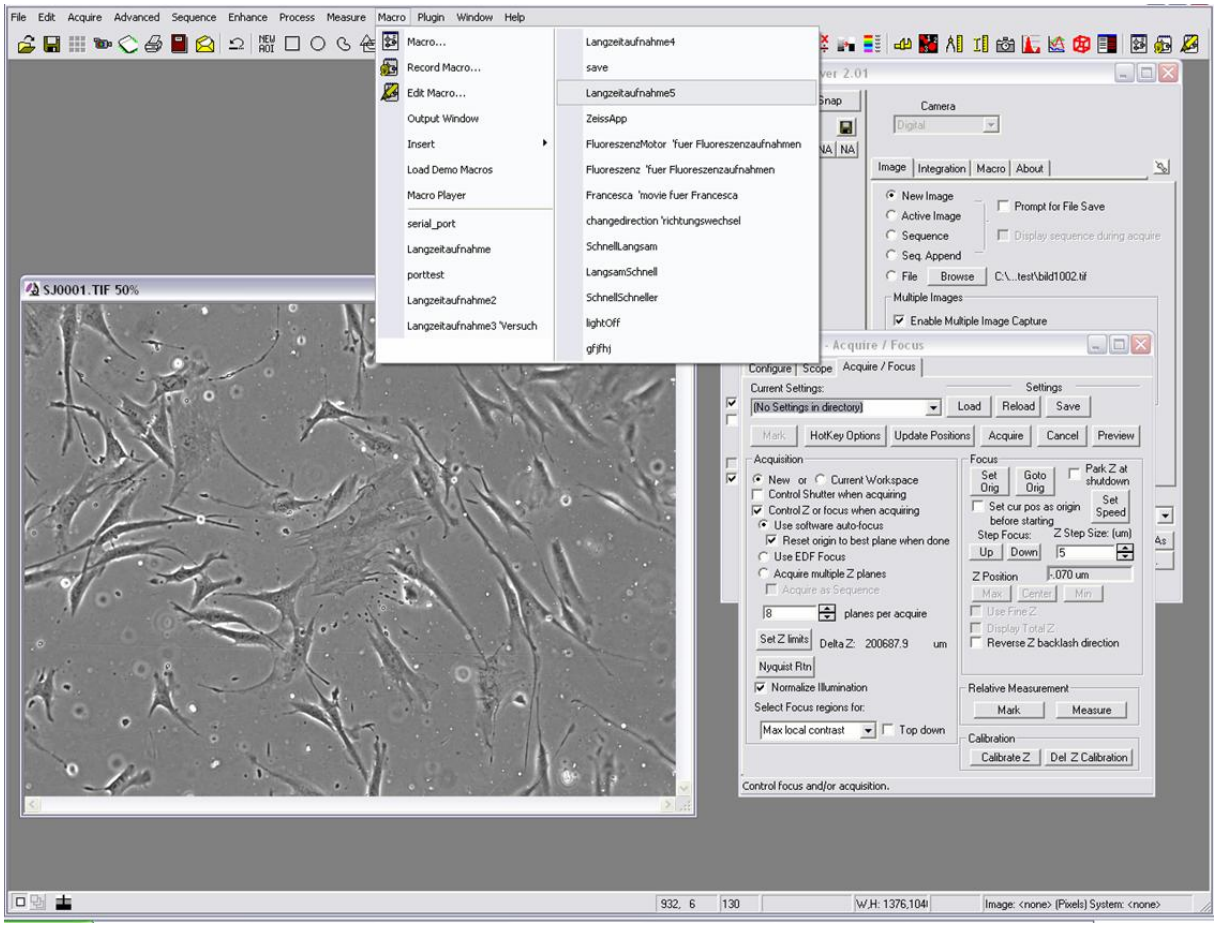


**Fig. 2.12: Layout of the ImageProPlus software. The microscope is controlled by the ScopePro software, and the camera (PCO Sensicam) is also controled by the ImageProPlus software. The experimental set-up can be controlled via self-programmed macros).**

To create more sophisticated experiments, and for better usability, a Visual Basic for Applications program was developed. A self-programmed Visual Basic plug-in was embedded in the AxioVision software (Zeiss; Fig. 2.13) of controlling the microscope. Using this software, one can also vary the stretch frequency, the duration of the experiment, the interval between the images, and the calibration of the autofocus. Furthermore, one can obtain several images during a single observation, with different microscope settings. Thus, for example, it is possible to take phase-contrast images and fluorescence images in the same experiment, or fluorescence images with two different dyes. The Visual Basic plug-in enables the use of all features of the Zeiss AxioVision 4.6 software.

Before starting the experiment, it is necessary to measure the applied strain of the elastic membrane. Therefore, the Visual Basic plug-in has a function which enables the acquisition of images when the substrate is in the relaxed state, as well as at maximum stretch.

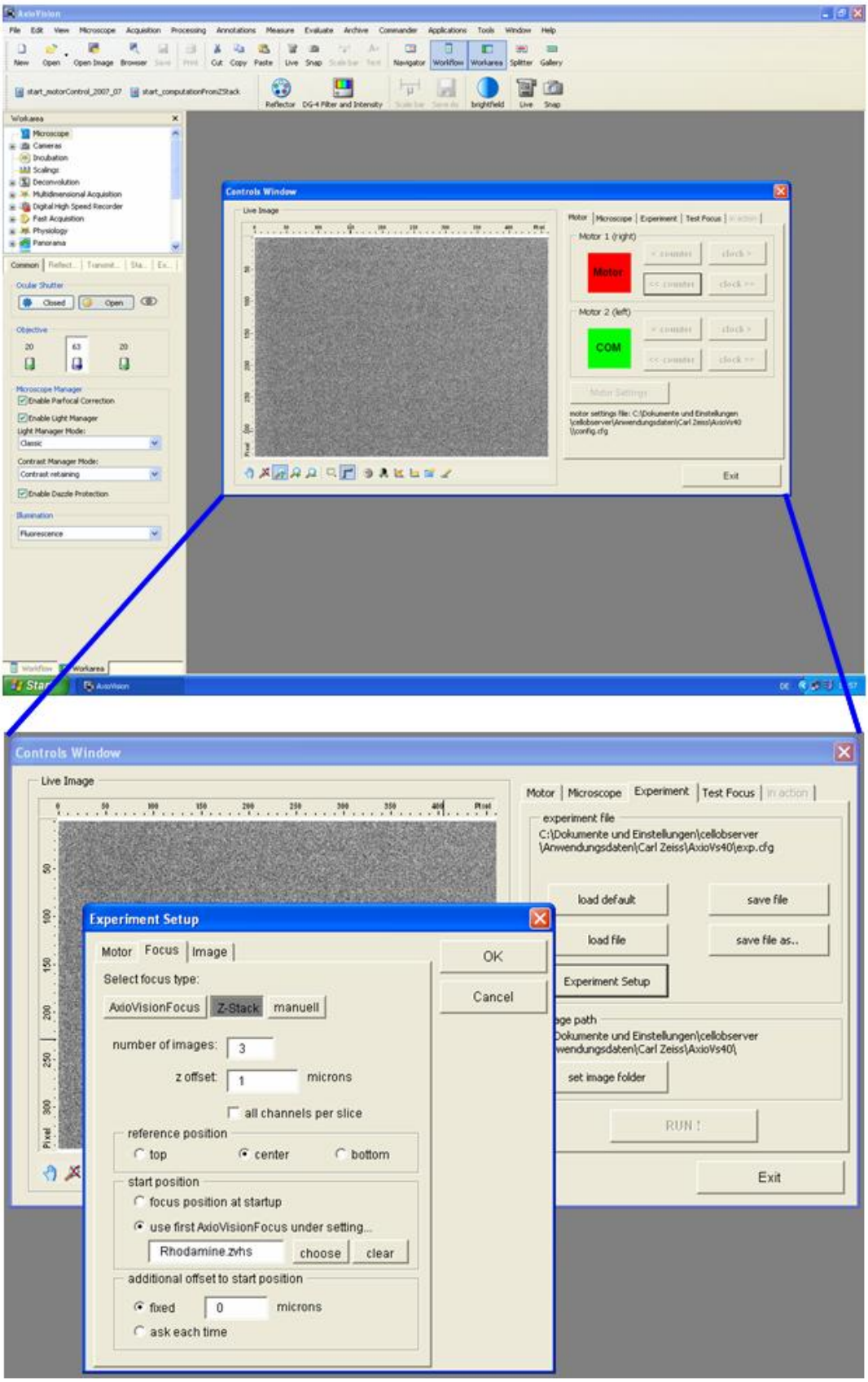


**Fig. 2.13: Screenshot of Zeiss Axiovision 4.6, with self-programmed software. A Visual Basic program for controlling the experimental set-up was included with the Axiovision software. The window in the middle depicts the self-made plug-in. On the lower side is a detailed view of the software for the experiment.**

# 2.2 Cell culture

## 2.2.1 Materials and chemicals

### 2.2.1.1 Buffers, chemicals, and media

Buffers were prepared with Millipore water. All solutions and glassware were sterilized by autoclaving (Varioklav, H+P, Oberschleißheim, Germany) or sterile filtration, if they were not already sterile from the manufacturer.

**Dulbecco's Modified Eagle's Medium DMEM (1x):** containing 1000 mg/L glucose, 4 mM L-glutamine and 110 mg/L sodium pyruvat. (GIBCO; Karlsruhe, Germany).

**Mesenchymal Stem Cell Basal Medium (Poietics MSCGM BulletKit):** containing 440 ml MSCGM: 50 ml Mesenchymal Stem Cell Growth Supplement; 10 ml L-Glutamine; 0,5 ml Penicillin-Streptomycin. (LONZA; Walkersville, MD, USA).

**Phosphate-buffered saline (PBS) tablets**: consisting of 0.14 M NaCl; 0,01 M $PO_4$ buffer; and 0,003 M KCl. Each 5 g tablet was dissolved in 500 ml distilled water. (GIBCO).

**Fetal Bovine Serum (FBS):** Origin: EU-Approved (South America). (GIBCO).

**Trypsin-EDTA :** 0,05% Trypsin, and 0,53 mM EDTA (Ethylendiamintetraacetat). (GIBCO).

**Paraformaldehyde (PFA) (**Sigma), 3.7% in PBS.

**Glutaraldehyde** (Sigma), 3% in PBS.

**Fibronectin powder from human blood plasma** (Sigma) dissolved in PBS**.**

**PenStrep Solution** (Sigma): 10000 U/ml penicillin, 10000 µg/ml streptomycin.

**Fibronectin staining kit:** Alexa568 protein labeling kit (Invitrogen; Karlsruhe, Germany)

#### 2.2.1.2 Lab materials

For the cell culture, plastic pipettes (Greiner, Germany) and Pasteur pipettes (Karl Hecht Glaswaren, Germany) were used. Plasticware such as Petri dishes or cell culture flasks were provided by various companies (Greiner, Germany; Nunc, Denmark; BD (Becton, Dickinson and Company) Bioscience, USA; Eppendorf, Germany).

#### 2.2.1.3 General lab equipment

**Centrifuges:** Hermle Z 300; Wehingen, Germany.

**Incubator:** Binder; Tuttlingen, Germany.

**Microscopes:** Axiovert 200M, Axiovert CL40, Imager Z1; Zeiss, Jena, Germany.

**Oven:** Binder; Tuttlingen, Germany.

**Sterile working bench:** Herasafe; Heraeus, Hanau, Germany.

**Vortexer:** Heidoloph Reax top; Schwabach, Germany.

**Waterbath:** Memmert, Schwabach, Germany.

## 2.2.2 Cultured cell types

Different types of fibroblasts were used in our experiments. Most of the experiments were carried out using a rat embryonic fibroblast cell line (REF52wt) (Franza *et al.* 1986) and primary human fibroblasts (HDF). The REF52wt cells were kindly provided by Benny Geiger from the Weizmann Institute, Rehovot. The fluorescence experiments were performed, using stable transfected REF cells (see Section 2.2.6, below) (Zamir *et al.* 1999). Human fibroblasts from donors of different ages were used. The approximate ages of the cell donors ("young", between 11 and 32 years; "old" between 43 and 54 years) are listed in Table 2.2 and Table 2.3.

| NAME | ORGANISM | TISSUE | DESCRIPTION | CULTURE MEDIA | REFERENCE |
|---|---|---|---|---|---|
| REF52 | Rat | Embryo | Fibroblast | DMEM-complete | Franza 1986 |
| REF52 YFPpaxillin | Rat | Embryo | Fibroblast | DMEM-complete plus G418 | Zamir,1999 |
| HDF 1 | Human | Dermis | Fibroblast (young donor) | DMEM-complete | Kaufmann,2001 |
| HDF 2 | Human | Dermis | Fibroblast (young donor) | DMEM-complete | Kaufmann,2001 |
| HDF 3 | Human | Dermis | Fibroblast (young donor) | DMEM-complete | Kaufmann,2001 |
| HDF 4 | Human | Dermis | Fibroblast (old donor) | DMEM-complete | Kaufmann,2001 |
| HDF 5 | Human | Dermis | Fibroblast (old donor) | DMEM-complete | Kaufmann,2001 |
| HDF 6 | Human | Dermis | Fibroblast (old donor) | DMEM-complete | Kaufmann,2001 |
| hMSC | Human | Human bone marrow | Human mesenschymal stem cell | MSCBM-complete | Lonza technical sheet |

**Table 2.2: List of cells used in our experiments.**

### 2.2.3 Maintenance of fibroblasts in culture

To avoid contamination, all the steps involving eukaryotic cells were performed under a sterile hood, using sterile techniques and materials. All cells were maintained in DMEM (DMEM complete with 2mM L-Glutamine; GIBCO) supplemented with 10% FBS (GIBCO). The cells were cultured in an incubator (Binder) at 37°C and a 5% $CO_2$ humid atmosphere. The media was changed every 2 days. After the cells had reached a confluent state, they were split. For splitting, they were washed with sterile PBS and then released with a trypsin-EDTA 2.5% (GIBCO) solution for 5 min. After diluting in 5 ml DMEM medium, they were centrifuged at 750 rpm for 6 min. The cell pellet was then suspended in the media, and cells were plated again in cell culture flasks (Nunc).

### 2.2.4 Primary cell cultures (human fibroblasts)

Primary human dermal fibroblasts (HDF) from donors of varying ages were kindly provided by Dr. Dieter Kaufmann (Department of Human Genetics, University of Ulm) (Kaufmann *et al.* 2001). These fibroblasts were cultured in complete medium (DMEM) and used between passage 4 and 16. The age of the fibroblasts is indicated in Table 2.3 which also describes the tissue source from which the cells were extracted.

| NAME | DATE OF DONOR BIRTH | DATE OF CULTIVATION | AGE OF DONOR AT EXTRACTION | TISSUE |
|---|---|---|---|---|
| HDF 1 | 1961 | 1993 | 32 (young) | Human foreskin |
| HDF 2 | 1969 | 1992 | 23 (young) | Human foreskin |
| HDF 3 | 1981 | 1992 | 11 (young) | Human foreskin |
| HDF 4 | 1939 | 1989 | 50 (old) | Neck dissection |
| HDF 5 | 1941 | 1994 | 43 (old) | Eyelid |
| HDF 6 | 1939 | 1993 | 54 (old) | Eyelid |

**Table 2.3: Primary human fibroblasts with different donor age. (provided by Dr. Dieter Kaufmann, University of Ulm) (Kaufmann *et al.* 2001).**

### 2.2.5 Human mesenchymal stem cells (hMSC)

For the investigations involving the impact of cyclical stretch on stem cells, Poietics™ human mesenchymal stem cell systems were used. The cells are commercially available from Lonza (Lonza, USA) and are derived from human bone marrow (Minguell *et al.* 2001). Bone marrow contains a population of rare progenitor cells known as mesenchymal stem cells (MSC) capable of replication as undifferentiated cells, or as cells capable of differentiating into bone, cartilage, fat, muscle, tendon, and marrow stroma. Such cells are cultivated with a special medium MSCGM Bullet Kit, containing Mesenchymal Stem Cell Basal Medium, Mesenchymal Stem Cell Growth Supplement, L-Glutamine and Penecillin-Streptavidin, as described in the company manual. For splitting the cells, we used the same splitting protocol as we used for the fibroblasts (section 2.2.3). In this study, we used undifferentiated stem cells, and therefore no differentiation media was added (Engler *et al.* 2006).

### 2.2.6 Fusion proteins and transfection of cells

The REF52 cells expressing YFP(yellow-fluorescent-protein)-paxillin fusion proteins were kindly provided by Prof. Benjamin Geiger (Weizmann Institute of Science, Rehovot, Israel). The paxillin was cloned into pEYFP-C3 plasmid (Clontech, Mountain View, CA, USA) using *Hin*dIII and *Xba*I. REF 52 fibroblast were cultured in DMEM (GIBCO) supplemented with 10% FBS (GIBCO) and 2 mM L-glutamine. Superfect (Qiagen, Hilden, Germany) was used according to the manufacturer's recommendations for stable transfection. The cells were cultured in the media, to which 1 mg/ml G418 (GIBCO) was added for the development of stable and YFP-expressing clones (Zamir *et al.* 1999).

### 2.2.7 Experimental conditions

The cells in culture were trypsinized and, after counting, plated within the self-made adhesive stretching chambers (see Section 2.1.2). The cells were counted by means of light microscopy (10x objective) and a hemocytometer. Two different cell densities were investigated in dependency of the stretching frequency. The standard cell density was 50 cells/mm². For experiments with confluent cell layers a cell density of 100 cells/mm² was used. To avoid bacteria contamination 1% Penicillin-Streptavidin solution was added to the medium. The experiments were performed at 37°C, in an atmosphere of 5% $CO_2$, humidity.

### 2.2.8 Immunofluorescence staining procedure

Cultured cells were washed with PBS at 37°C, and fixed with 3.7% paraformaldehyde (Sigma) for 10 min. Permeabilization was achieved by applying a 0.1 % Triton X-100/PBS solution for 3 min. In order to block the non-specific binding of antibodies, the samples were incubated in a 0.5% BSA (Sigma)/PBS solution. The cells were then incubated for 1 h with the primary antibodies. The non-specifically bound antibodies were removed by washing the samples 3x with PBS. The samples were then incubated with the secondary antibodies for 30 min at ambient temperature.
In this study, rabbit-anti-fibronectin (F3648, Sigma) was used as primary antibody, and goat-anti-rabbit Alexa 568 (A11036, Invitrogen) was used as a secondary antibody. The actin staining was done with Alexa 488 Phalloidin (A12379,Invitrogen) together with the secondary antibody. Both the primary and the secondary antibodies were diluted 1:400 in PBS. The phalloidin was added in a concentration of 1:60.

### 2.2.9 Scanning electron microscopy (SEM)

Cells were prepared for electron microscopy using a the method known as critical point drying (CPD 030 ceitical point dryer; BAL-TEC, Balzers, Liechtenstein). Critical point drying is based on the process of “the continuity of state”, in which there is no apparent difference between the liquid and gas state of the medium used. Therefore, the surface tension between these interfaces is reduced to zero. This continuity of state occurs at a specific temperature and pressure, and results in a density known as the critical point. This condition of zero surface tension can be used to dry biological specimens, thereby avoiding the damaging effects of surface tension. If the cells are air-dried, the evaporation of water molecules can disrupt the cell membrane because of the surface tension of water. For this reason, the water was replaced by ethanol, before the biological specimens were prepared for the SEM. In the critical point dryer, the ethanol was then replaced by liquid $CO_2$. The critical temperature and pressure for $CO_2$ is 31°C and 75 bar, at which point liquid $CO_2$ becomes hypercritical, and the evaporation of this “liquid” leaves the cell membrane and other cell structures unscathed. Following removal of the culture media samples were then fixed in 4% glutaraldehyde in PBS (Sigma) for 15 min; dehydration was achieved by incubating the samples in a series of solutions with a graded ethanol (JT Baker, Phillipsburg, NJ, USA) content, beginning with 50%, and followed with 60%, 70%, 80%, 90%, 96% and, finally, three times 100% ethanol. Each incubation step lasted at least 30 min. Samples were then transferred into a shallow glass dish and placed in the chamber of the critical point dryer which was filled approximately one-third with 100% dry ethanol, and the cap sealed airtight. Once a temperature of 10°C and a pressure of 50 bar was reached, the chamber was

repeatedly emptied of liquid and filled with $CO_2$ (approximately 6–8 times) without uncovering the sample, so that all ethanol was removed. The chamber was then filled to the top with liquid $CO_2$, and heated to a temperature of 40°C and a pressure of 90 bar. Finally, the glass samples were sputter-coated with a 5 nm gold layer in a BAL-TEC MED020 Coating System Sputter, in preparation for SEM imaging.

Images were acquired by a Zeiss Gemini Ultra 55 scanning electron microscope.

# 2.3 Image analyses and evaluation routine

## 2.3.1 Analyzing the phase contrast images

Time-lapse movies of different experiments were made. Images of certain time points were chosen and analyzed. Images taken at time points 0, 250, 500, 1250, 2500, 3750, 5000, 6250, 7500, 8750, 10000, 11250, 12500, 15000, 17500, 20000, 25000, 30000, 32500, 35000, 37500, 40000, 45000, 50000, 55000, 60000 and 65000 seconds were used in most of the experiments. At the beginning of the experiment, the cells react faster to the applied stretch; for that reason, the time interval between the consecutive images is shorter. The stretch is stopped after 30000 seconds; therefore, the interval between images lessens once again, to observe the relaxation of the cells.. It is possible to choose different time points for analysis, theoretically, a time resolution of 50 seconds could be realized.

The phase contrast images could not be analyzed by means of a simple automatic image processing routine, because the images were taken through PDMS, and artifacts or dirt in the PDMS can disturb the automatic analyses. Therefore, the images were edited by a common image software called NIH Object Image, compatible with an Apple MacIntosh computer. The cells were marked by hand. Each marked cell represents a region of interest (ROI) (Fig. 2.14). These ROIs can be analyzed by means of a self-made macro embedded in the NIH software. The macro provides the cell area, the cell perimeter, the cell center and it fits then an ellipse to the ROIs so it is possible to obtain the major and minor axes and the orientation angle of the fitted cell. The data obtained constitute the raw data to be used for the further evaluation.

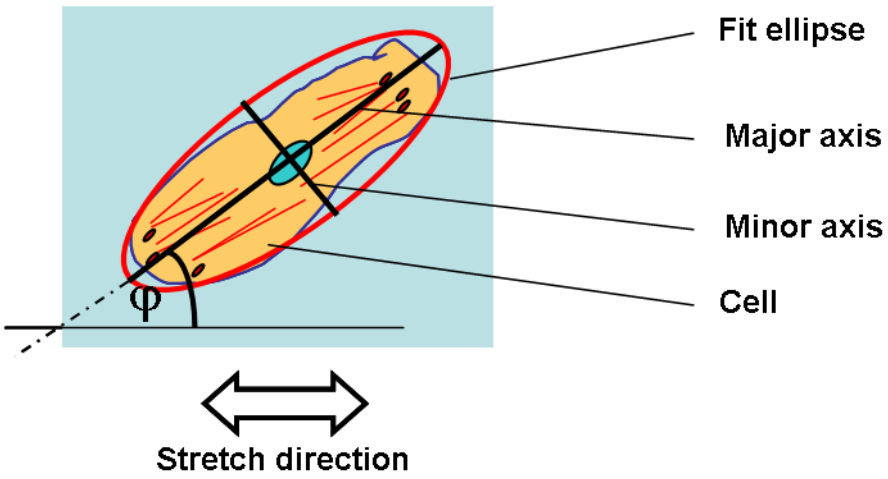


**Fig. 2.14: Measuring a cell. Cells were marked with the image software NIH Object Image. A self-programmed macro was used for analysis of regions of interest (ROI). An ellipse is fitted to a cell (red). In this manner, specific values such as orientation angle in respect to the stretch direction and the major and minor axes of the cell are obtained.**

## 2.3.2 Evaluating the raw data

The data we obtain from the analysis of the phase contrast images can be quantitatively evaluated. The mean value of the cellular orientation, the cell area or the cell elongation for all cells at a certain time point can be determined. The statistical analysis provides the standard deviation of the mean value which corresponds to the error in our results.

### 2.3.2.1 Morphological parameters

Analysis of data yields morphological parameters such as the mean cell area, or the perimeter of a cell. It also provides the major and the minor axes of the ellipse, to which the cell is fitted. The major axis can be divided by the minor axis. The dimensionless result <ε> gives a quantitative value for the elongation of a cell. The higher the value, the more a cell is elongated and a value of 1 corresponds to a perfectly round cell.

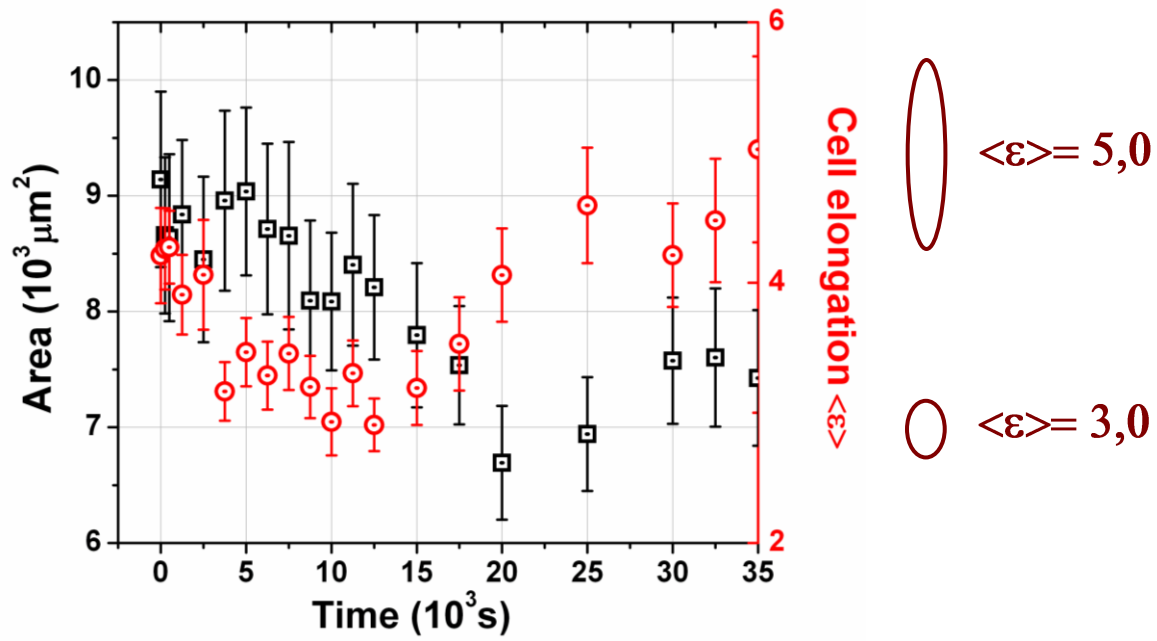


**Fig. 2.15: Example for the quantification of cell morphology. (HDF1, frequency = $2s^{-1}$, amplitude = 8%). Black squares indicate the change in cell area over time, during cyclic stretch. Red circles indicate the change in the cell elongation <ε>. Cell elongation is measured by dividing the major axis by the minor axis of the cell. The higher the resulting value, the more the cell is elongated. A value of 1 means a perfectly round cell.**

The mean values for the area, or the elongation of cells at a certain time point, were determined and plotted (Fig. 2.15). The plot shows the data of morphological change (area and elongation) of a cell over time.

### 2.3.2.2 Orientation of the cells

Cellular behavior during extracellular stimulus can be described with a simple phenomenological mathematical model, as described in other studies (Jungbauer *et al.* 2004; Kemkemer *et al.* 2006; Kemkemer *et al.* 1999; Kemkemer *et al.* 2002). In these studies, a theory of automatic controller was used. The automatic controller describes a cell in macroscopic terms, as illustrated in the information flux diagram (Fig. 2.16). Many processes in the cell can be described with this model. The controler model itself consists of a detection unit which is characterized by the known function *g(φ,signal)* and the reaction unit which is described by the coefficient *k*. The system also requires a feedback loop, in order to compare the actual value of, for example, the cell orientation with the set point. Compared with a cell, the detection unit could consist of signal receptor proteins and the amplifier could be a second messenger. Actin, for example, could be an essential part of the motor unit.

In our case, the controlled variable is the angle of orientation, *φ*, with respect to the stretch direction. The system must be able to measure the cell's actual angle of orientation, with respect to the applied stretch. In the summation unit, the extracellular signal and the feedback signal are compared. The angle- and field-dependence of the detection unit is described by the unknown function *g(φ,signal)*, and the strength of the reaction unit by the coefficient *k*.

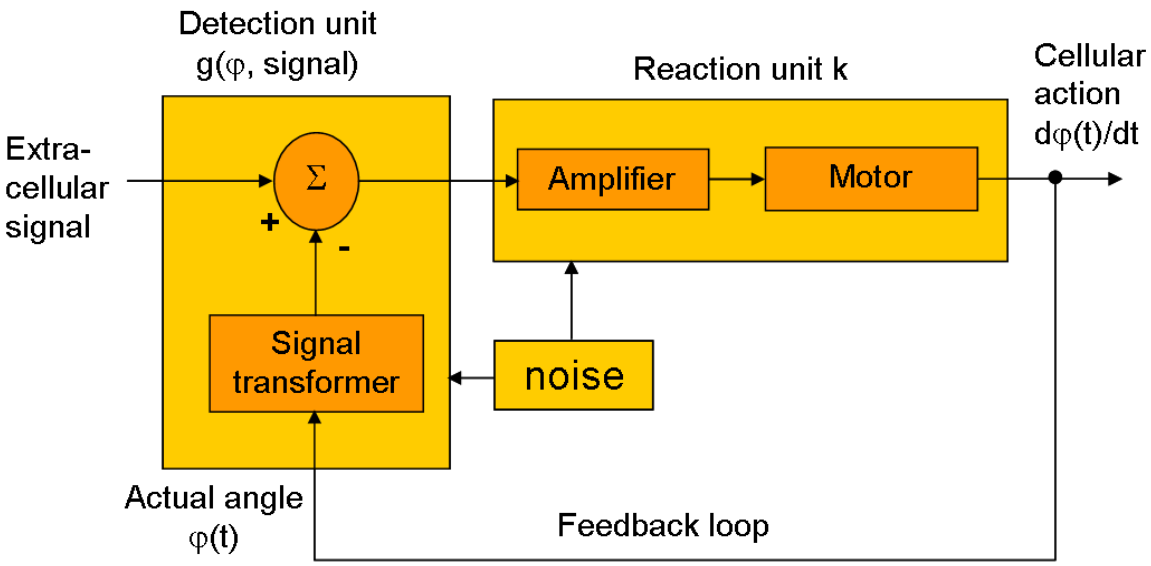


**Fig. 2.16: Schematic drawing of an automatic controller.**

The temporal change of the angle of orientation, dφ/dt, quantifies the cellular reaction. It can be described as follows:

$$d\varphi / dt = -kg(\varphi, signal) + \Gamma(t) \qquad \text{(Eq.1)}$$

The first term on the right side (deterministic part) describes the cellular response to an extracellular signal. The second term (stochastic part, noise) represents a function that must be introduced, since random orientation is observed, in cases of no external signal.
Equation 1 describes the behavior of a single cell, and can be used for simulations. To describe the distribution of an observed variable, for example the orientation angle $\varphi$, it is necessary to transform the Langevin equation into a Fokker-Planck equation. The resulting equation describes the density distribution of the orientation angle of a cell ensemble, and the solution can be compared to experimental results. A special case for the solution is given in Equation 3, in Section 2.3.2.3.

### 2.3.2.3. Apolar order parameter and dose-response curve

To quantify the cell's cellular response to stretching, density distributions *f(φ)*, derived from the Fokker-Planck equation, of the orientation angle and mean values for the order parameter <cos2φ> were calculated from the analysis of the image sequences.
The order parameter is defined as:

$$S = <\cos 2\varphi> = \int f(\varphi) \cos 2\varphi d\varphi \qquad \text{(Eq.2)}$$

Consequently, we should obtain $S$ = 0 if the cells are randomly orientated; $S$ = 1 if they are orientated in parallel and $S$ = -1 if they are orientated perpendicularly to the stretching direction. Fig. 2.17 shows a dose-response curve for the order parameter over time.

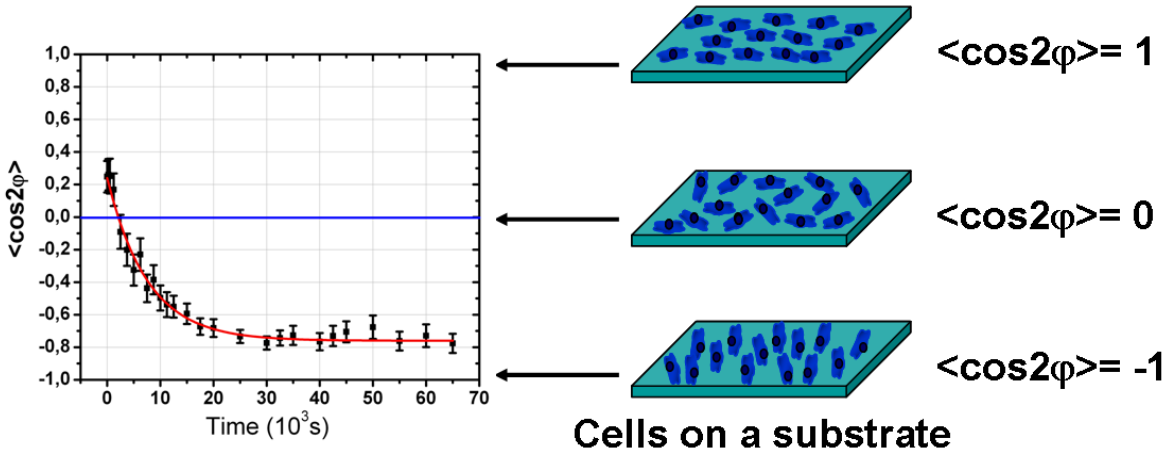


**Fig. 2.17: Example of a quantitative analysis of cellular orientation by the order parameter <cos2φ>. The order parameter is S=<cos2φ>=1, if the cells are orientated parallel to the stretch direction. S=0 if the cells are oriented randomly. S=-1, if the cells are oriented perpendicular to the stretch direction. The graph on the left represents temporal characteristics of the order parameter during an experiment with HDF1 cells (20Hz, 8%, stretch stopped after 30000 seconds). The time characteristic was fitted to a mathematical model of "automatic controller". From this fit, one may obtain the characteristic time τ for cellular reorientation.**

The aforementioned procedure, based on a stochastic differential equation (Eq.1), leads to the following expression, used to evaluate the time dependence of the order parameter:

$$\langle\cos 2\varphi\rangle(t) = \langle\cos 2\varphi\rangle_{st2} + [\langle\cos 2\varphi\rangle_{st1} - \langle\cos 2\varphi\rangle_{st2}]e\text{-}(t/\tau)+\ldots \qquad \text{(Eq. 3)}$$

This equation indicates that, starting at a steady state orientation $\langle\cos 2\varphi\rangle_{st1}$, a new steady orientation state $\langle\cos 2\varphi\rangle_{st2}$ is reached, with a characteristic time τ, describing the dynamics of cellular reorientation. In our experiments, the characteristic time τ was determined by matching Eq. 3 to the experimental data via a least-square fit, using Origin Lab software.

This characteristic time τ gives a value for the duration of the orientation process during the cyclic strain. It describes the time until the value <cos2φ> reached the value of 1/e (approximately 63% of the maximum orientation).

For the evaluation of the maximum orientation $\langle\cos 2\varphi\rangle_{MAX}$, the last three time points before the stretch was disabled, were analyzed. The average of these three values results in the value representing the steady state of the maximum orientation.

For calculations and analysis of the data, Microcal Origin 7.0 software (Microcal, Northampton, USA) was used.

## 2.4 Parameters of the stretching experiments

The parameters of the stretching experiments can be varied in different ways. These parameters include values used to analyze the raw data, or it can be parameters which can be used to change the experimental set-up. In Table 2.4, the possible variations of the different parameters are listed.

| Analyzed parameters | Variable experimental parameters |
|---|---|
| • Determination of the characteristic time $\tau$ of the reorientation process, using a phenomenological mathematical model.<br>• Evaluation of the maximum of cellular orientation<br>• Determination of the response lag times.<br>• Evaluation of the cell morphology. Investigations of the change of the cell elongation and the cell area during cyclical stretch.<br>• Evaluation of the cell divisions<br>• Observation of the cells after stopping the stretch | • Stretch frequency *f*.<br>• Stretch amplitude *A*.<br>• Cell types.<br>• Cell density.<br>• Stretch direction.<br>• Stretching rate.<br>• Adhesive micro-pattern on the stretching substrates.<br>• Phase-contrast or fluorescence microscopy. |

**Table 2.4: Different changeable parameters of the experiments, sub-divided in different parameters of the data analyzes and in parameters of the experimental setup.**

# 2.5 Structuring the PDMS surface by micro-contact printing (µCP)

To pre-orient cells with respect to the stretch direction, cells are only allowed to adhere to certain adhesion islands. For this purpose, the common method of microstructuring was used (Chen *et al.* 1998;$_{H}$ Ostuni and Whitesides 2000; Weibel *et al.* 2007). The PDMS surface was made totally non-adhesive via spin coating star PEG (polyethyleneglycol), as described by Gasteier (Gasteier *et al.* 2007). StarPEG is a starlike prepolymer with arms on PEG basis and reactive isocyanate endgroups. Lines of different sizes as cell-adhesive islands were stamped on the passivated star PEG layer by the micro-contact printing (µCP) of fibronectin. The passivation of the surface was verified following a stretching for 10 hours.

## 2.5.1 Fabrication of the master substrates by photolithography

The stamps for the µCP were created by the commonly used method of soft photolithography (Xia and Whitesides 1998). Master substrates were fabricated as shown in Fig. 2.20. Silicon wafers (ChrysTec, Berlin, Germany) were cleaned for photolithography with isopropanol and Millipore water, and dried. A photoresist layer (AZ1505, Microchemicals, Ulm, Germany) of 1.0 µm height was spin coated (Convac, Wiernsheim, Germany) on the wafer. The photoresist was then illuminated (3-5 sec) with UV light through a lithography mask. The shapes on the mask depended on the desired pattern and could consist of lines, circles or ellipses. Fig. 2.18 shows a photolithography mask with lines of different width and different spacing in between. Fig. 2.19 shows a silicone wafer spin-coated with photoresist AZ1505, and a microstructured silicone wafer.

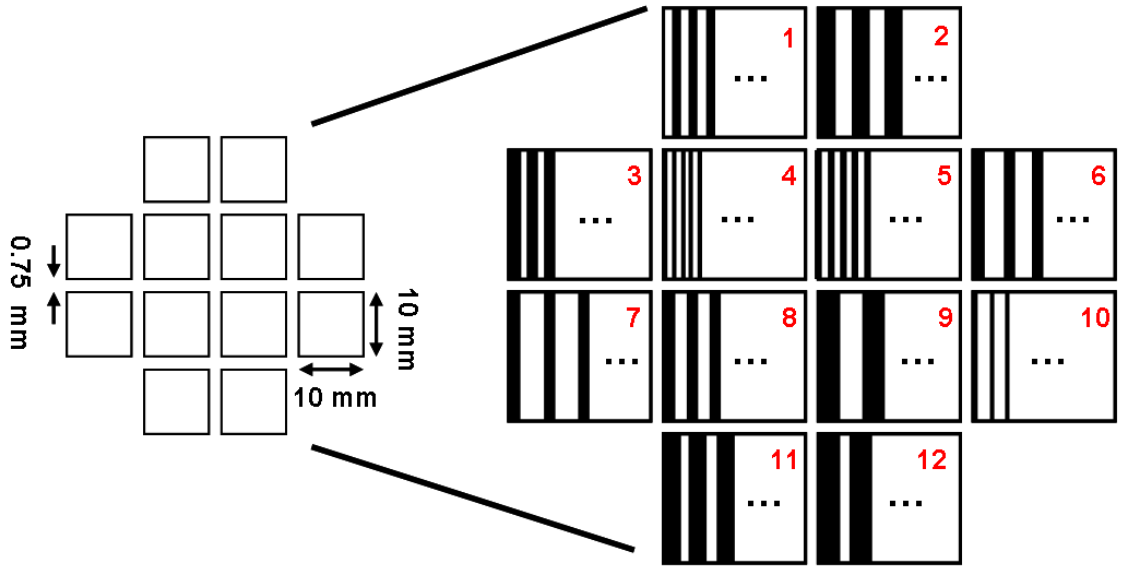


| Field | 1 | 2 | 3 | 4 | 5 | 6 | 7 | 8 | 9 | 10 | 11 | 12 |
|---|---|---|---|---|---|---|---|---|---|---|---|---|
| **Line width (µm)** | 4 | 8 | 5 | 2 | 3 | 5 | 5 | 5 | 10 | 2 | 8 | 10 |
| **Spacing (µm)** | 4 | 8 | 2 | 2 | 3 | 8 | 10 | 5 | 10 | 5 | 5 | 5 |

**Fig. 2.18: Scheme of a photolithography mask with lines of varying widths.**

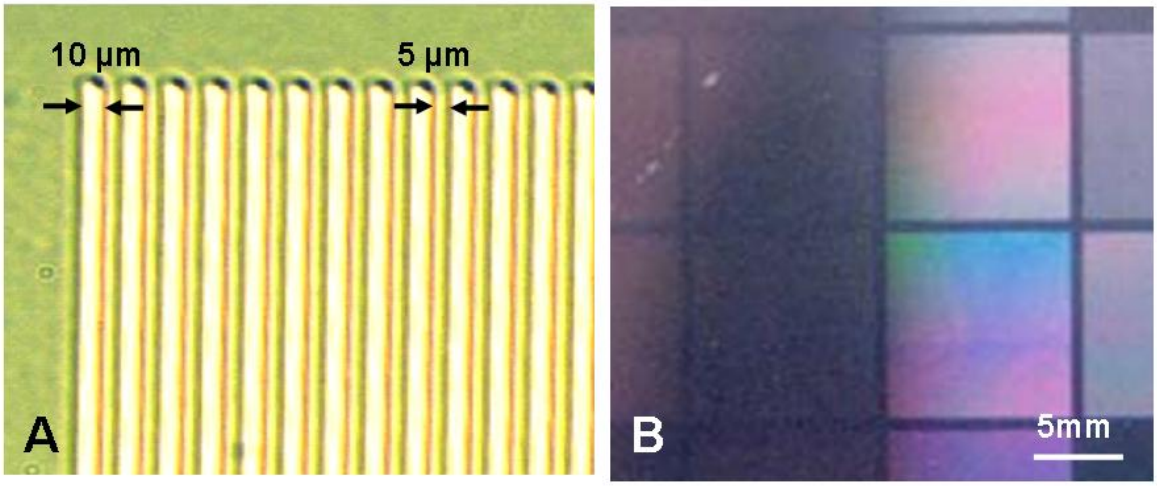


**Fig. 2.19: A: Picture of photoresist (AZ1505) lines on a silicone wafer. B: Picture of the central region of a wafer with different fields of varying line widths**.

The illumination of the resist was carried out with a Suess MJB3 and MJB4 mask aligner (München, Germany). Afterwards, the resist was developed in a developer solution and a line pattern was transferred onto the silicone wafer. The wafer was baked a second time, in order to make the photoresist stable. Before the wafers could be used as molds for the PDMS stamps, the wafers underwent silanization to prevent damage to the microstructure, and to simplify the peeling-off process of the PDMS stamps.

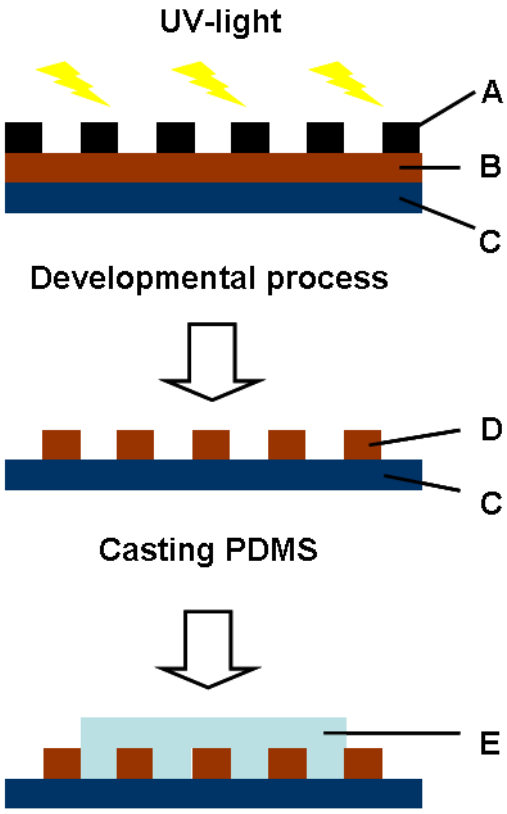


**Fig. 2.20: Lithography process. A: Lithography mask. B: Photoresist (AZ1505). C: Silicone wafer. D: Photoresist grooves. E: Casted PDMS.**

## 2.5.2 Use of the master substrates as PDMS molds

The structured silicone wafers were used as master substrates for the µCP stamps (Ning Wang and Ingber 2002). The stamps were made by casting PDMS onto the master substrates. The PDMS was mixed in a ratio of 10:1 with the two compounds, the elastomere (base) and the cross-linker (curing agent), as described in Section 2.2.2. Air bubbles were removed by putting the PDMS into an exsiccator. After pouring the PDMS onto the master substrates, any remaining air bubbles were removed. The molds were then placed in an oven at 65°C overnight, for the cross-linking process. Subsequently, the PDMS substrates could be easily peeled away from the silanized master substrates. The PDMS could then be cut, and the required stamp employed to print adhesive lines on the nonadhesive starPEG layer.

The surface of the stretching chambers was modified in the following manner. In cooperation with the Department Möller DIW Aachen, a non-adhesive layer for cells was established by spin-coating a starPEG layer (Gasteier *et al.* 2007) onto the surface of the stretching chambers. Alexa568-labeled fibronectin (Alexa Fluor 568 Protein Labeling Kit) as cell adhesion protein was printed onto this layer by micro-contact printing. The stamps were incubated with 5

µg/ml fibronectin solution, and the pattern was transferred onto the center of the stretching chamber. For our purposes, we used a pattern of 10 µm wide adhesive lines, with non-adhesive spacing of between 5 µm and 40 µm separating lines.

The lines were stamped in different orientations (parallel, perpendicular and at an angle of 30°) with respect to the stretching direction. Control experiments were carried out for 10 hours stretching, to show that the lines and the passivation layer were not damaged by the cyclical stretch. The stability of the lines was verified with phase-contrast microscopy of cells adhering to the lines, and fluorescence microscopy of the stained fibronectin lines themselves. If the adhesive lines would be damaged by the stretch, the cells would detach from the surface.

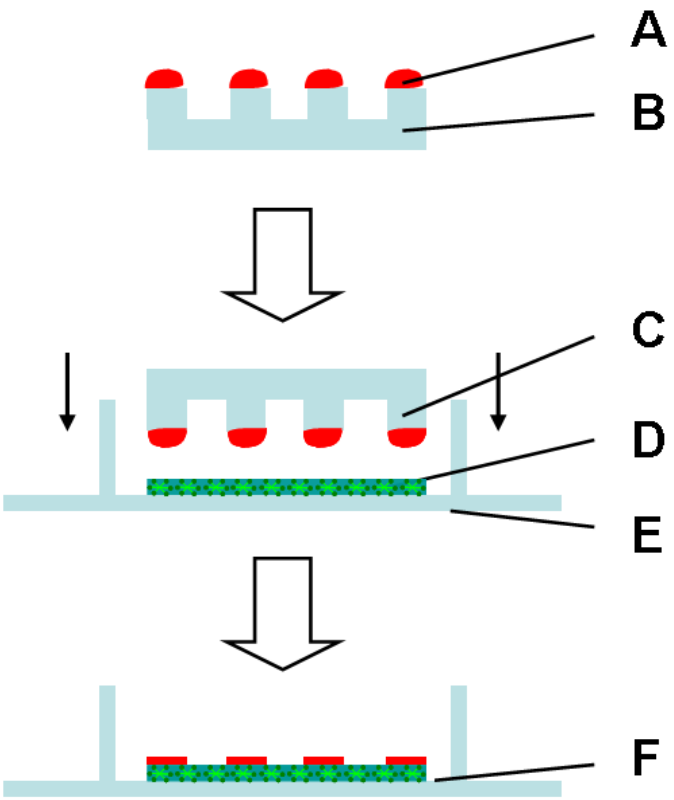


**Fig. 2.21: Micro-contact printing (µCP) of fibronectin (dyed with Alexa 568). A: Dyed fibronectin. B: PDMS stamp. C: Up side down version of the PDMS stamp. D: Non-adhesive layer with star PEG. E: Stretching chamber. F: Stretching chamber with non-adhesive layer and adhesive islands (lines).**

# 3. Results and Discussions

The Results chapter is divided in nine subchapters. The first subchapter describes the specification of the stretching system. The next subchapter describes the results for the phenotype and the morphology observation of cells during cyclical stretch. In the third part, the results for the cellular reorientation process in dependence of the stretch frequency as main results of this study are presented. Our results concerning the amplitude dependency, the studies of old and young cells, the change of the stretch direction, focal adhesion behavior, and the influence of stretch on cell division are described in the subsequent subchapters. In the last subchapter a conclusion of the results is shown and small additional experiments are presented in the appendix.

## 3.1 Characterization and calibration of the stretching system

To characterize the topography of the stretching chambers, surface roughness was examined by means of atomic force microscopy. The center area of the stretching chamber was investigated when the chambers were in a relaxed state, and during maximum stretch (Fig. 3.1.1). The AFM images show no wrinkles on the surface of the substrates, apart from some dirt in the nanometer range. No difference in the surface roughness was found between substrates in the stretched and the unstretched condition.

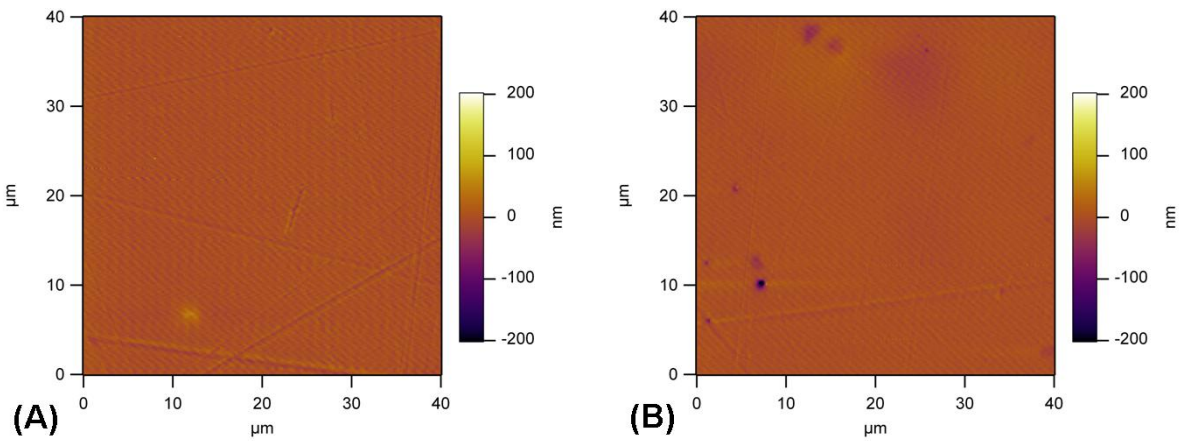


**Fig. 3.1.1: AFM images of the surface of the stretching chamber without stretch (A) and in a stretched condition (B). We could not observe surface differences prior and following stretch.**

The elasticity of PDMS was measured in various studies (Carrillo and L. & Puttlitz 2005) and is also described in the technical sheet (Sylgard 184). Our investigations showed that cyclic strain caused more damage to the material than static strain, and the chambers broke at lower

amplitudes, than during simple elongation. During cyclic strain with a stretch frequency of 0.5 $s^{-1}$, the chambers began to break at an amplitude of 17%. Therefore, the threshold for the maximum amplitude of the experiments was shown to be 15%; higher amplitudes could break the stretching chambers. Our experimental studies were carried out at amplitudes between 1%, the lowest possible amplitude, and 15%.

The homogeneity of the strain field in the center region of the stretching chamber was then measured. Phase-contrast images in both the relaxed state and the maximum stretched state were acquired, and compared.

The results demonstrate a homogenous strain distribution in the stretched state. The elongation of the chambers creates a biaxial strain at the center of the stretched membrane which may be described as a longitudinal elongation and a transverse contraction. Amplitudes of 1%, 2%, 6%, 8%, 12.5% and 15% were applied as shown in Table 3.1.1, and compared to the measured values.

| Amplitude | Mean longitudinal elongation in% (x-axis) | Standard deviation in % (x-axis) | Mean transverse contraction in % (y-axis) | Standard deviation in % (y-axis) |
|---|---|---|---|---|
| 1 | 1.2 | 0.07 | 0.03 | 0.02 |
| 2 | 1.93 | 0.05 | 0.04 | 0.02 |
| 6 | 5.8 | 0.12 | 1.0 | 0.25 |
| 8 | 7.99 | 0.7 | 1.55 | 0.1 |
| 12,5 | 12.49 | 0.5 | 1.95 | 0.95 |
| 15 | 15.00 | 0.2 | 3.37 | 1.19 |

**Table 3.1.1: Characterization of the strain field. Different stretching amplitudes were applied to the stretching chamber. Afterwards the transfer of the strain on the substrate was measured as described in Section 2.1.3.**

The measured values were found to be close to the theoretically expected values. For instance, for an applied strain of 8%, the measured longitudinal elongation was 7.99% ± 0.7%, with a transverse contraction of 1.55% ± 0.1%. The measurements showed that within the limits of the experimental uncertainty, the applied strain was fully transferred to the stretching chamber. For a pure uniaxial strain the substrate is stretched only in one direction and shows no compression orthogonal to the stretch direction. In our experimental set-up, a perfect uniaxial strain is not possible, since a transverse contraction can not be totally excluded; however, we can reduce it to a very low value, as shown in Table 3.1.1.

The stretch was also calibrated following the experiment, at an amplitude of 8%, to see if the stretch characteristic had changed during the experiment. In this case, we obtained the following values: 7.5% ± 0.6% for the longitudinal elongation and 1.1%± 0.2% for the transverse contraction. These results indicate that the substrate characteristics concerning the strain field do not change during the experiment. Even a cyclic stretch of more than 8 hours had no effect on the substrate characteristics and the corresponding elasticity.

It was then necessary to demonstrate, that the substrate stretch was actually transferred to the cells adhering to the substrate. Therefore, the cells on the substrate had to be marked and measured, both before and following the stretch. These calibration experiments were carried out at amplitudes of 2%, 6%, 8%, 12.5% and 15%. The measurement error in this case was higher than that of the polystyrene beads, because cells were stretched as a two- dimensional object, and the strain was distributed over the entire cell. The easiest way to analyze if the strain is transferred to the cells is the observation of cells which are perfectly aligned with the x- or y-axis. We observed cells in the relaxed state and in the maximum elongation of the stretching chamber measured them and compared the results in the relaxed and the stretched state. Table 3.1.2 shows the average of the measurement results.

| Amplitude (%) | Mean longitudinal elongation in % (x-axis) | Standard deviation in % (x-axis) | Mean transverse compression in % (y-axis) | Standard deviation in % (y-axis) |
|---|---|---|---|---|
| 2 | 2.3 | 0.47 | 0.5 | 0.3 |
| 6 | 6.02 | 0.5 | 1.23 | 0.15 |
| 8 | 7.54 | 0.83 | 0.99 | 0.1 |
| 12,5 | 12.2 | 0.18 | 2.93 | 0.92 |
| 15 | 15.65 | 0.73 | 5.05 | 1.23 |

**Table.3.1.2: Characterization of the strain transferred to the cells.**

The measurement of the cells indicates, for example, that an amplitude of 8%, results in a longitudinal elongation of 7.54% ± 0.7% and a transverse contraction of 0.99% ± 0.1% of the cells. This implies that the strain is transferred very well to the cells. This is also the case for the other amplitudes used in our experiments. The ratio between the longitudinal elongation and the transverse contraction was nearly constant for the high amplitudes.

If one does not clamp the substrates at the side, resulting in free movement orthogonal to the stretch direction, the ratio between the longitudinal elongation and the transverse contraction corresponds to the Poisson ratio. The Poisson ration is the ratio between the relative contraction strain divided by the relative extension, or axial strain. In the case of PDMS, the Poisson ration described in the literature is 0.5 which we also observed in our measurements.

## Discussion

The characterization and calibration of the stretching system we developed showed that it is possible to apply a defined strain to the substrates. The difference between the applied amplitude and the measured strain of the substrate was within an acceptable range, the divergence between the given strain and the measured strain was between 5% and 10%. A homogenous strain field was measured in the observation area of the stretching chambers. Furthermore, a comparison between the strain transferred to the cells on the substrate, and the strain to the substrate itself, showed that the strain of the substrate, was, indeed, transferred to the cells.

AFM measurements indicated that pre-stretching of the substrates avoids the generation of wrinkles on the surface of the substrate.

The measurements were taken several times, so that we could be certain that both the homogenous strain field and the stretching amplitude were highly reproducible.

## 3.2 Phenotype and morphology of cells during cyclical stretch

As noted in the Introduction, cells subjected to cyclical stretch orient themselves perpendicular to the stretch direction. The general principle governing our experiments was to plate cells on cyclical, deformable elastic substrates. The dynamic behavior of the cells was observed by phase-contrast microscopy and live cell imaging.

Fig. 3.2.1 shows excerpts of a typical image sequence, taken from a stretching experiment with REF52 cells, a stretching frequency of 10 $s^{-1}$, and a stretching amplitude of 8%. At the beginning of an experiment, cells adhering to the PDMS substrates initially oriented themselves in a random fashion. After stretching the membrane for a certain period of time, they increasingly aligned themselves perpendicular to the uniaxial stretching direction, as previously observed (Dartsch, 1986). Fig. 3.2.1 depicts different time points during the cyclical stretch of REF52 cells (Image 1: 0 s; Image 2: 1800 s; Image 3: 6000 s and Image 4: 30000 s). After 30000 s, the cyclical stretch was stopped, and the behavior of the cells after stretch was observed (Image 5: 37500 s; Image 6: 65000 s). In the case of the REF52 cells, we could observe a subsequent relaxation of the cells oriented perpendicularly to a random orientation.

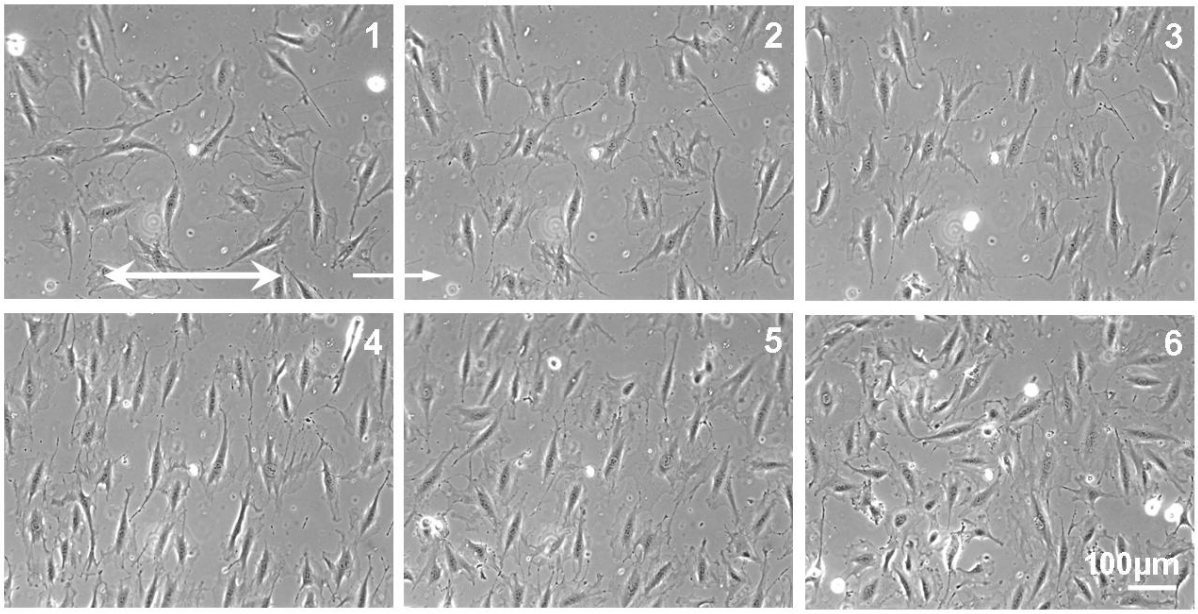


**Fig. 3.2.1: Light microscopy image sequence of REF cells adhering to a cyclically stretched substrate at strain amplitude *A*=8% and strain frequency *f* =10 $s^{-1}$. Each image corresponds to a particular time point, *t*, after the start of stretching: 1 (t=0 s); 2 (t=1800 s); 3 (t=6000 s); 4 (t=30000 s); 5 (t=37500 s); 6 (t=65000 s). The substrate was stretched in the x-direction (double arrow in Image 1). After 30000 s (4) the applied stretch was stopped; subsequently, relaxation and the cells return to a random orientation was observed (Images 5 and 6).**

### 3.2.1 Scanning electron microscopy images

Fig. 3.2.2 shows scanning electron microscopy images of HDF1 human fibroblasts adhering to a PDMS substrate after 8 hours of stretching. The stretching experiment was carried out at a stretch frequency of 2 $s^{-1}$, and a stretching amplitude of 8%. The white double arrow visualizes the stretch direction.

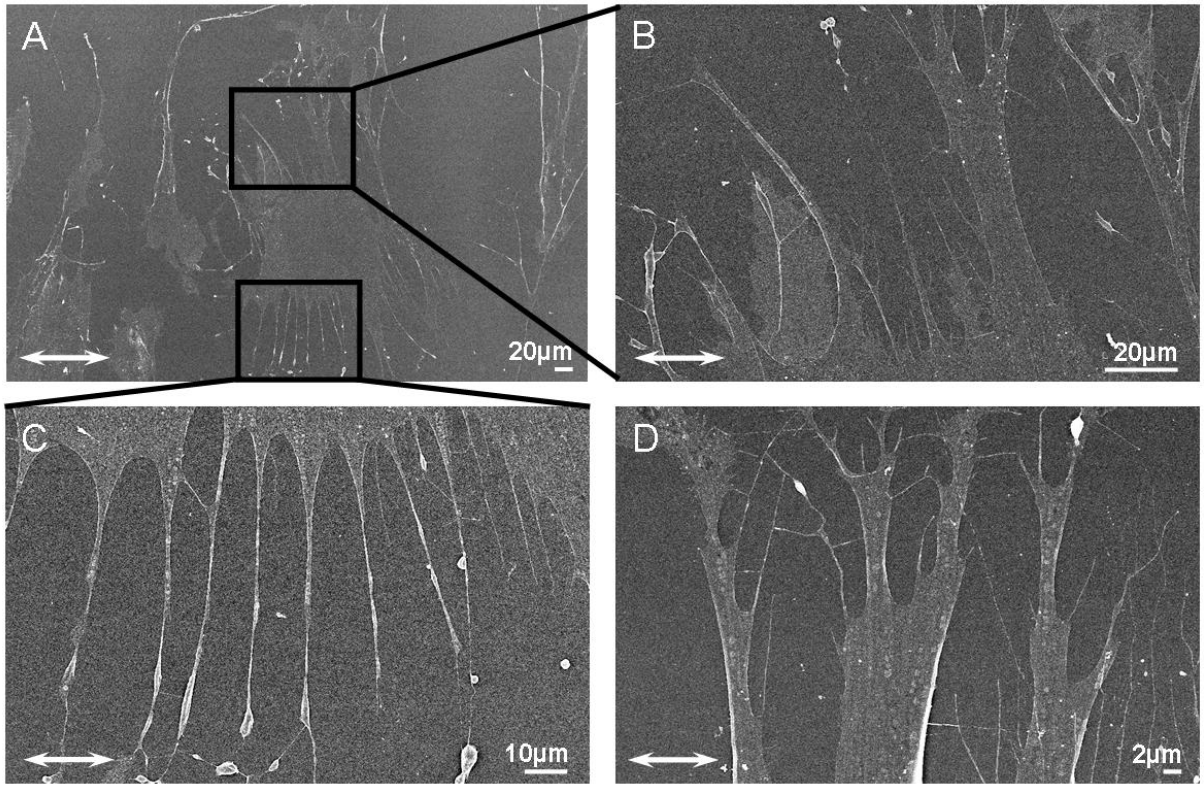


**Fig. 3.2.2: Scanning electron microscopy images of HDF1 fibroblasts after being stretched for 8 hours with a stretch frequency of 2 $s^{-1}$, and a stretch amplitude of 8%. A: Overview of fibroblasts oriented perpendicular to the stretch direction. B and C: Close-up view of filopodia-like cell extensions. D: Filopodia-like cell extensions oriented perpendicular to the stretch direction. White double arrows indicate the stretch direction.**

The cells aligned themselves perpendicular to the stretch direction, and elongated along the orientation axis, as may be seen in the overview image (Fig. 3.2.2 A). The fibroblasts built small filopodia-like cell extensions, as they do during cell migration. These cell extensions were built in the direction of the orientation axis, meaning that the cell extensions were also orientated perpendicular to the stretch direction (Fig. 3.2.2 B-D). Image 3.2.2.D also shows that the filopodia-like cell extensions of different cells are in contact with one another.

### 3.2.2 Temporal change of cell elongation and cell area

Cell morphology was evaluated at each time point. Therefore, we determined the cell area and, furthermore, also analyzed the length of the major and minor axes of the fitted ellipse. After these parameters were measured, the mean value at different time points was plotted over time. Figs. 3.2.3 and 3.2.4 show the time course of the cell orientation, the cell elongation and the cell area of REF52 cells and HDF1 cells for an experiment carried out at 2 $s^{-1}$ stretch frequency and 8% stretch amplitude. The vertical red line indicates the time point at which the mechanical stretch was stopped.

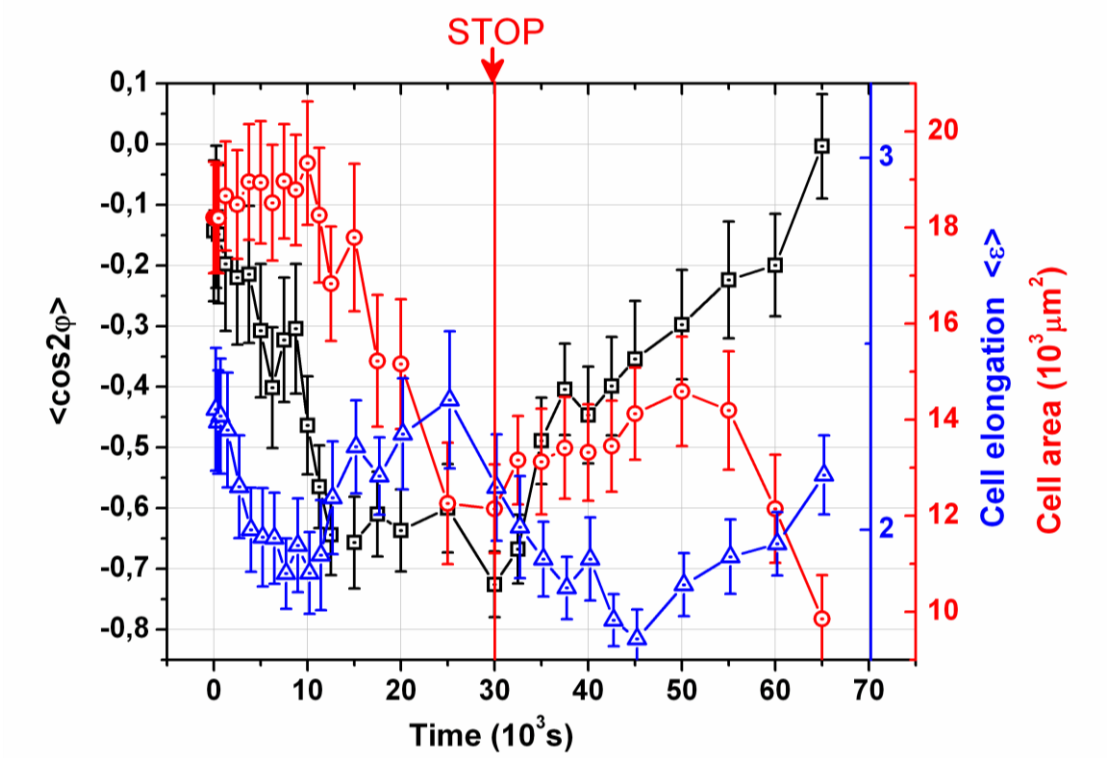


**Fig. 3.2.3: Changes in cell morphology of sub-confluent REF52 cells during cyclical stretch (2 $s^{-1}$, 8%). □ = change of mean orientation <cos2φ> over time; ○ = change of cell area over time; Δ = change of cell elongation over time. The stretch was stopped after 30000 s (vertical red line).**

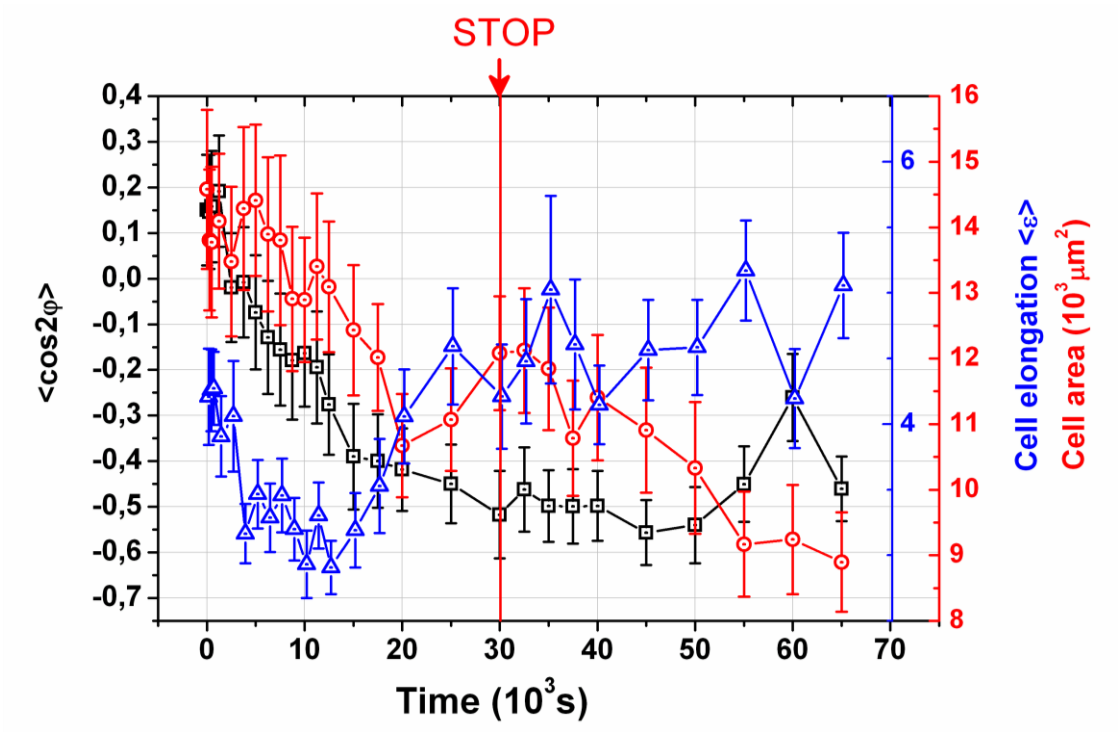


**Fig. 3.2.4: Changes in cell morphology of sub-confluent HDF1 cells during cyclical stretch (2 $s^{-1}$, 8%).□ = change of mean orientation <cos2φ> over time; ○ = change of cell area over time; Δ = change of cell elongation over time. The stretch was stopped after 30000 s (vertical red line).**

The changes in cell morphology observed during cyclical stretching indicate that both cell types behave in a similar manner: the mean cell area remains constant at early stages, what means in the first 10000 seconds of the experiment, and decrease to one third of the initial mean cell area with time.

Both cell types are slightly rounding up in the first 10000 seconds of the experiments (mean cell elongation decreases) and elongate again in a new direction around the characteristic time of reorientation which is in detailed described in Section 3.2. We determined the time point at which the cell area begins to changes (≈ 10000 s for REF52 cells; Fig. 3.2.3) and the time point when cell elongation is at its minimum (between 6000 s and 7000 s for the REF52 cells; Fig. 3.2.3) and compared these times with the characteristic time of cell reorientation (between 5000 s and 6000 s for REF52 cells).

This comparison indicated that the change in cell area began after the characteristic time of the reorientation process. The cells first begin to orientate themselves perpendicular when cyclical stretch was applied; once they had completed this process, they began to reduce the cell area. After the mechanical strain had ceased, the cell area remained constant for a period of time (~ 25000 s) and then diminished, due to the fact that the cells were dividing and growing to form a confluent layer.

Cell elongation decreased from the start of the experiment, until the cells had orientated themselves. This means that the cells assume a rounded shape during the orientation process; however, once they are orientated, they begin elongating again in the new direction of the orientation.

## Discussion

Changes in cell morphology can be interpreted as an attempt of the cell to avoid the stress caused by the cyclical strain (Dartsch *et al.* 1986). Cell reorientation requires the continuous remodeling of both the focal adhesions and the actin cytoskeleton (Hayakawa *et al.* 2001; Kaunas *et al.* 2005; Na *et al.* 2007). The actin stress fibers need to be depolymerized and then repolymerized in a new direction to re-establish a state of equilibrium, following an adaptive process. The disassembly of the cell's focal adhesions and actin cytoskeleton may be the reason why the cell assumes a rounded shape when stress is first applied (Keller *et al.* 1991). The disassembly of the actin cytoskeleton causes a loss of stability within the cell, as a result, they begin to round up. At the same time, the cell's cytoskeleton may reassemble itself, but perpendicular to the stretch direction (see Section Appendix A.4). As soon as the assembly process and the disassembly process are balanced, the cell assumes its least rounded state. As the reassembly process continuous, the cell begins to elongate once again, until a certain "steady state" is reached. In both cell types observed, this "steady state" usually involves greater elongation than that seen in the initial state. Once the cell is no longer exposed to external stress, it returns to a relaxed state. In the case of REF52 cells, they assume a more rounded shape, while the human fibroblasts remain elongated in a perpendicular orientation.

To clarify our assumption that the actin cytoskeleton is responsible for this behavior, it is necessary to observe the dynamics of the actin fibers. This can be realized with an improved experimental set-up, enabling, for example, the tracking of fluorescently labeled actin fibers in fibroblasts. Our evaluations of the cell area indicate that both cell types begin to shrink in area either during or at the end of the orientation process. The shrinking of the cell area may also constitute an attempt by the cell to avoid mechanical strain. If the contact area is reduced, the force transmitted to the cell is reduced because of the relation $F = A * \sigma$, while $F$ is the applied force, $A$ the cell area and $\sigma$ the stress. Once the external force ceased, the cells retained the area they had reached, or even shrank further. The shrinking effect we observed could have been resulted from cell growth and proliferation from a single-cell state to a confluent cell layer.

# 3.3 Reorientation dynamics of cells in dependence of the stretching frequency

In this part of the study, we mainly focused on the influence of stretching frequency on the degree of reorientation and the reorientation dynamics of cells. The frequency dependent cellular reaction can also be cell-type dependent. For that reason, we examined two different fibroblast cell types, REF52 wild-type cells (a rat embryonic fibroblast cell line) and HDF1 (primary human fibroblast) cells. The cells were stretched for 30000 seconds; afterwards the stretch was stopped and the cells were observed for a further 35000 seconds to investigate the behavior of the cells following stretch. The time-lapse movies obtained were analyzed, and the mean values of the orientation $S = \langle\cos 2\varphi\rangle$ at certain time points were plotted over time. The error bars represent the standard deviation, and result from the statistical fluctuations of the single values for the cells around the mean value. The characteristic time for the reorientation process was determined by fitting Equation 3 (Section 2.3.2.3) to the experimental data. Furthermore, the influence of cell density, and the influence of the stretching rate on the cellular response were observed.

## 3.3.1 Reorientation dynamics of sub-confluent REF52 cells

A layer of single REF52 cells (30 to 50 cells/mm²) was observed during cyclical stretch. The stretch frequency was changed for each experiment. In Fig. 3.3.1 we can see that the mean orientation of the REF52 cells rises exponentially over time. The cells increasingly align themselves nearly perpendicular to the stretching direction, up to a certain maximum angle. This is shown in the graph, where the order parameter changes from nearly 0 (random orientation) to a new, maximum value. When this angle is reached, the reorientation process stops and goes into saturation and the cells do not orient further over time. We investigated this dynamic for different stretching frequencies. Measurements of the cellular orientation were made with a frequency of $f = 0.0001\ s^{-1}$, up to a frequency of $f = 20\ s^{-1}$. The results of these measurements, what means the time course of the cellular orientation during cyclical stretch were then compared for the different stretching frequencies.

In control experiments, in which no mechanical strain was applied, the cellular orientation varies between $S = \langle\cos 2\varphi\rangle = 0.2$ and $S = -0.2$. This temporal variation of the cellular orientation is caused by cell migration and cell movement. At a stretch frequency of $f_{t1} = 0.01\ s^{-1}$, REF52 cells behaved like cells in the control experiment, in which the cells were randomly oriented. This means that $f_{t1} = 0.01\ s^{-1}$ is a threshold frequency for the activation of the reorientation process (Fig. 3.3.1 B), because at the next measured frequency of $f = 0.05\ s^{-1}$, a low-level cell reorientation can already be observed.

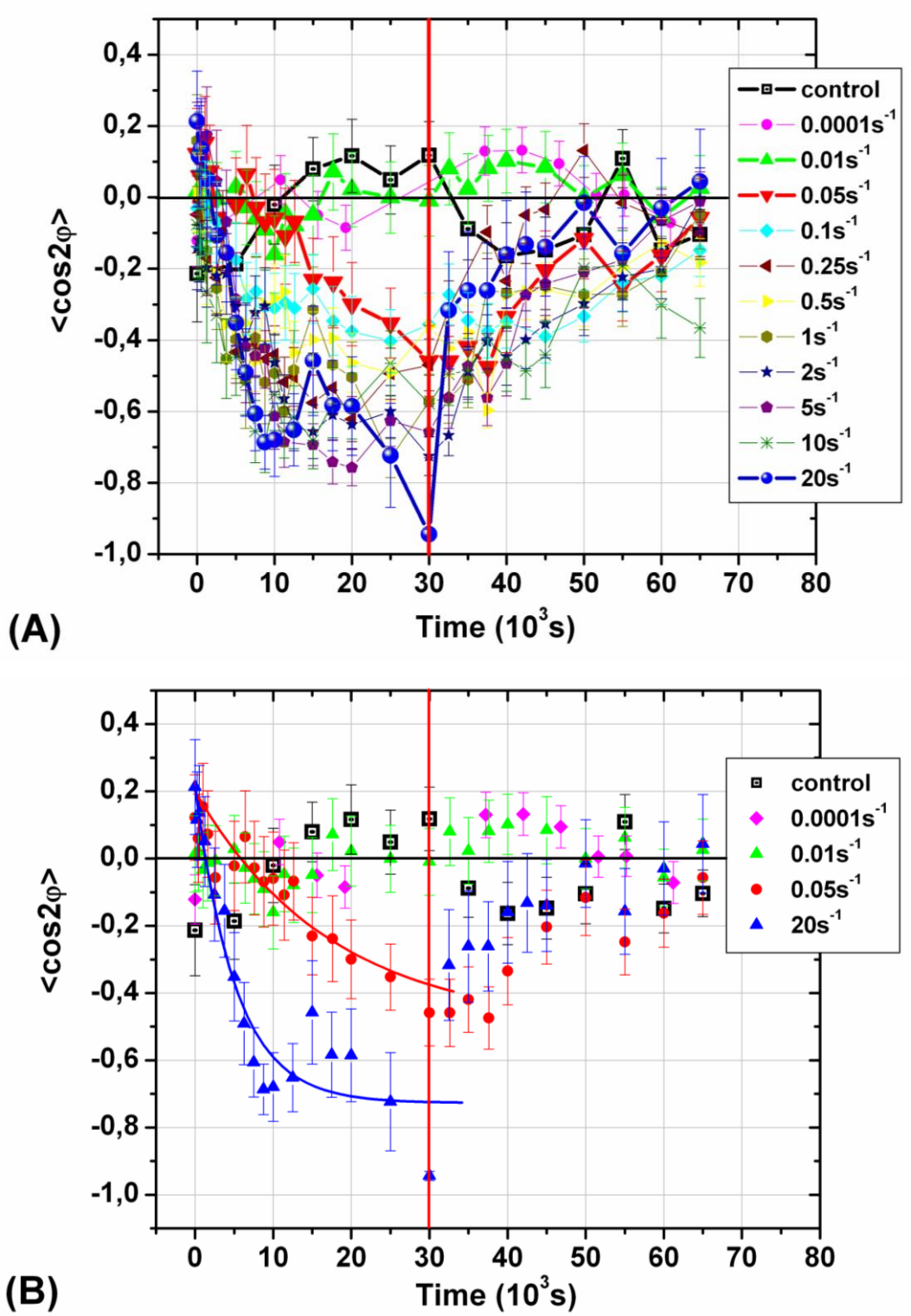


**Fig. 3.3.1: A: Exponential decrease of the order parameter *S*=<cos2φ> for REF52 cells from a random orientation (*S* ≈ 0) to a saturation value in dependence of the stretch frequency. The stretching amplitude was a constant 8%. B: Different selected frequencies:(□): Control experiment with no stretch; (♦): The lowest possible frequency, 0.0001 $s^{-1}$; (▲): The threshold frequency at which the cells show no cellular response, $f_{t1}$ = 0.01 $s^{-1}$; (●): The frequency at which the cellular reaction began, *f* = 0.05 $s^{-1}$; and (▼): The maximum possible frequency, *f* = 20$s^{-1}$. The REF52 cells return to a random alignment after the stretching ceases (t = 30*$10^3$ s; vertical red line). Error bars represent the standard deviation of the mean value. The characteristic time τ is determined by fitting the exponential expression to the experimental data points (B: *f* = 0.05 $s^{-1}$ and *f* = 20 $s^{-1}$).**

The obtained time courses for the different frequencies were plotted in Fig. 3.3.1. We can observe that the REF52 cells reacted faster and align more perpendicular as the stretching frequency increased. After 30000 s, the mechanical stretch was deactivated (vertical red line in the figures), and the cells were observed for another 35000 s. Theses observations showed that the cells began to relax and reorganize into a random orientation, once the strain had ceased. The relaxation process was also exponential in nature, but with a longer time constant of the order of approximately 10000 s.

### 3.3.2 Reorientation dynamics of sub-confluent HDF1 cells

To ascertain if the results observed in the REF52 fibroblasts are cell-type specific, or characterize a general behavior of various fibroblasts, we performed the same experiments, this time using human dermal fibroblasts. The experiments were carried out with the same frequency variations, and the results compared with those of the REF52 cells.

In both the HDF1 cells and the REF52 cells, we observed a similar behavior during cyclical stretch. From an initially random orientation, the cells begin to align themselves perpendicular to the stretch direction once cyclical stretch was applied. A detailed analysis showed, however, that there were several differences in cellular behavior.

The most obvious difference was that the HDF1 cells began to reorient perpendicular to the stretch direction at a higher stretching frequency. In order to observe the reorientation process of the HDF1 cells, a stretch frequency above the threshold frequency $f_{t1}$ = 0.1 $s^{-1}$ (Fig. 3.3.2) had to be applied. This means that the threshold frequency for a cellular reaction involving HDF1 cells is 10 times higher than that measured for the REF52 cells (threshold frequency HDF1 cells: $f_{t1HDF1}$ = 0.1 $s^{-1}$; threshold frequency REF52 cells: $f_{t1REF52}$ = 0.01 $s^{-1}$).

Like the REF52 cells, the reorientation of the HDF1 cells also increased with the stretching frequency, but compared to the REF52 cells, the HDF1 cells reorient slower and less perpendicular (Fig. 3.3.2).

All in all, the reorientation of the in a perpendicular direction occurs slower for the human fibroblasts than for the REF52 cells. Our findings indicate that REF52 cells are more sensitive to cyclical stretch than the HDF1 cells.

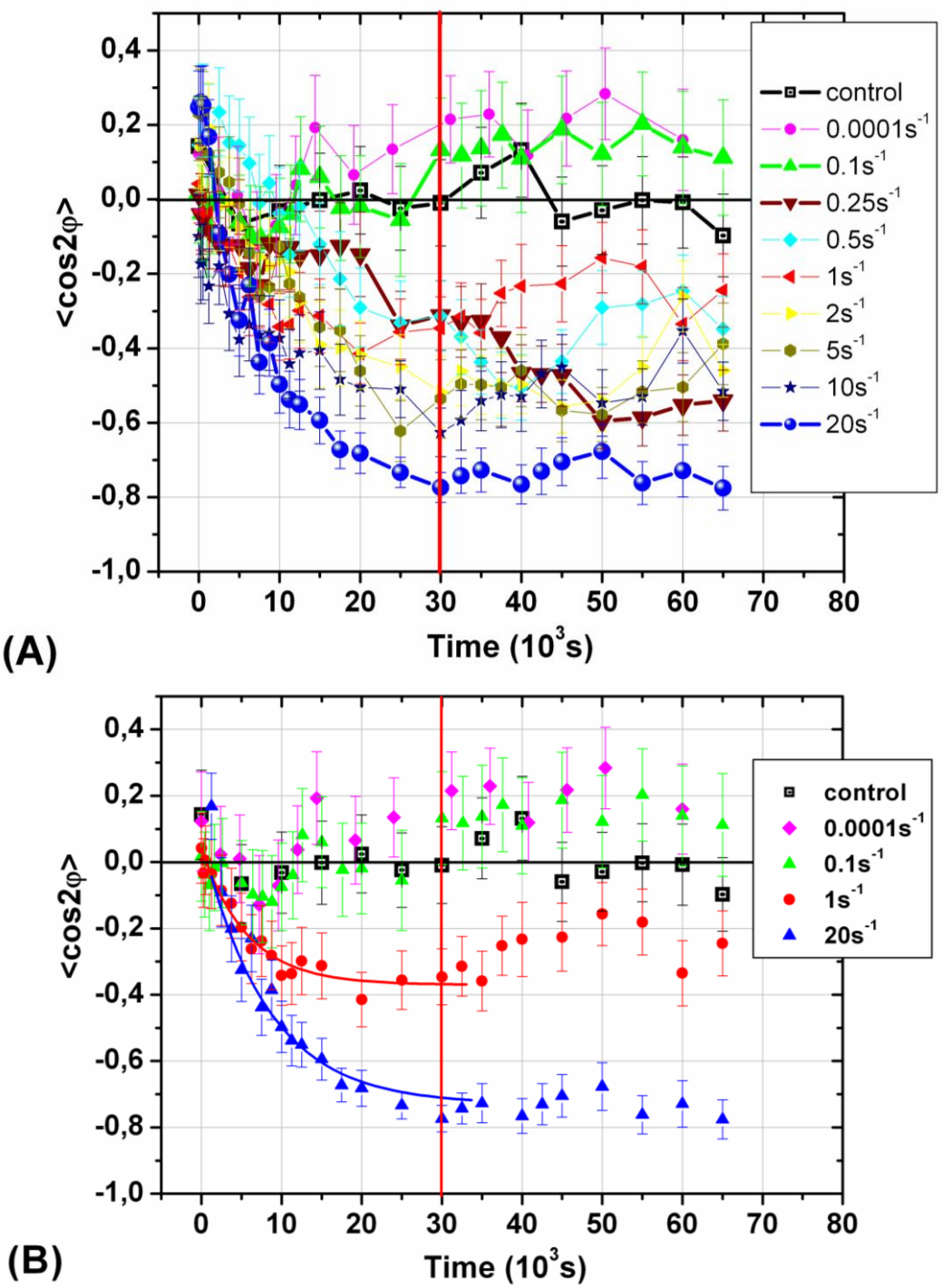


**Fig. 3.3.2: A: Exponential decrease of the order parameter $S$=<cos2φ> for REF52 cells, from a random orientation ($S \approx 0$) to a saturation value in dependence of the stretch frequency. The stretching amplitude was a constant 8%. B: Different selected frequencies:(□): Control experiment with no stretch; (♦): The lowest possible frequency $f$ = 0.0001s$^{-1}$; (▲): The threshold frequency where the cells show no cellular response, $f_{t1}$ = 0.1s$^{-1}$; (●): A stretch frequency of $f$ = 1s$^{-1}$; and (▼): The maximum possible frequency, $f$ = 20s$^{-1}$. In contrast to the REF52 cells, the HDF1 cells remained in an orientation perpendicular to the stretching direction, even after the stretching is ceased (t = 30*10$^3$ s; vertical red line). Error bars represent the standard deviation of the mean value. The characteristic time τ is determined by fitting the exponential expression to the experimental data points (B: $f$ = 1 s$^{-1}$ and $f$ = 20 s$^{-1}$).**

A further difference between the two cell types lies in their behavior after the cyclical mechanical stretch was stopped. In contrast to REF52 cells which relaxed into a random orientation, the HDF1 cells remained in a perpendicular orientation and demonstrated a quasi-plastic behavior.

### 3.3.3 Characteristic regimes in frequency dependent dynamic reorientation

The plots of time characteristics obtained (Figs. 3.3.1 and 3.3.2) were analyzed by a simple phenomenological model, mentioned in Section 2.3.2. The data curves were fitted to the following equation:

$$y = \langle \cos 2\varphi \rangle_{MAX} + \left( \langle \cos 2\varphi \rangle_0 - \langle \cos 2\varphi \rangle_{MAX} * \exp\left( -t/\tau \right) \right) \qquad \text{Eq. 4}$$

with the fit parameters $<cos2\varphi>_0$ and $<cos2\varphi>_{MAX}$ , while $<cos2\varphi>_0$ represents the mean orientation <cos2φ> of the cells during the initial state of the experiments which is always around 0 and $<cos2\varphi>_{MAX}$ , the maximum mean orientation $<\cos 2\varphi>_{MAX}$ of the cells, at which point the reorientation process goes into saturation. $<cos2\varphi>_{MAX}$ can not become smaller than - 1 (see Section 2.2.3).

Equation 4 is derived from the time-dependent solution of the differential equation describing the mathematical model (Section 2.3.2.3, Equation 3)

The fit curve yields a value for the characteristic time τ of the reorientation process of the cells. Examples of a fit are given in Fig. 3.3.1 B and Fig. 3.3.2 B. Fig. 3.3.1 B illustrates the data for the time course of the cellular orientation (<cos2φ>) at different stretch frequencies applied to REF52 cells, the exponential fit for the two active frequencies, $f = 0.05\ s^{-1}$ (●) and $f = 20\ s^{-1}$ (▲), is shown. In a similar fashion, Fig. 3.3.2 B, shows the data for time course of the cellular orientation (<cos2φ>) at different stretch frequencies applied to the HDF1 cells, and the exponential fit is demonstrated at stretching frequencies of $f = 1\ s^{-1}$ (●) and $f = 20\ s^{-1}$ (▲).

.In Fig. 3.3.3, the characteristic times for both cell types were plotted as a function of the various frequencies.

The characteristic time represents the time it takes for the cells to reorientate themselves by a fraction of 1/e (i.e., approximately 63% of the maximum orientation).

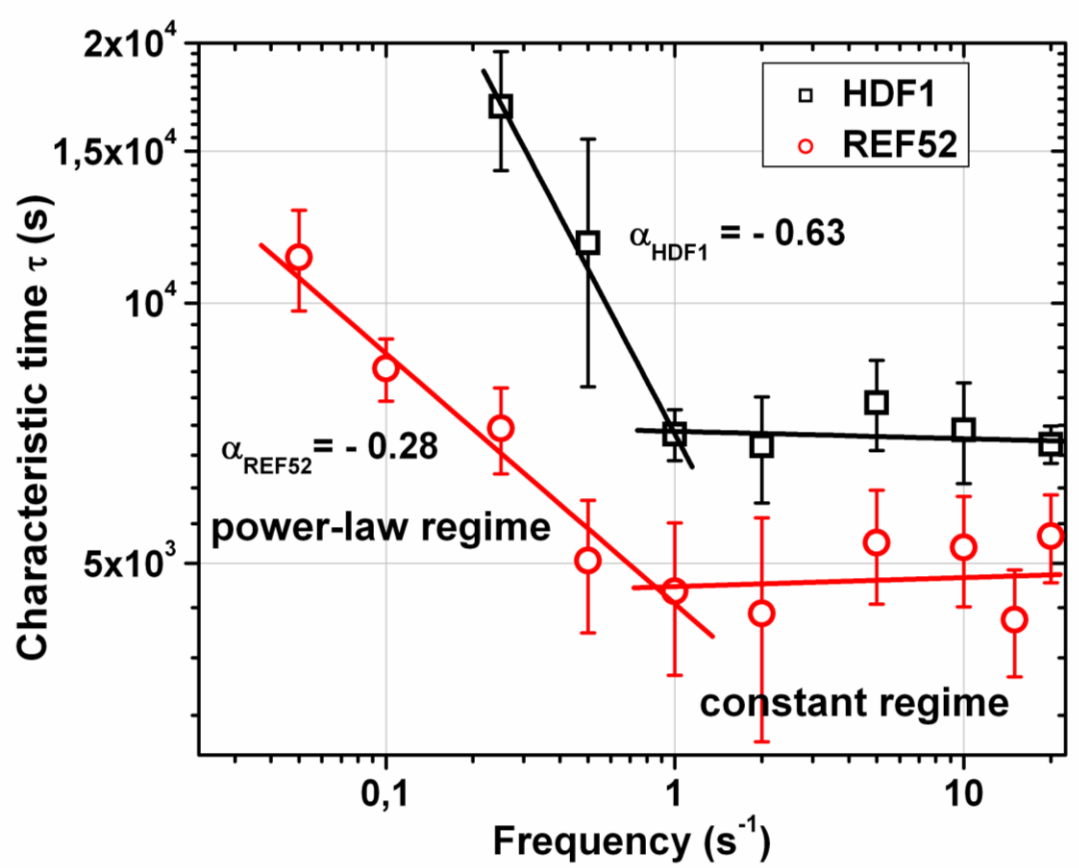


**Fig.3.3.3: Biphasic characteristics of dynamic cell reorientation for sub-confluent cells (□ and ○). The characteristic time $\tau$ decreased according to a power law for $f$ < 1 $s^{-1}$ (power-law regime) and then remained constant for $f$ >1 $s^{-1}$ (constant regime) (note the log/log diagram!). Reorientation of HDF cells (□) was slower than that of REF cells (○) for all frequencies. The threshold frequency for the onset of cellular response was higher for the HDF1 cells than for the REF cells. The slopes seen during the power law regime were $\alpha_{HDF1}$ = -0.63 (±0.13) for the HDF1 cells and $\alpha_{REF52}$ = -0.28 (±0.06) for the REF52 cells. This shows in general, the HDF1 cells reoriented themselves more rapidly than the REF cells.**

In order to reorient themselves during cyclical stretch, cells required a characteristic time of between 5000 and 15000 seconds. We demonstrate that the characteristic time τ decreases according to a power law for an increase in frequency up to a frequency of $f_{t2}$ = 1 $s^{-1}$, indicating that reorientation occurs more rapidly, as the stretching frequency increases.

Above this certain threshold ($f_{t2}$ = 1 $s^{-1}$), the characteristic time is constant with increasing frequencies. In fact, two different regimes were observed, a power-law regime for frequencies below $f_{t2}$ = 1 $s^{-1}$, and a constant regime for frequencies higher than $f_{t2}$ = 1 $s^{-1}$. This behavior could be observed for both cell types and may be typical for other cell types.

REF52 cells reorient themselves faster, at all frequencies. We therefore assume that REF52 cells are more sensitive to mechanical stretch than the human dermal fibroblasts.

The different slopes [($\alpha_{HDF1}$ = - 0.63 (± 0.13) for the HDF1 cells and $\alpha_{REF52}$ = - 0.28 (± 0.06) for the REF52 cells] of the power-law regime, indicate that the characteristic time of the reorientation decreased more rapidly for the HDF1 cells.

### 3.3.4 Influence of cell density on the dynamics of cell reorientation.

We expected that the cell density would have an impact on the reorientation of cells during cyclical stretch. Accordingly, and in contrast to the experiments performed with single cells, we then chose to observe a layer of confluent cells with cell-cell contacts. REF52 were plated at double density compared to the single cell experiments (100 cells/mm²) on the stretching chambers. Other experimental parameters, such as the used stretching frequencies, were the same as those used for the single cell experiments. Fig. 3.3.4 depicts the time course of the mean cellular orientation for a stretching experiment with a stretch frequency of $f$ = 10 $s^{-1}$ and an amplitude of 8% for single cells, and for a confluent cell layer.

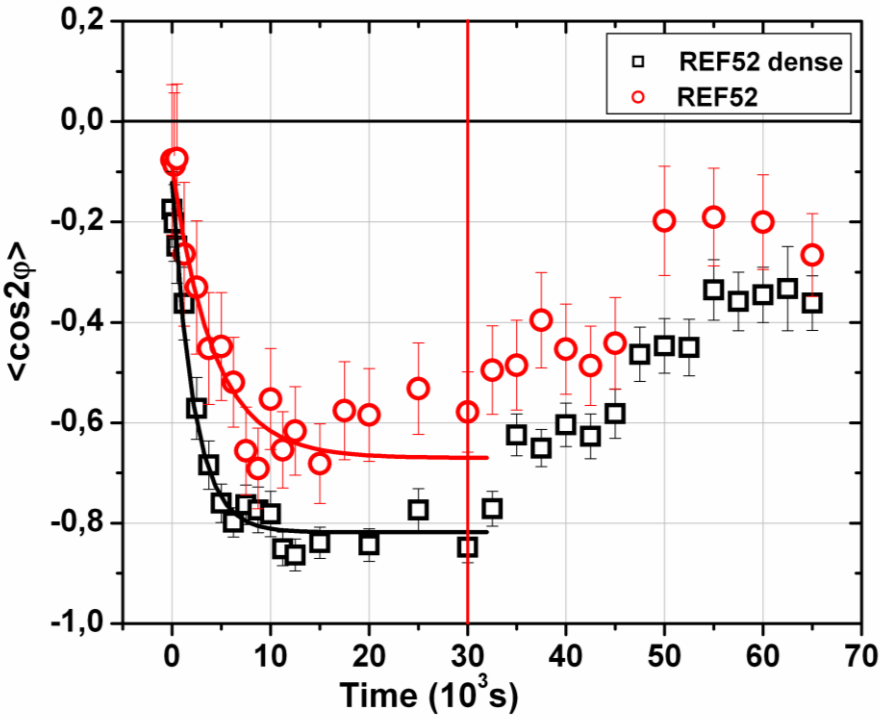


**Fig.3.3.4: Comparison of the time course of the mean cellular orientation of single REF52 cells and confluent REF52 cells ($f$=10 $s^{-1}$; $A$=8%). [(□)=REF52 confluent cells;(○)=REF52 single cells). The vertical red line indicates thetime point at which stretch was stopped.**

In principle, confluent REF52 cells behave like single cells. In both cases, the cellular alignment to a perpendicular orientation occurred in an exponential manner. Once the stretch was stopped, both single and confluent cells relaxed into a random orientation. Compared to the single cells, the confluent cells reoriented themselves faster, and the maximum degree of orientation ($<\cos 2\varphi>_{MAX}$) was also higher (single cells: ≈ - 0,63; confluent cells: ≈ - 0,8; Fig. 3.3.4:). As in the other experiments, the data were fitted by an exponential function (see Section 3.3.3) for each applied frequency. The characteristic times τ were plotted as a function of the frequencies, and the results compared with the single cell experiments involving the REF52 cells (Fig. 3.3.5).

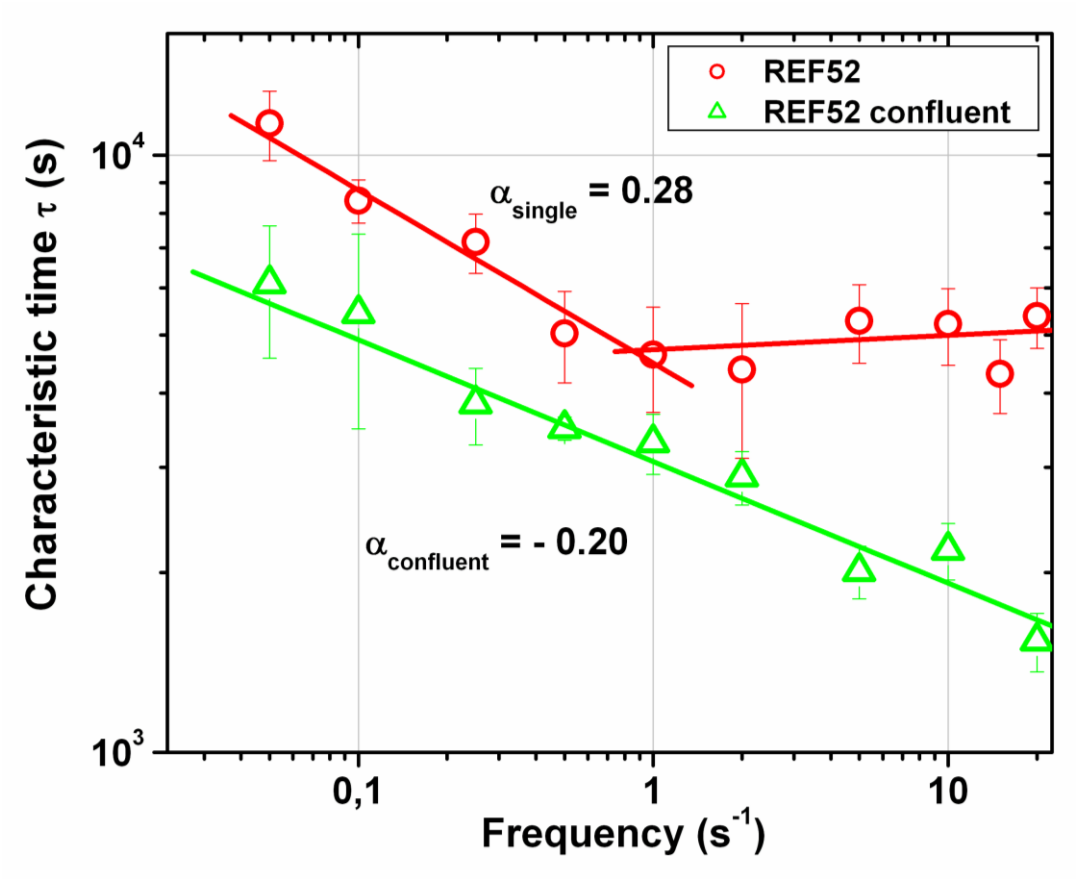


**Fig.3.3.5: Comparison of the characteristic time τ of sub-confluent REF52 cells, and a confluent layer of REF52 cells. [(○)=REF52; (Δ)=REF52 dense]. While the single cells showed a biphasic characteristic (power-law and constant regimes; note the log/log diagram!), the confluent cell layer showed no biphasic characteristic. It is only possible to observe a power–law regime for the characteristic time and in general faster cellular responses for the confluent cells compared to the single-cells. The slopes seen during the power law regime were $\alpha_{single}$ = - 0.28 (± 0.13) for the single cells and $\alpha_{confluent}$ = - 0.20 (± 0.06) for the REF52 cells in a confluent layer. The characteristic time for cells in a confluent layer decreases faster compared to single cells.**

The characteristic time τ for the confluent cells was consistently found to be between 1.5 and 2 times shorter than for the single cells, indicating that confluent cells with cell-cell contacts react faster than single cells. A comparison of the slopes $\alpha_{single}$ = - 0.28 (± 0.13) for the single cells and $\alpha_{confluent}$ = - 0.20 (± 0.06) for cell sin a confluent layer demonstrates that the characteristic time for cells in a confluent layer decreases faster with an increase of the stretch frequency.

Furthermore, in contrast to the single cells, cells in a confluent layer behaved differently at high frequencies. For single cells, we observed a characteristic biphasic behavior for the characteristic time in dependency of the stretch frequency, while the characteristic time for confluent cells decreases with a power law. In the case of cells in a confluent layer, we could not observe a threshold frequency of $f_{t2}$ = 1 $s^{-1}$ and a constant regime for the characteristic time could not be shown.

### 3.3.5 Change of the maximum orientation $<\cos 2\varphi>_{MAX}$ with frequency

The orientation versus time plots (Figs. 3.3.1 and 3.3.2) indicated that the cells reoriented themselves in a manner that was not totally perpendicular to the stretch direction. They oriented themselves up to a certain maximum angle of orientation. After reaching this angle, the reorientation process went into saturation. This maximum angle was determined by calculating the average of the measured angles in the plateau. Fig. 3.3.6 shows the frequency-dependent maximum orientation $<\cos 2\varphi>_{MAX}$, we observed for both single cells and cells in a confluent layer.

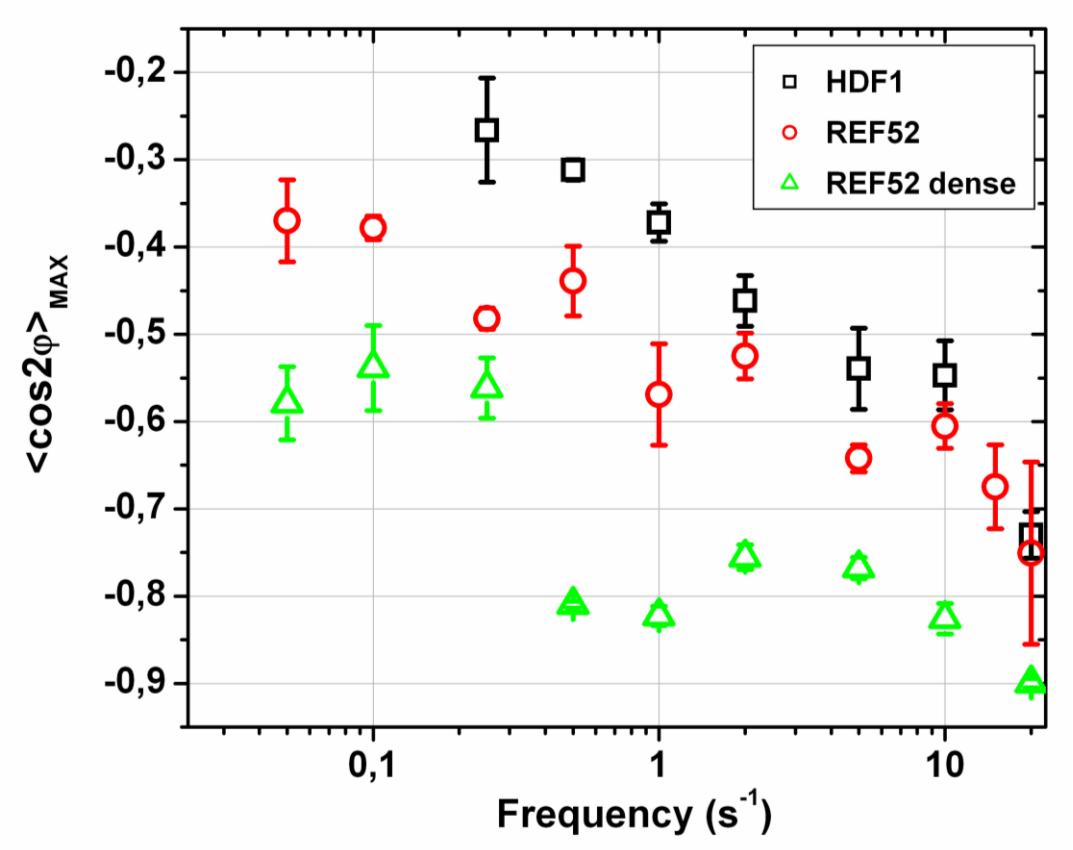


**Fig. 3.3.6: Maximum orientation $<\cos 2\varphi>_{MAX}$ for different stretching frequencies. Comparison between single HDF1 cells, single REF52 cells and confluent REF52 cells. [(□)=HDF1;(○)=REF52; (Δ)=REF52dense]. In the sub-confluent cell layer, the maximum orientation approached a value that was asymptotic to $S_{MAX} = <\cos 2\varphi>_{MAX} = -1$. In the confluent cell layer, a step between 0.25 $s^{-1}$ and 0.5 $s^{-1}$ could be observed.**

Evaluation of the maximum orientation $<\cos 2\varphi>_{MAX}$ indicated that the maximum orientation was not only influenced by the longitudinal elongation and the transverse compression (Wang *et al.* 2001), but was also dependent on the stretch frequency.

Our experiments with single cells demonstrated that the maximum angle of orientation approached asymptotic to $<\cos 2\varphi>_{MAX} = -1$, as the stretch frequency increased [Fig 3.3.6 **(□)**

and **(○)]**. At higher frequencies, the cells oriented themselves more perpendicularly to the stretching direction.

Cells in a confluent cell layer behaved differently from the single cells. In Fig. 3.3.6 we could not observe a continuous approach toward $<\cos 2\varphi>_{MAX} = -1$ for an increase of the frequency. The maximum orientation angle of cells in a confluent layer for low frequencies up to $f = 0.25$ $s^{-1}$ was more or less constant and at a frequency of $f = 0.5$ $s^{-1}$, we could observe a discontinuity. At higher frequencies, the maximum orientation, $<\cos 2\varphi>_{MAX}$, again displayed more or less constant behavior, respectively, $<\cos 2\varphi>_{MAX}$ approaches the perfect perpendicular orientation of $<\cos 2\varphi>_{MAX} = -1$, at high frequencies near $f = 20s^{-1}$.

At all frequencies, we found a higher maximum orientation for cells in a confluent layer, as compared to the sub-confluent cells.

### 3.3.6 Lag time of the cellular reorientation process

The lag time is in our case defined as the time difference between the start of the experiment, when the mechanical stretch was first applied, and the first observed reaction of the cells. This lag time was evaluated for each experiment, and plotted for each frequency (Fig. 3.3.7).

In the experiments with single cells, we observed a decrease in lag time with increasing frequencies up to a threshold of $f_{t2} = 1$ $s^{-1}$. Above a frequency of $f_{t2} = 1$ $s^{-1}$, the lag time was around 500 seconds in almost all experiments.

For cells in a confluent layer, we observed a different result: at all frequencies, the lag time was found to be constant, around 500 s. The time resolution of 500 s used to evaluate our experiments was not high enough to enable more detailed predictions.

However, our results do indicate that the lag time was lower for cells in a confluent layer as compared with single cells.

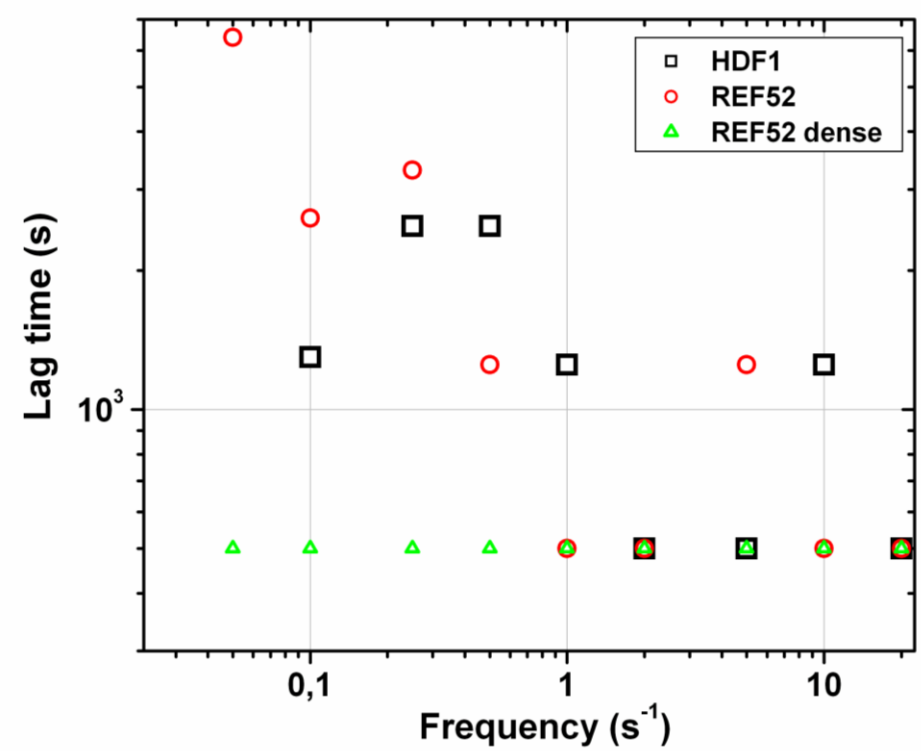


**Fig. 3.3.7: Lag time of the experiments (time between application of the cyclical stretch, and the first reaction of the cells). Comparison of the lag time at different frequencies between single HDF1 cells, single REF52 cells, and confluent REF52 cells. [(□)=HDF1;(○)=REF52; (Δ)=REF52dense].**

## 3.3.7 Cellular response during cyclical stretch with different stretching rates

Cells response to cyclical stretch is frequency dependent as shown in Section 3.3.1 – 3.3.6. Following question arises: is the strain of a major importance for the cellular reorientation process or the back relaxation of the substrate from the maximum strain to the point of no strain? Therefore, we conducted experiments with asymmetric stretching rates. Three different types of experiments were performed (Fig. 3.3.8). In type (A) we applied a slow substrate stretch in the range of the threshold frequency $f_{t1}$ where not yet a cellular reorientation is observed ($f_{t1REF52}$ = 0.01 $s^{-1}$ and $f_{t1HDF1}$ = 0.1 $s^{-1}$, see Section 3.3.1 and 3.3.2). For the relaxation from the maximum strain back to position of zero strain, a frequency of $f$ = 1 $s^{-1}$, where the cells during an experiments with symmetric stretching rates reorient very well, is applied. An observation of a cellular orientation would mean that the back relaxation of the substrate causes the cellular response. In type (B) (Fig. 3.3.8) we exchanged the frequencies used in type (A). In this case a cellular response would lead to major importance of the strain process for the cellular response. In type (C) we stretched with f = 1 $s^{-1}$ and for the back relaxation we applied 5 $s^{-1}$ to determine if a higher frequency for the relaxation leads to a cellular reorientation.

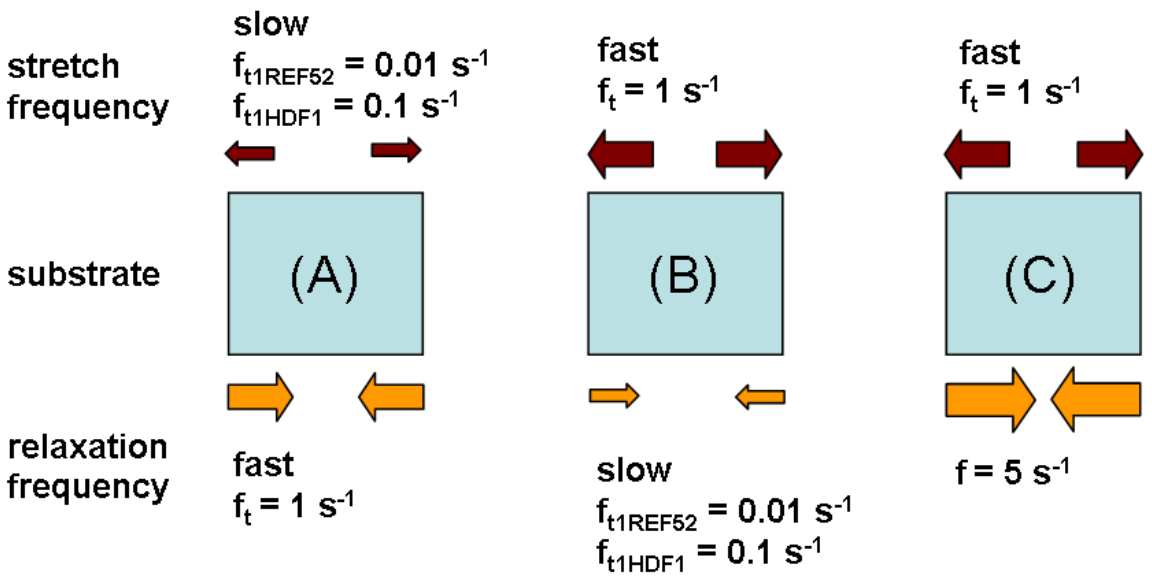


**Fig. 3.3.8: Scheme showing the different types of experiments to investigate the influence of different stretching rates. (A): the cells were stretched with the threshold frequency where not yet a cellular reorientation is observed and substrate relaxed back from the maximum strain to the zero position with a frequency at which the cells respond. If the cells react, the back relaxation of the substrate plays the major role for the cellular response. (B): the frequencies of type (A) were applied in the other way round. A cellular response leads to a major role of the substrate stretch. Type (C) was done to proof, if a faster back relaxation can influence the cellular response.**

Results for the time course of the mean order parameter $\langle\cos 2\varphi\rangle$ of both cell types are shown in Fig. 3.3.9. We discovered that both cell types do not react to a slow stretch and a fast relaxation (Fig. 3.3.9 A), but rather behave like cells in the control experiments without applied stretch.

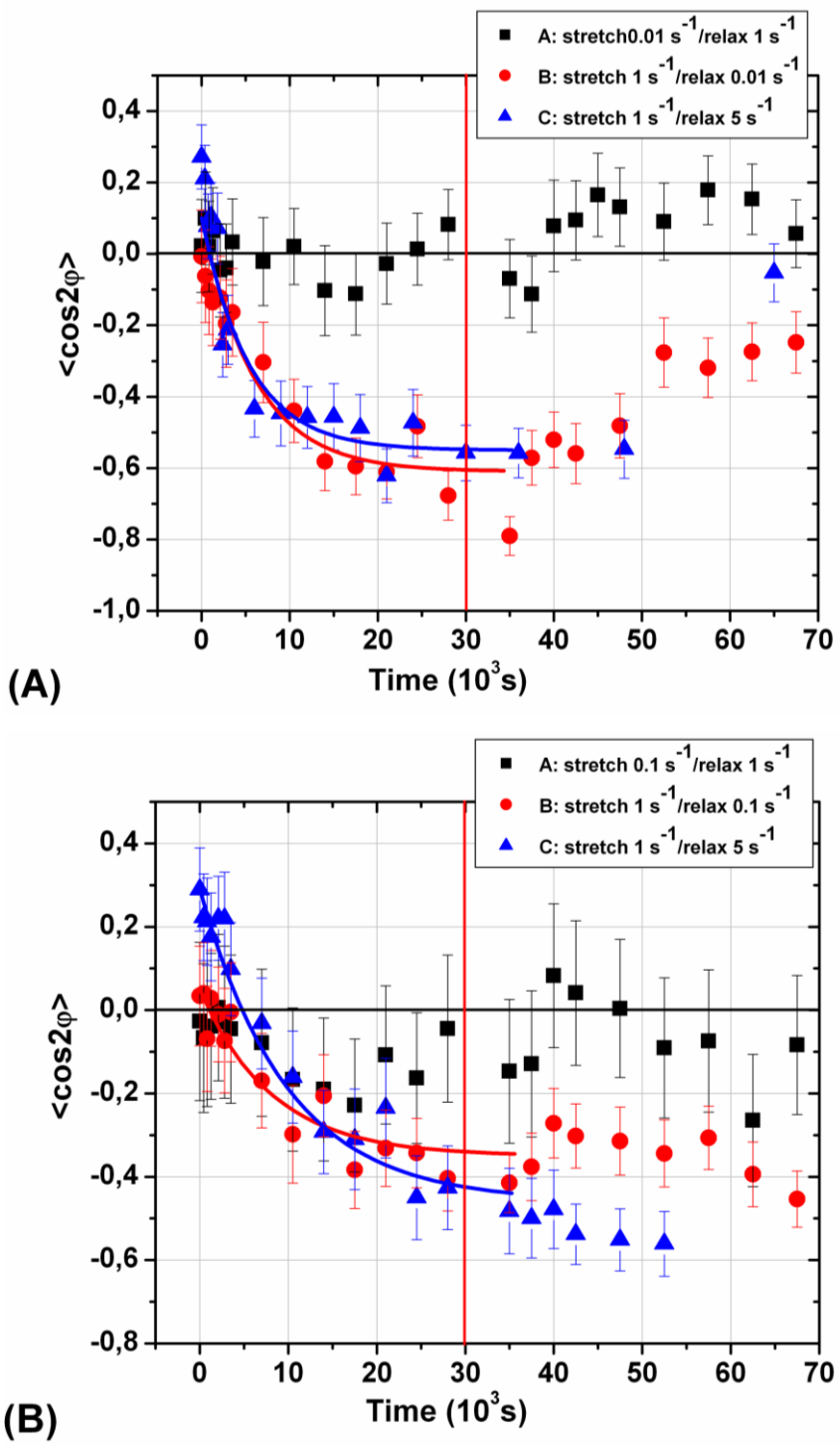


**Fig. 3.3.9: The influence of asymmetric stretching and relaxation rates on cells. (A): REF52 cells: *A*: substrate stretch: 0.01 $s^{-1}$ (no cellular reaction expected, according to Section 3.3.1); substrate relaxation: 1 $s^{-1}$ (cellular response expected, according to Section 3.3.1). *B*: substrate stretch: 1 $s^{-1}$; substrate relaxation: 0.01 $s^{-1}$. *C*: substrate stretch: 1 $s^{-1}$; substrate relaxation: 5 $s^{-1}$ (cellular response in saturation expected according to Section 3.3.3). (B): HDF1 sub-confluent cell layer: *A*: substrate stretch: 0.01 $s^{-1}$ (no cellular reaction expected according to Section 3.3.2); substrate relaxation: 1 $s^{-1}$ (cellular response expected according to Section 3.3.2). *B*: substrate stretch: 1 $s^{-1}$; substrate relaxation: 0.01 $s^{-1}$. *C*: substrate stretch: 1 $s^{-1}$; substrate relaxation: 5 $s^{-1}$ (cellular response in saturation expected according to Section 3.3.3). Stretching amplitude was a constant 8%. The vertical red line indicates the time point at which the stretch was stopped (30000 s).**

However, at a stretch of $f$ = 1 $s^{-1}$ and a relaxation of $f_{t1}$ = 0.01 $s^{-1}$, the REF52 cells reorient perpendicular to the stretch direction with a characteristic time of 6012.2 (± 851.7) s (Fig. 3.3.8, B) and in the experiment with $f$ = 1 $s^{-1}$ stretch and $f$ = 5 $s^{-1}$ relaxation they reorient perpendicular with a characteristic time of 5412.81 (± 10007.7) s (Fig. 3.3.8, C). These three types of experiments show that the relaxation of the substrate had hardly any influence on the cellular orientation response of the cells. If we compare the characteristic times we obtained in these experiments with asymmetric stretch and relaxation rates and the characteristic time for an experiment with a symmetric stretching rate at $f$ = 1 $s^{-1}$, we obtain a smaller characteristic time at the experiment with the symmetric stretching rate. This indicates a faster reorientation of the cells at symmetric stretching rates. We got similar results for the same measurements with HDF1 cells.

| | **REF52 Stretch:1 $s^{-1}$ Relax:0,01 $s^{-1}$** | **REF52 Stretch:1 $s^{-1}$ Relax:5 $s^{-1}$** | **REF52 1 $s^{-1}$ 8%** | **HDF1 Stretch:1 $s^{-1}$ Relax:0,01 $s^{-1}$** | **HDF1 Stretch:1 $s^{-1}$ Relax:5 $s^{-1}$** | **HDF1 1 $s^{-1}$ 8%** |
|---|---|---|---|---|---|---|
| **Characteristic time (s)** | **6012.2** | **5412.81** | **4376.2** | **8145.64** | **9821.1** | **7049.237** |
| **Error(s)** | **851.7** | **1007.7** | **1269.1** | **1287.42** | **771.84** | **477.8** |

**Table 3.3.1: Characteristic time for experiments REF52 and HDF1 cells involving different stretching rates, as compared to experiments performed with the same stretching rate. Stretching amplitude was a constant 8%.**

### 3.3.8 Discussion

The cellular reorientation process necessitates the continuous remodeling of focal adhesions and the actin cytoskeleton (Hayakawa *et al.* 2001; Kaunas *et al.* 2005; Na *et al.* 2007) as previously discussed (Section 3.2). The actin stress fibers need to be depolymerized and repolymerized; moreover continuous remodeling of focal adhesion sites is needed in cell migration, reorientation and shape changes. The temporal dynamics of these processes should correspond with the exponential time course of reorientation observed in our experiments. For both cell types, we observed the same time characteristic in dynamic behavior during cyclic stretch. Furthermore, the exponential characteristic was found to be independent of the frequency, if the signal is above a certain threshold. In previous studies researchers reported that the cellular reorientation process is primarily dependent on the stretch amplitude and not the stretching rate (Wang *et al.* 2001). However in our studies, we observed that the reorientation process is stretch rate dependent, so that we could not verify the findings of Wang *et. al*.

Apart from the exponential characteristic of the time course of the perpendicular cell alignment, some differences specific to cell types could be found. These differences included the various thresholds at which the cells began to respond to the cyclical stretch. The REF52 cells already began to respond at a stretch frequency of $f_{t1REF52}$ = 0.01 $s^{-1}$, while the HDF1 cells reacted only at a frequency that was ten times higher ($f_{HDF1}$ = 0.1 $s^{-1}$). This finding and the general faster reorientation of the REF52 cells led us to assume that REF52 cells are more sensitive to cyclical mechanical stretch.

Furthermore, when the mechanical stimulation was stopped the REF52 cells orient back into a random orientation, while the HDF1 cells remained oriented more or less perpendicular to the stretch direction. Compared to the REF52 cells, the HDF1 cells displayed greater quasi-plasticity, as also indicated by the ten times higher threshold for the reaction of the HDF1 cells. It seems that the HDF1 cells reorganize slower than the REF52 cells which could be attributed to variations in their cytoskeletal structures.

For a cell density of approximately 50 cells/$mm^2$, we observed two distinctive regimes for the frequency dependence of the characteristic time of reorientation. This behavior is analogous to the phase transition that occurs during cell spreading as described by Sheetz *et. al* (Dobereiner *et al.* 2004). The characteristic time decreased according to a power law, from a threshold frequency at which a response first becomes visible, to a saturation frequency of approximately $f_{t2}$ = 1 $s^{-1}$. For frequencies above $f_{t2}$ = 1 $s^{-1}$, we observed a regime in which the characteristic time remained constant, and an increase in frequency failed to accelerate the rate of cell reorientation. It seems that the molecular machinery of either sensory or actuation type reached a saturation level at frequencies above $f_{t2}$ = 1 $s^{-1}$, and was incapable of reacting any faster.

As sensory machinery we define all cellular elements which might be involved in the sensation of mechanical forces, such as focal adhesion or cadherins, while we define the actuation machinery as all cellular elements which are involved in the cellular reorientation process, such as the actin cytoskeleton.

It seems that for confluent cells, the molecular machinery was not in saturation which might be due to the fact that in addition to cell-matrix contacts via integrins, cell-cell contacts via cadherins were also present, and cadherins provide an additional mechanical sensing mechanism. Further studies involving the specific inhibition of individual signal transduction pathways or proteins, such as cadherins, could prove this hypothesis. Another way to gain deeper insight into the temporal characteristics of the mechanotransduction machinery would be to perform fluorescence recovery after photo bleaching (FRAP) experiments, so that we could observe the length of time required, for example, to reassemble focal adhesions.

One might speculate about the molecular origins of the lower threshold frequency and the saturation frequency $f_{t2}$ = 1 $s^{-1}$. By definition, mechanosensing requires at least one element that responds to an applied mechanical stimulus. However, there is yet to be a fully accepted, detailed understanding of which cellular components measure specific mechanical signals (Janmey and McCulloch 2007; Janmey and Weitz 2004). Elements known to play important roles in the cell's response to mechanical signals include cadherins in cell-cell contacts, and integrins in cell-substrate contacts (Chen *et al.* 2004; Ko and McCulloch 2001).

In experiments carried out with confluent cells we obtained no biphasic behavior and the cells could reorient themselves faster at all frequencies compared to the single cells. This finding suggests that the sensory system of the single cells is probably in saturation, rather than the actuation system. If the actuation system were the limitation factor, it would not be possible for the confluent cells to reorient themselves faster than the single cells, if we assume that there is no drastic structural or functional difference in their actin cytoskelet.

Previous studies revealed that the cytoskeletal architecture of cells tends to remodel itself in response to stretching (Hayakawa *et al.* 2001; Kaunas *et al.* 2005). This remodeling of the cytoskeletal architecture is an active cellular process controlled by signaling proteins; it has also been demonstrated that the level of Rho activity controls the extent and direction of orientation of stress fibers in stretched cells, and thus their elongation. Rho GTPase is known to be activated by integrin-triggered pathways (DeMali *et al.* 2003). Investigations of cells subjected to cyclical stretch by means of fluorescence resonance energy transfer measurements (FRET) could give more insight in the influence of these enzymes (Katsumi *et al.* 2002).

Typical time scales of focal adhesion formation and actin remodeling are on the order of 30 to 90 minutes (Geiger *et al.* 2001), stretching may influence directionality of protein polymerization or depolymerization (Hayakawa *et al.* 2001). Fast compression, for example, can lead to the disassembly of actin fibers within a minute (Costa *et al.* 2002).

Furthermore, our studies of fibroblasts during cyclcial stretch at different frequencies may advance the development of biophysical motivated modeling aimed to improve our understanding of mechanically induced cellular responses. There is currently no realistic theoretical model which could explain the actual force sensing mechanisms, and the internal reorganization of cellular components associated with the cellular response to stretch. On the other hand, a number of initial modeling approaches have been proposed to take into account different degrees of molecular detail in predicting certain aspects of cell orientation in response to periodic stretching (Chen 2006; De Rumi *et al.* 2007; Lazopoulos and Stamenovic 2006; Wei *et al.*).

A recent cell mechanical model centers on the concept "tensional homeostasis", and assumes that cells attempt to keep constant certain mechanical properties such as an optimal internal stress (Na *et al.* 2007; Rehfeldt and Discher 2007). Based on such an idea one model describes the cell as an elastic dipole interacting with a periodic external strain field (De Rumi *et al.* 2007), while assuming that an intrinsic relaxation time exists for the remodeling and readjustment of the cell orientation. This relaxation time is of unknown magnitude, and corresponds to the reorganization of actin stress fibers and focal adhesions. The theoretical model of De *et al.* predicts how the combination of active cellular forces due to (i) reorganization of the cytoskeleton and (ii) elastic forces exerted by the matrix, determines cellular orientation in the presence of both static and dynamic strains. The model predict that at high frequencies, the cells align nearly perpendicular to the stress direction, since they do not have sufficient time to relax the forces to relax and reorganize their cytoskeleton to establish the optimal stress (set point) in the adjacent matrix. In other words, they cannot instantaneously follow the external stress, and can only respond to the time average of the cyclical applied external force (De Rumi *et al.* 2007). Therefore, the cell response and the characteristic time are almost always frequency- independent, as was corroborated by our experiments (Section 3.3.3). As the frequency decreases, however, the characteristic time for the cells to reorient themselves increases, since the cells do have sufficient time to relax and reorganize their cytoskeleton, in order to establish the optimal stress (set point) in the adjacent matrix.

The model of De *et. al* predicts that in the low frequency regime, cells will orient themselves more parallel to the external stress direction, since internal cellular relaxation plays a crucial role, and eventually sets the characteristic time of the steady-state alignment. Besides the parallel cellular alignment at low frequencies, our findings demonstrate a qualitative agreement with the theoretical predictions which intuitively explain our observed bi-phasic characteristic frequency regimes (Safran *personal communication*). In contrast to other experiments (Brown *et al.* 1998; Eastwood *et al.* 1998) and the theoretical prediction (De Rumi *et al.* 2007), we did not detect significant cellular alignment in the direction parallel to the strain at very low frequencies ($0.0001s^{-1}$ and $0.001s^{-1}$). We assume that this difference might be explained by the cellular environment in our experiments, in which the cells were cultured on rather stiff PDMS substrates (Young's modulus approximately 1 MPa) coated

with a low concentration of fibronectin whereas Eastwood *et al.* (Eastwood *et al.* 1998) used a rather thick collagen lattice. The parallel orientation they observed might have been due to a mechanical alignment of collagen fibers and subsequent contact guidance of the fibroblast cells (Poole *et al.* 2005). However, preliminary experiments (detailed in Section Appendix A.1) with a different cell type (human mesenchymal stem cells) showed a parallel orientation at low frequencies, indicating a cell-type specific response. Of course, our experiments could not verify the accuracy of the theoretical model (De Rumi *et al.* 2007), but our experimental data do show some consistency with the model. Therefore, our results might provide important insights into a physically motivated understanding of these cell mechanical phenomena.

We also measured whether different frequencies could influence the maximum cell orientation. Previous studies by Wang *et al.* (Wang *et al.* 1995a; Wang 2000) suggested that the maximum angle of orientation was dependent on the elongation and the transverse compression of the cells. In addition to these results, we could show that in the case of the single cells, the cells align themselves more perpendicular to the stretching direction as the frequency increases. The reason that the maximum orientation is dependent on the frequency remains unclear, but it could represent an effect of the mechanosensing and mechanotransduction machinery.

When we conducted the same evaluation with a confluent cell layer, we observed a discontinuity between $f = 0.25\ s^{-1}$ and $f = 0.5\ s^{-1}$. Below $f = 0.25\ s^{-1}$, the maximum orientation of the cells remained more or less constant and above $f = 0.25\ s^{-1}$, the degree of orientation strongly increased. Furthermore, we observed some fluctuation between $\langle\cos 2\varphi\rangle_{MAX}$ =-0,75 and -0.9. As in the evaluation of the characteristic time, the cell-cell contacts likely played a certain role in mechanosensation and mechanotransduction. Perhaps there was a mechanical switch between $f = 0.25\ s^{-1}$ and $f = 0.5\ s^{-1}$, in which parts of the molecular machinery such as cadherins, became involved in mechanosensing and mechanotransduction. Therefore, experiments in which the cadherins are “knocked down” could give further insights into this process.

An explanation into the two effects, the biphasic behavior of the frequency dependence of the characteristic time, and the increase in the maximum orientation $\langle\cos 2\varphi\rangle_{MAX}$, could be found in the mechanotransduction and mechanosensory machinery of the cell. The time- dependent reaction kinetics of the reorientation process may be explained as previously mentioned, by a saturation of the sensory molecules. For a cell to sense an external force, a certain amount of time is required if, for example, a conformational change of the sensory protein, or for a phosphorylation of a protein such as focal adhesion kinase, is to occur. Above the threshold frequency of $f_{t2} = 1\ s^{-1}$, the time of 0.5 s is too short for relaxation of the protein, or for rephosphorylation process to occur, the sensing process cannot be done any faster. As a result, the characteristic time stays constant, at higher frequencies.

The maximum orientation angle is a degree for the strength of the cellular response and the amount of molecules involving the mechanosensation process could be crucial for this maximum orientation. If more molecules were stimulated, the maximum orientation angle would increase. We could not observe biphasic behavior for the maximum orientation, a finding which indicated that this process is not yet in saturation. It is also possible that over time, the expression of genes controlling the activity of the involved molecules increased, thereby preventing the saturation of the process.

Results of experiments in which cadherins were inhibited on a confluent cell layer could also help to explain the differences in lag time between sub-confluent and confluent cells. The lag time gives a value for the inertia of the cellular mechanics. In sub-confluent cell layers, we observed a decrease of the lag time as the frequency increased, implying an earlier response to the external force. For the confluent cells, the lag time was found to be constant and faster, compared to that of the sub-confluent cells. Experiments undertaken at higher time resolutions must be performed, in order to obtain more detailed results for the lag time. A “knockout” of the cadherins could also provide similar results for the lag time of the sub-confluent cell layers.

The results of the experiments with asymmetric stretch and relaxation rates that the stretch of the substrate to which the cells adhere, rather than the reverse relaxation of the substrate, is crucial to the cellular response.

This finding provides insight into how the cell measures cyclical stretch. It indicates that sensing is a stretch-dependent process, and relaxation plays a minor role. The mechanosensors themselves must involve mechanisms such as a stretch-dependent ion channel, stretch dependent proteins, or the stretch of the whole cytoskeleton.

Notably, we found that cells reoriented faster under experimental conditions in which relaxation and the stretch were equal, for example, with a symmetric stretching rate, a frequency of $f = 1\ s^{-1}$ than to an asymmetric stretching rate. The reasons for this effect remain unclear, and can only be explained by means of additional molecular biological methods. But whatever the exact reason is, it is clear that the complex process of mechanosensation and mechnaotransduction can be activated more easily under conditions of a constant, rather than changing stretch.

## 3.4 Reorientation dynamics of single cells in dependence of the stretching amplitude

Besides the stretching frequency, the stretching amplitude influences the cellular reorientation process of cells (Neidlinger-Wilke *et al.* 2001; Takemasa *et al.* 1997). Therefore, we conducted a study into how the amplitude affects the reorientation dynamics. The experiments were performed in a manner similar to those of the frequency studies. The frequency was kept constant at 1 $s^{-1}$, and the amplitude was varied between 1% and 15%, the limits of the experimental set-up. Both cell types, REF52 and HDF1, were tested. Fig. 3.4.1 depicts a sequence of a phase-contrast images of HDF1 cells for 3 different amplitudes.

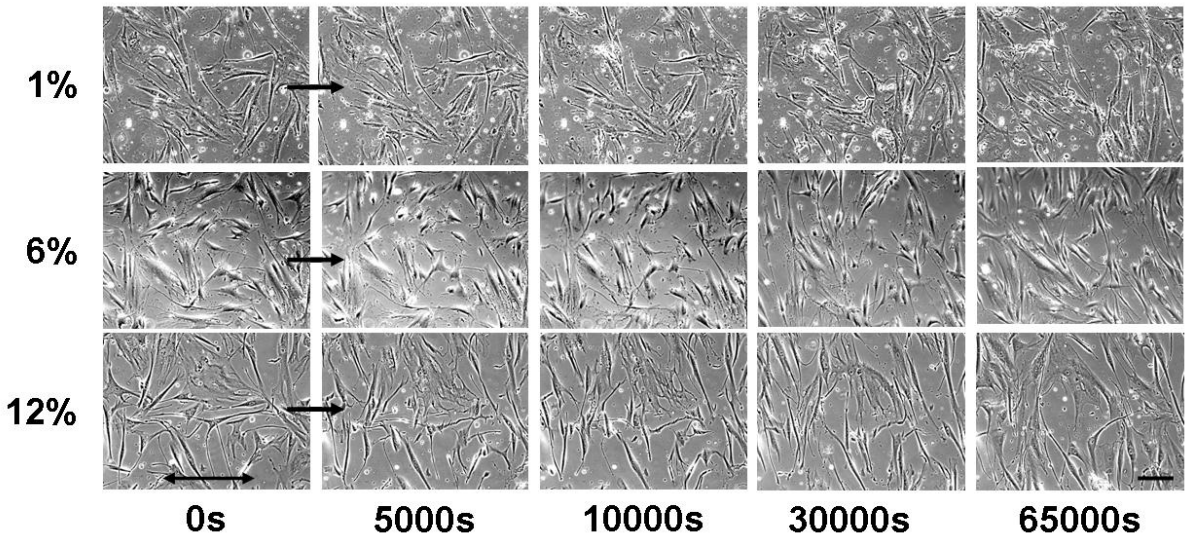


**Fig. 3.4.1: Phase-contrast images of human fibroblasts exposed to 3 different stretching amplitudes (1%, 6% and 12%). HDF1 cells showed no reaction at an amplitude of 1%, and a faster reaction as the amplitude increased. After 30000 s, the stretch was stopped. In contrast to the REF52 cells (Fig. 3.2.1), HDF1 cells remained in a perpendicular orientation. Black bar: 100µm**

HDF1 cells showed no orientation response to cyclical stretch at a frequency of $f = 1\ s^{-1}$, and a stretching amplitude of $A$ = 1%., Increasing amplitude correlated with an increased cellular response. At 6% amplitude, the cells reorient slower, compared to cellular reorientation at 12% amplitude.

The mechanical strain was stopped after 30000 s, and the cells were then observed for an additional 35000 s. The HDF1 cells remain oriented perpendicular to the stretch direction. The cells were then marked, and the order parameter $\langle\cos 2\varphi\rangle$ was plotted over time (Fig. 3.4.2).

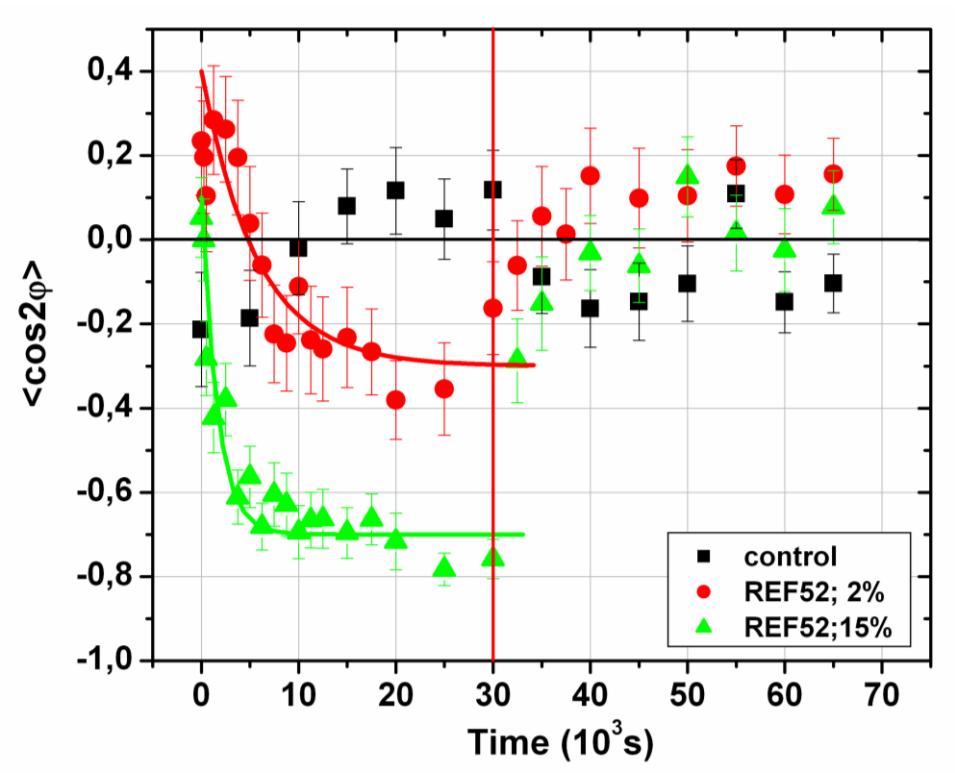


**Fig. 3.4.2: Order parameter <cos2φ> of REF52 cells during cyclical stretch for high (15%) and low amplitudes (2%). The stretch frequency was fixed at 1 $s^{-1}$. The characteristic time τ was determined by an exponential fit to the data. The vertical red line indicates the stop of the mechanical stretch.**

As in the frequency studies, the characteristic time τ was determined by an exponential fit of the time course of the mean order parameter.

In contrast to the frequency dependence of the reorientation dynamics, we can not observe a biphasic characteristic or a power-law characteristic in dependency of the amplitude. Furthermore, we could not observe much difference between the two cell types. The characteristic times for different amplitudes were nearly the same, and the slopes of the fit curves were also similar [REF52: - 510.57 (± 155.9); HDF1: - 673.75 (± 83.4); Fig. 3.4.3]. The only difference between the two cell types is the lowest amplitude, when cellular reorientation can be observed. The REF52 cells already began to reorient themselves at an amplitude of 1%, while the HDF1 cells first began to react at an amplitude of 2%.

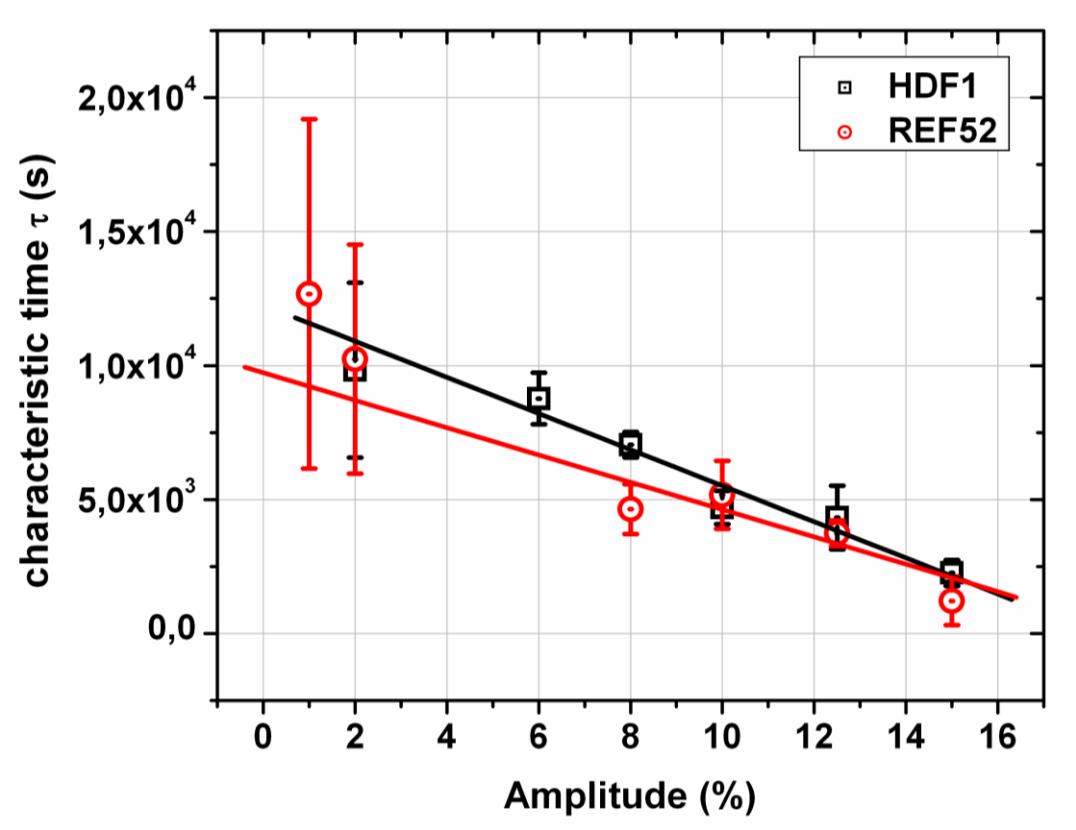


**Fig. 3.4.3: Characteristic time τ of REF52 and HDF1 cells, at different stretching amplitudes. As the stretch amplitude increase, the characteristic time decrease in a linear fashion [(□) =HDF1;(○) =REF52].**

We also evaluated the maximum angle of orientation, $<\cos 2\varphi>_{MAX}$, and its dependence on the amplitude, observing that $<\cos 2\varphi>_{MAX}$ decreased in a linear fashion, as the amplitude increased. These findings implies that the higher the amplitude, the more the cells aligned themselves perpendicular to the stretch direction. The degree of change of $<\cos 2\varphi>_{MAX}$ with the change in amplitude was similar for both cell types [slope of the fit: REF52: -0.048 (± 0.003); HDF1: -0.05 (± 0.003); Fig. 3.4.4]. At high amplitudes (15%), both cell types did not increase their angle of perpendicular orientation to the stretch direction. At this amplitude, it seems as if the orientation is approaching saturation, but this is speculation and must be proved by experiments which would include a 17% amplitude and even higher amplitudes.

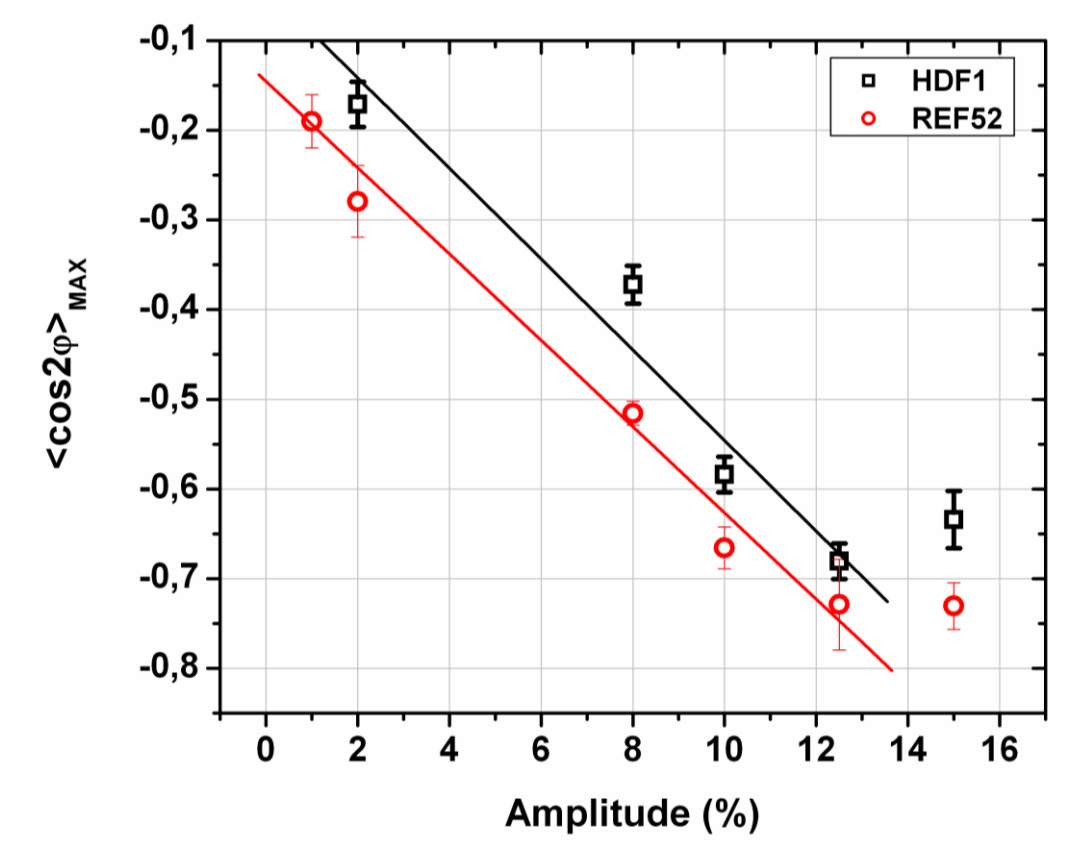


**Fig. 3.4.4: Maximum degree of orientation effecting dependency of different amplitudes for two different cell types. [(□)=HDF1;(○)=REF52]. $<\cos 2\varphi>_{MAX}$ increased in a linear fashion as the amplitude increased, and reached saturation at around 12%. The fit slopes were similar for both cell types [REF52: -0.048 (± 0.003); HDF1: -0.05 (± 0.003)].**

## Discussion

Investigations of the influence of the amplitude on the characteristic time τ of the reorientation process showed a linear dependency, in contrast to the power law and biphasic characteristic in dependency of the frequency. The larger the amplitude, the faster the cells reorient.

We observed that the REF52 cells were more sensitive to mechanical stimulation because they already respond at amplitudes of 1%, while the HDF1 cells respond at amplitudes of 2%. These threshold amplitudes are similar to the amplitudes which Dartsch (Dartsch *et al.* 1986) published for arterial smooth muscle cells (2%-3,5%). Apart from this difference between the REF52 cells and the HDF1 cells, the results for the characteristic time and the maximum orientation for both cell types were comparable. No major differences were found among the characteristic times for the different amplitudes. The slope of the linear dependency was nearly equal for both cell types. The reason for the decrease of the characteristic time with an increase of the amplitude is probably that the cytoskeleton is more easily disrupted and destroyed at higher amplitudes. This finding also implies the assumption that the disassembly of the actin fibers is accelerated, and the reorientation process occurs more rapidly.

In our experiments, evaluation of the maximum angle of orientation showed that the cells aligned themselves more perpendicular, as the amplitudes increased between 1% and 10%. The maximum orientation remained constant above a 10% stretch. These findings are in contrast to the studies of Neidlinger-Wilke (Neidlinger-Wilke *et al.* 2001) and Wang (Wang *et al.* 1995b), who reported that the strength (maximum orientation) of the cellular response was dependent on both the elongation and the compression of the cell. This implies that the strength of the cellular response is dependent on the kind of strain applied -- pure uniaxial strain, or equibiaxial, strain. These researchers suggested that the cellular orientation response constitutes an attempt to avoid both tensile and compressive axial surface strains. Wang *et al.* further hypothesized that the maximum orientation constituted an attempt by the cell to avoid the two stress factors, compression and elongation. Based on the assumption that greater elongation causes increased compression, the maximum orientation would be lower at higher amplitudes which we did not find to be the case.

The reason that we did not find a less perpendicular orientation at high amplitudes is probably due to the fact that in our experiments we did not use simple elongation strain. The substrates were clamped at all four sides and we had an almost pure uniaxial strain and we obtained a low transverse compression. As could be seen for the elongation amplitude, a certain threshold of strain was necessary, in order to generate a cellular response. In our case, the transverse compression was always around this threshold, indicating that the cells probably did not react to the compression. Therefore, we suggest that the cells respond faster and align more perpendicular as the amplitude increased. The reason and the underlying cellular causes for this behavior are still not clear.

We would expect that the cellular response can be dependent on the total inserted energy. We expected that this energy was a product of the external signals frequency and amplitude. Our measurements, however, showed a power law behavior for the variation of the frequency, and a linear behavior for the variation of the amplitude. This result shows that the stretching frequency influences the characteristic time of reorientation more than the amplitude. Therefore, we cannot simply predict that the inserted energy is a product of the external signals, obtained by multiplying the stretching frequency and the stretching amplitude.

## 3.5 Comparison of reorientation dynamics of cells from young and old donors

The age of the cell can also influence the dynamics of reorientation during cyclical stretch. We would expect that old cells would react slower than young cells. To investigate the role of cell age on cellular behavior, we examined human fibroblasts of three different young human donors (HDF1, HDF2 and HDF3) and cells from three different old human donors (HDF4, HDF5 and HDF6). The experiments were performed as described before (Section 3.3), dynamic reorientation of each of these cell types was observed. Following the quantitative analysis we compared the characteristic times of cell reorientation and the maximum angles of cell orientation.

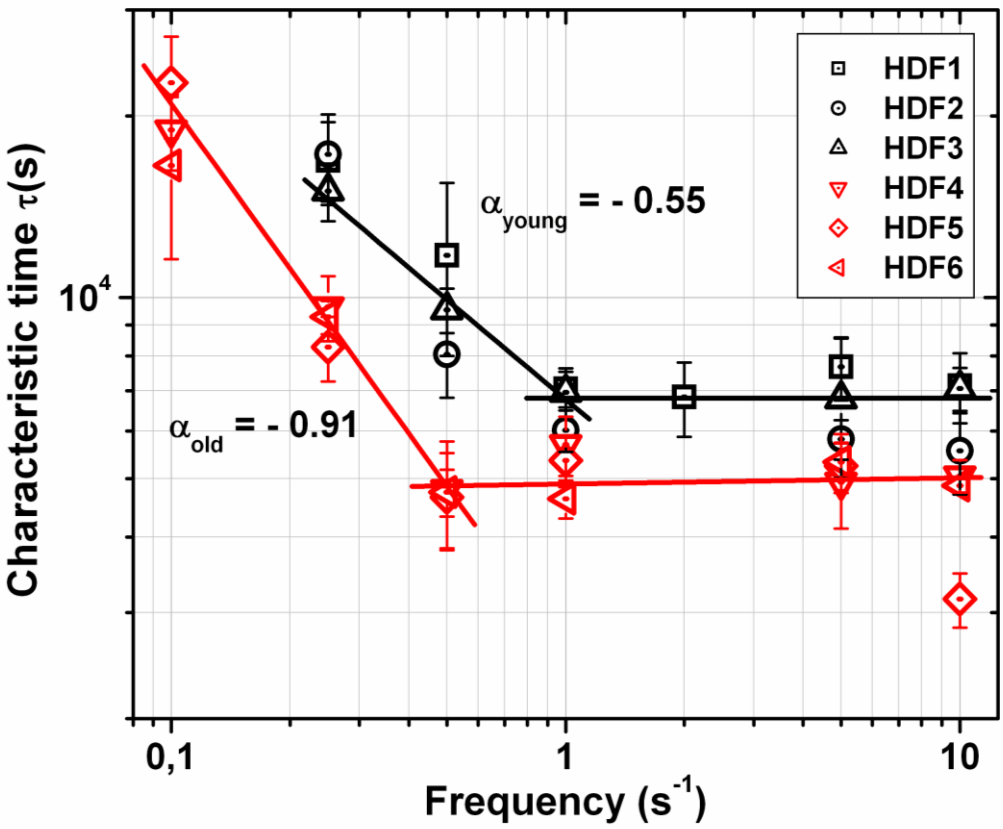


**Fig.3.5.1: A comparison of the characteristic times of reorientation of young (HDF1, HDF2 and HDF3) and old (HDF4, HDF5 and HDF6) fibroblasts. It is possible to clearly distinguish between young (black) and old (red) cells. The cells of old donors reorient faster during cyclical stretch. The slopes $\alpha_{young}$ = - 0.55 and $\alpha_{old}$ = - 0.91 demonstrate a faster decrease for the characteristic time for old cells with increasing frequencies. Furthermore, the threshold frequency for the start of the cellular reaction is ten times smaller for the old cells.**

Fig. 3.5.1 shows the characteristic times for the reorientation of cell types of different age. Contrary to our expectations, the old cells reoriented themselves faster than the young cells. For both cell types the characteristic time decreased with a power-law up to a certain threshold frequency $f_{t2}$ for an increase of the stretch frequency. For the old fibroblasts we

discovered a threshold frequency of $f_{t2}$ = 0.5 $s^{-1}$ while $f_{t2}$ = 1 $s^{-1}$ is the threshold frequency for the young fibroblasts. The old fibroblasts have lower characteristic times at all measured frequencies, meaning, that the old fibroblasts reorient themselves faster in general. This difference between the young and old cells is corroborated by a t-test between the mean characteristic times of the group of young and the group of old fibroblasts at all measured frequencies (Table 3.5.1). All p-values were below 0.05, indicating that the difference between young and old cells was, indeed, significant. Furthermore we can distinguish very well the difference between the results of the group of young and old cells. The slopes $\alpha_{young}$ = - 0.55 and $\alpha_{old}$ = - 0.91 during the power-law regime demonstrates that the characteristic time decreases faster with a frequency increase for the old cells compared to the young cells.
And if we are looking on the threshold frequency $f_{t1}$ at which the cells began to respond to the cyclic cal stretch this threshold frequency is ten times lower for the old cells ($f_{t1}$ = 0.01 $s^{-1}$) compared to the young cells ($f_{t1}$ = 0.1 $s^{-1}$). These findings demonstrate that the old cells are more sensitive to cyclical stretch than young cells.

| Frequency | P-Value of t-test |
|---|---|
| 0.25 | 0.000827 |
| 0.5 | 0.00947 |
| 1 | 0.03399 |
| 5 | 0.04484 |
| 10 | 0.04848 |

**Table 3.5.1: P-Value of the t-test when the characteristic times at different frequencies of young and old cells were compared. A p-Value of < 0.05 was considered to be a significant difference.**

The maximum angle of cellular orientation was also evaluated and is shown in Fig. 3.5.2. The results showed little fluctuation, but the higher the frequency, the closer to perpendicular was the cell alignment. In general, we observed that the old cells orient themselves more perpendicular to the stretch direction compared to the young cells.

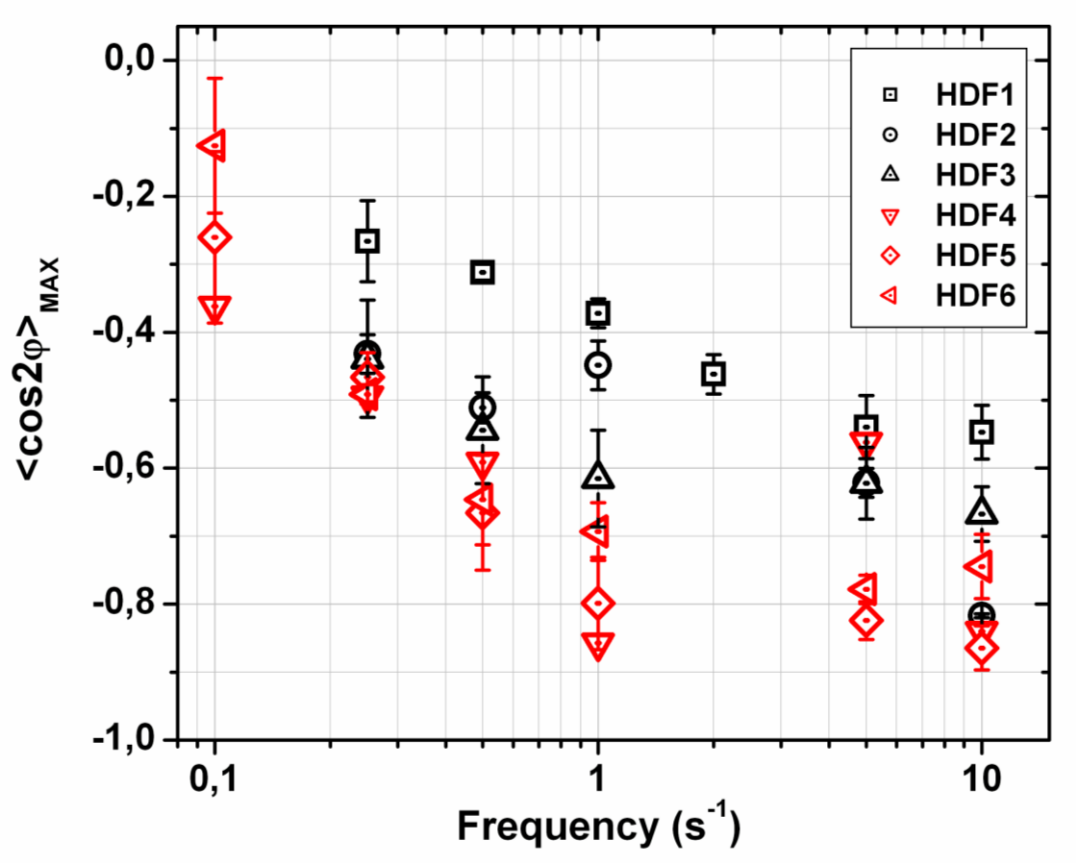


**Fig. 3.5.2: Comparison of the maximum orientation $<\cos 2\varphi>_{MAX}$ of young (HDF1, HDF2 and HDF3) and old (HDF4, HDF5 and HDF6) fibroblasts. $<\cos 2\varphi>_{MAX}$ increases with an increase of the stretch frequency. In general the old cells align more perpendicular compared to the young cells.**

## Discussion

We observed that fibroblasts from old donors respond faster to cyclical stretch than fibroblasts from young donors. Moreover, fibroblasts from old donors were found to be more sensitive to cyclical stretch and begin responding to such stretch at a lower frequency. The cells of old donors also showed two regimes for the characteristic time of the reorientation process, a power law decay of the characteristic time at frequencies below $f_{t2}$ = 0.5 $s^{-1}$, and a constant regime at frequencies above $f_{t2}$ = 0.5 $s^{-1}$. Furthermore, the old cells align more perpendicular with an increase of the stretch frequency.

The reason for this different behavior of old and young cells is not clear. One has to find certain differences between cells of old and young donors. The cell stiffness could be determined by probing the cells with an atomic force microscope (AFM) tip. Lieber and colleagues, for example (Lieber *et al.* 2004), demonstrated in rat cells that the stiffness of cardiac myocytes increased with age. Berdyyeva *et al.* (Berdyyeva *et al.* 2005) corroborated these results, showing that the stiffness of human epithelial cells increased with age. We did not yet test the mechanical properties of our cells by means of AFM, but if we assume that in our case, the cells of old donors are also stiffer than the cells of young donors, then our observation that the old cells react faster than the young cells could be caused by the

assumption that old cells have a more rigid cytoskeleton. Then we can assume, that mechanosensors linked to the cytoskeleton, such as p130CAS (Sawada *et. al* 2006), can be activated more easily, what leads to a faster reorientation.

Another explanation could be that young cells are more able to adjust to the external stress by means of cytoskeletal rearrangement: the younger cells were able to stabilize the cytoskeleton and work against the applied force, while the old cells could not.

The stability and turnover rate of the focal adhesions may differ between the cells of old and young donors, too. Therefore, experimental studies of the stability of the focal adhesions, carried out by means of fluorescence recovery after photobleaching (FRAP), could clarify the nature of differences between old and young cells.

Furthermore, it may also be possible that the genes expressed in old cells may differ from genes expressed in young cells. It is known, for example, that genes for DNA repair and stress response are up regulated in old cells of the human brain, while for example genes for vesicular transport or signaling are down regulated (Finkel *et al.* 2007; Lu *et al.* 2004). Difference in gene expression like in cells of the human brain can also occurs in other cell types, like our fibroblasts and this may influence the cellular response to cyclical stretch. This issue has not yet been investigated and to clarify the influence of the difference of the gene programs of cells from young and old donors on the cellular reaction has to be investigated. More studies such as the investigation of different specific genes, involved in the reorientation process, such as the genes encoding actin or Rhokinase, has to be done by means of polymerase chain reaction (PCR) and real-time polymerase chain reaction PCR (qRT-PCR) in dependency of cyclical stretch.

## 3.6 Change of strain direction

With our stretching device, it is possible to stretch the cells along the x- and y-axis. In the following experiment, we stretched the substrate twice in each direction, alternating between the x- and y- axes and, in the last phase, ending with a stretch along the y-axis. The duration of each stretching phase in a given direction was 30000 s; the entire experiment took 120000 s. The stretch frequency was 1 $s^{-1}$ and the stretch amplitude was 8%; moreover, both cell types, REF52 and HDF1, were investigated. Time-lapse movies of the experiment were taken, analyzed, and the results plotted as in previous experiments (Section 3.3).

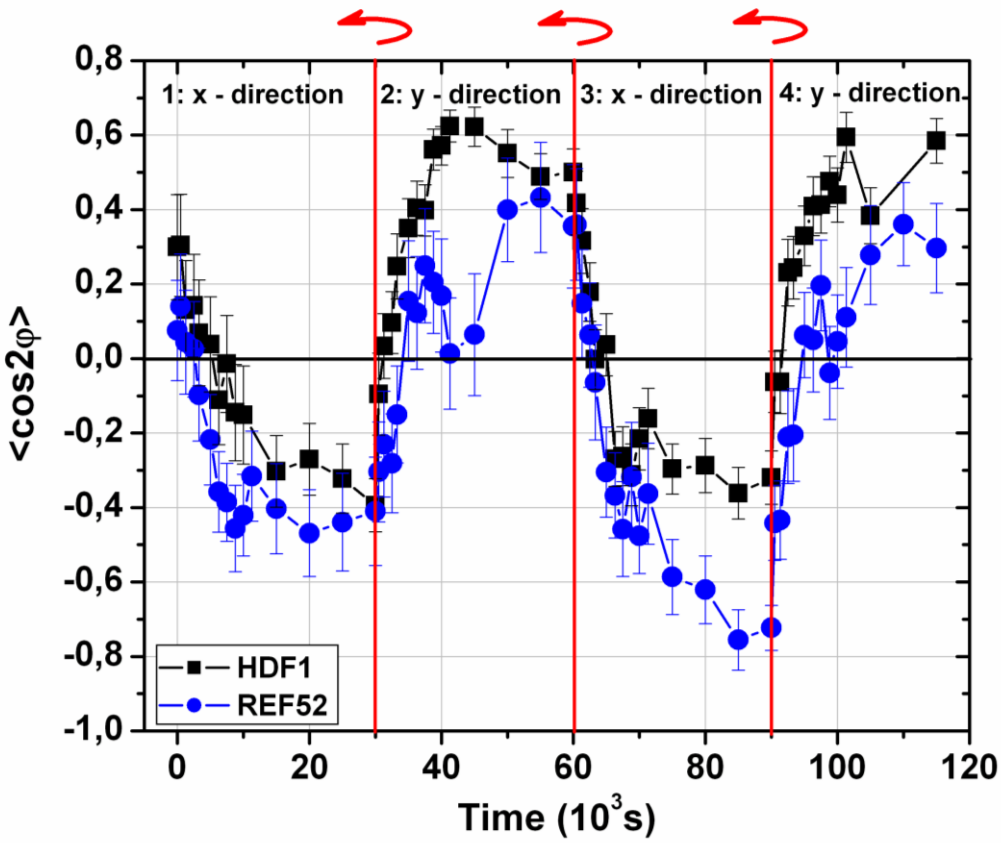


**Fig. 3.6.1: Temporal characteristics of the order parameter <cos2φ> after a change in the stretching direction. Stretch frequency: 1 $s^{-1}$; stretch amplitude: 8%. Phases 1 and 3: Stretch along the x-axis; Phases 2 and 4: Stretch along the y-axis.**

Figure 3.6.1 demonstrates that the cells behaved in the same manner as they did during the previous stretch experiments (Section 3.3). Following a change in the stretch direction, the cells began to realign themselves once again perpendicular to the new stretch direction. This behavior implied that the cells were turning from <cos2φ>= - 1 to <cos2φ>= + 1. As we had in the previous experiments (Section 3.3), we were then able to determine the characteristic times for these reorientation processes for all stretch phases, and compare the characteristic time in each stretch phase and compare them with each others.

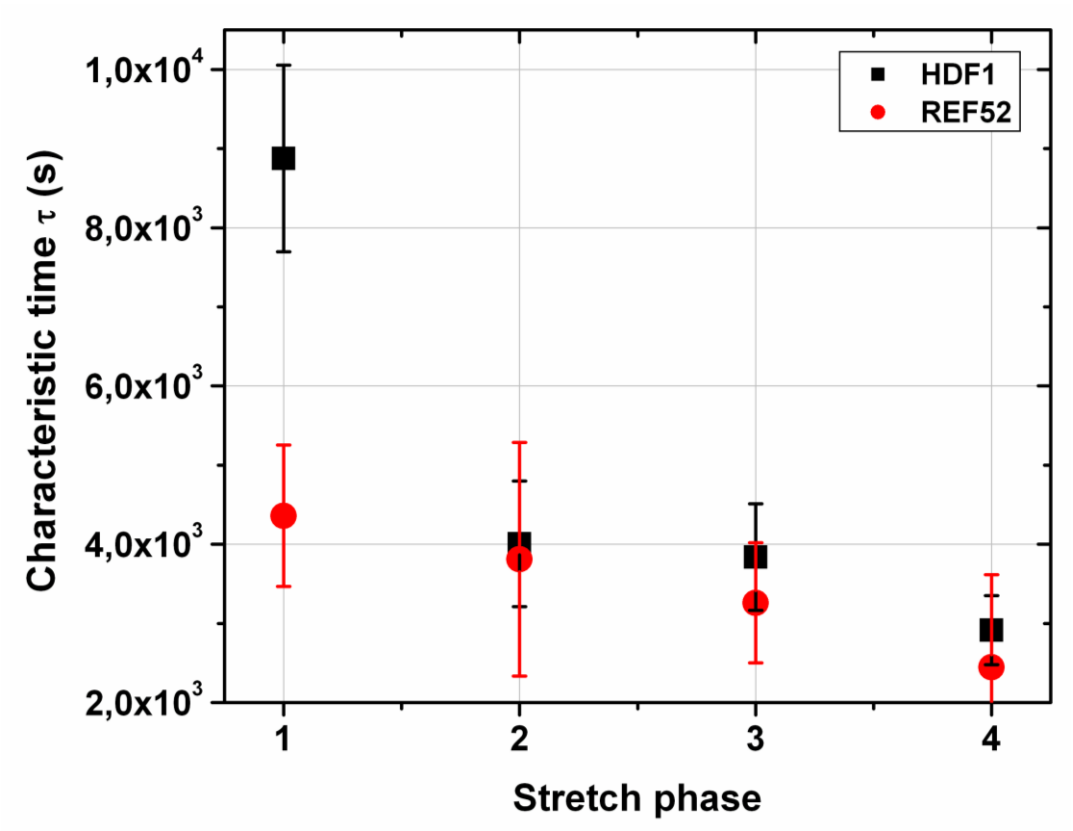


**Fig. 3.6.2: Characteristic time of the cell reorientation for the different stretch phases. Phases 1 and 3: Stretch along the x-axis; Phases 2 and 4: Stretch along the y-axis.**

For both cell types, we could see that the characteristic time for the cellular reorientation process decreased, with each change in the stretch direction (Fig. 3.6.2) and the cells reoriented themselves faster after each change. For REF52 cells, we observed a linear decrease in the characteristic time take, in all four stretch phases. The HDF1 cells displayed a linear decrease after the first change in direction.

## Discussion

The purpose of the experiments involving changes in the stretch direction was primarily to see if the cells adapt to externally applied stress. In this section we wanted to investigate if the cells can adjust to the stretch and react faster when we changed the stretch direction. If they react faster, this could represent a kind of “memory” of the stress, such that the cells could adapt faster to a state with less stress.

The results of these experiments demonstrated that the characteristic time for cellular reorganization became shorter each time the stretch direction was changed, meaning that the cells reacted faster after each change in direction. We can only speculate about the reason behind the decrease of the characteristic time. It could be caused by a passive mechanical process, or by an active process, meaning that the cell could actually memorize both the degree of stretch and the stretch direction and react accordingly by adjusting the organization of its cytoskeleton.

An explanation for the faster reorientation after each change of the stretching direction may be that the sensory and actuation machinery of a cell has to be activated. At the start of the experiment, the cells were in a relaxed state. After mechanical stress was applied in Phase 1, the cells had to respond to the stress. This reaction could have resulted from the activation of certain genes involved in cytoskeletal reorganization, or the expression of certain stress genes. By the time Phase 2 began, and the stretch direction was changed, the machinery underlying the cellular response to mechanical stress had already been activated; therefore the cells could reorient faster. One could say as soon as the cellular machinery is activated and the gene programs are switched on the cell can faster adjust to a change of the external signal. The fact that the HDF1 cells did not display a strong decrease between the first and the second stretching phases may have resulted that the activation of the cellular machinery for the reorientation process requires more time compared to the REF52 cells.

In order to better understand and even prove this hypothesis, certain reporter genes could be investigated at various time points during the different stretching phases, by means of real-time polymerase chain reaction PCR (qRT-PCR)

## 3.7 The reorganization of focal adhesions as a result of cyclical stretch

To investigate the dynamic behavior of cells during cyclical stretch, we observed the REF52 and human fibroblasts by means of phase contrast microscopy. In order to focus on the reorganization of the focal adhesions themselves, we tried to observe stable transfected REF cells by fluorescence microscopy. In our case, the focal adhesion protein paxillin was labeled with yellow fluorescent protein (YFP).

To avoid bleaching effects by the fluorescent light, fewer images were taken compared to the phase contrast experiments. The reorganization of the focal adhesions of single cells was analyzed in the same way as the phase contrast images. Therefore, the focal adhesions were marked by means of imaging software (NIH object image), and analyzed with the same software and in the same way as the fibroblasts in previous experiments (Section 3.2-3.5). Afterwards, both the orientation and the elongation of the focal adhesions were measured.

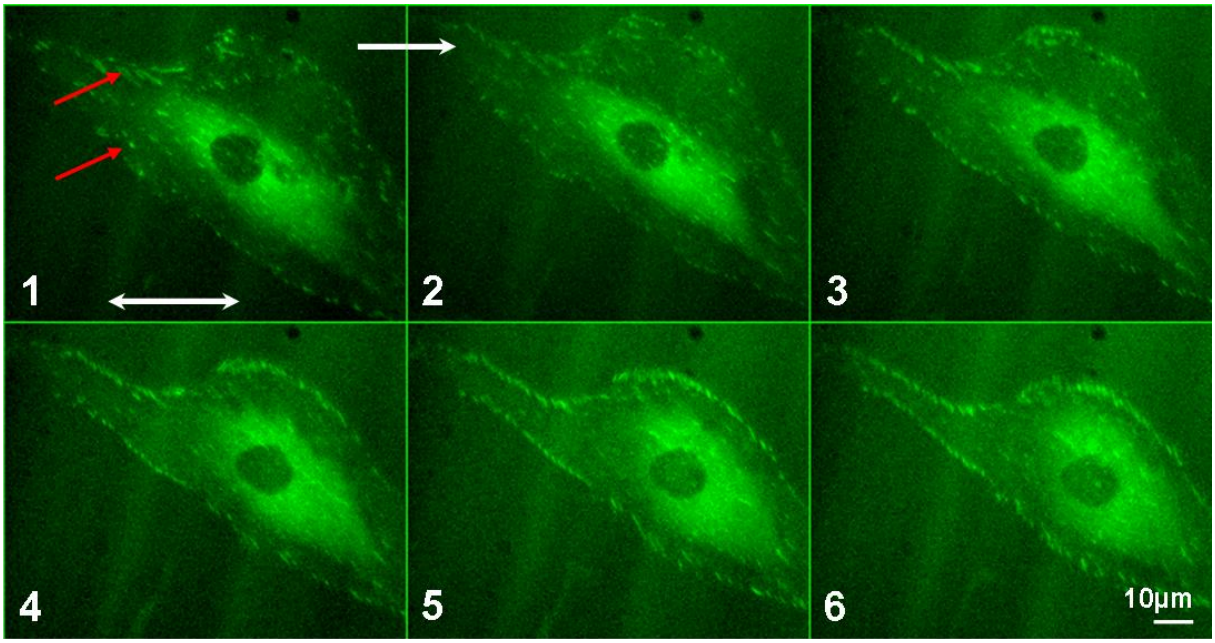


**Fig. 3.7.1: Sequence of fluorescent images of an REF-YFP-labeled cell. Stretch: 1 $s^{-1}$; 8%. Time points: 1: 0 s; 2: 600 s; 3: 1400 s; 4: 2200 s; 5: 3000 s; 6: 4200 s. Red arrow: focal adhesion. The focal adhesions disassemble and round up at the beginning of the experiment. Following the rounding up they reoriented perpendicular to the stretch direction, and elongated again.**

Figure 3.7.1 depicts a sequence of fluorescence images of a REF52-YFP-paxillin labeled cell. The images were obtained at 6 different time points (1: 0 s; 2: 600 s; 3: 1400 s; 4: 2200 s; 5: 3000 s; 6: 4200 s); the red arrow in Panel 1 indicates a focal adhesion sites.

Once the stretch begun, the focal adhesions start to disassemble. During the reassembly period they begin to orient themselves perpendicular to the stretching direction, as we observed for the whole cell itself. After the reorientation process the focal adhesions grow along the orientation direction. The focal adhesions in the center region of the cell begin to

disappear when the stretch begins while at the periphery of the cell, more focal adhesions appear.

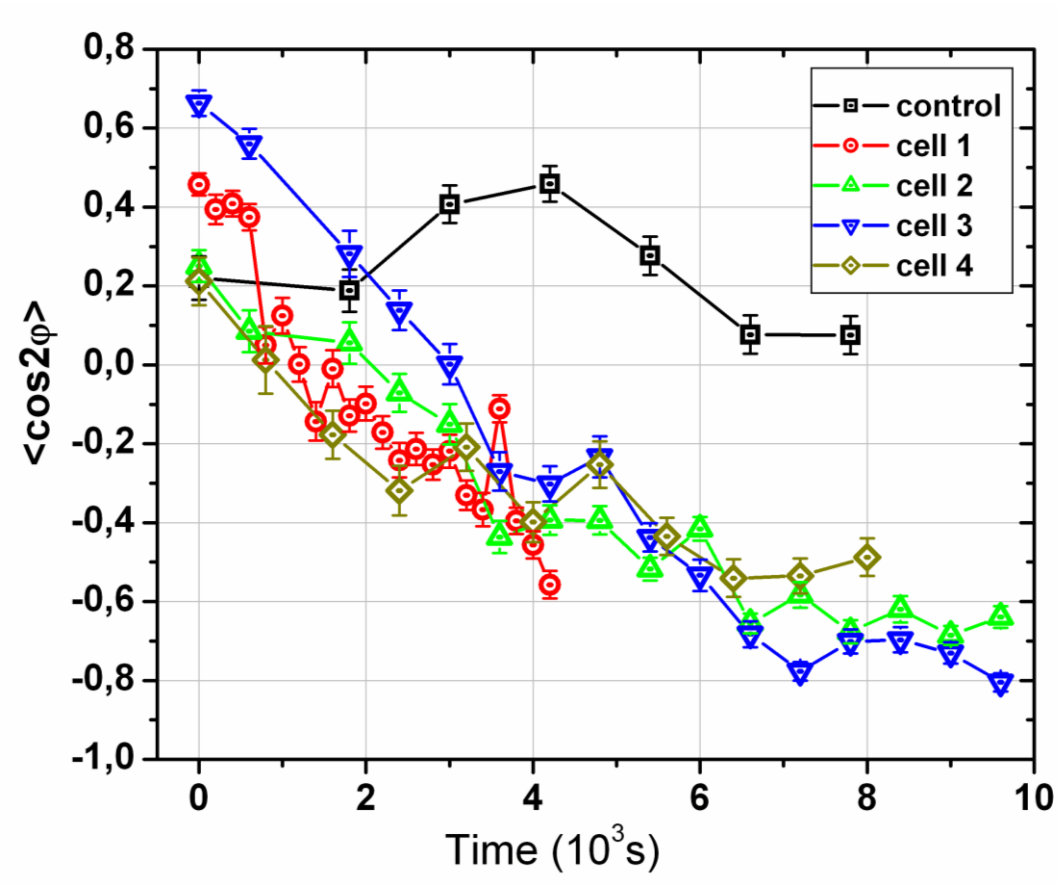


**Fig.3.7.2: Time course of the mean orientation <cos2φ> of focal adhesions during cyclical stretch for four different cells (stretch frequency 1 $s^{-1}$ and stretch amplitude 8%). The black line shows the control cell without any stretch.**

Results concerning the focal adhesions were evaluated in a manner similar to the results for the entire cell; the time course of the mean orientation was then plotted (Fig. 3.7.2). Results were fitted by a curve by means of a simple exponential function, and the characteristic time $\tau_{FA}$ for the reorientation process for the focal adhesions was determined, plotted and compared with the results we obtained for the entire cell (Fig.3.7.3)

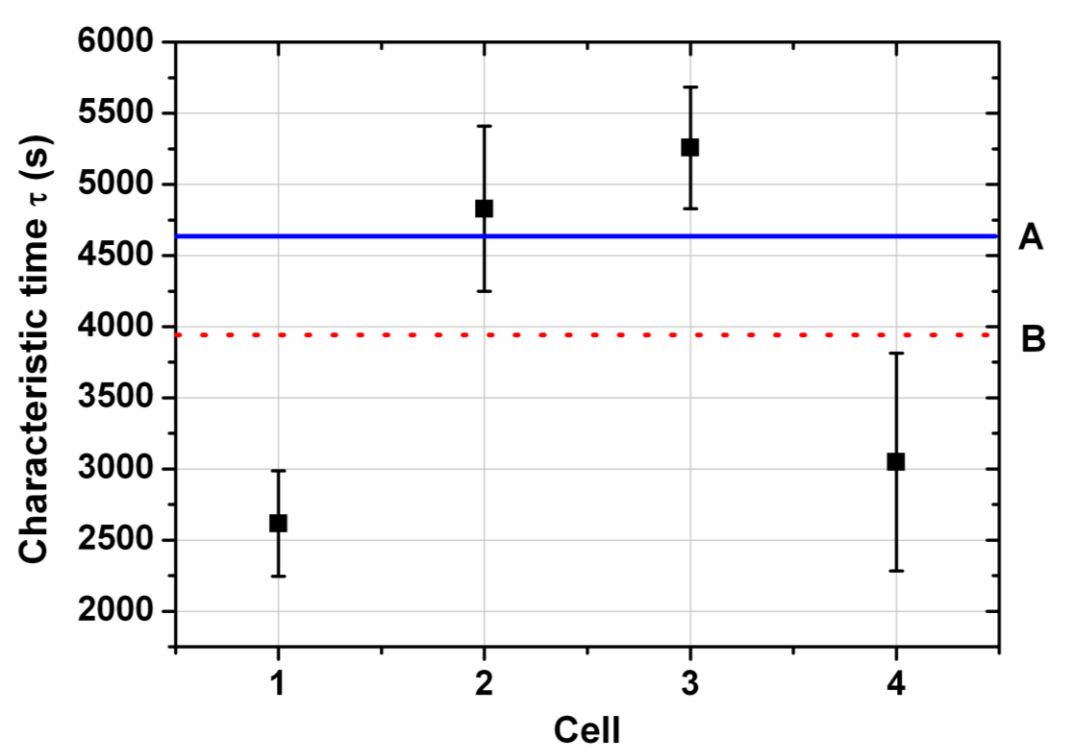


**Fig.3.673: Characteristic time of focal adhesion reorientation during cyclical stretch ($1s^{-1}$; 8%). A: Characteristic time of REF52 cells (Section 3.3). B: Mean value of $\tau_{FA}$ of cell 1- cell 4. The focal adhesions reorient faster than the entire cell.**

The mean value for the characteristic time of all four cells was found to be 3937.8 s. Compared with the characteristic time of the reorientation of the entire cells (4625.2 s), under the same experimental conditions, we found that the focal adhesions reoriented themselves faster. However, the characteristic time for the reorientation of the focal adhesions could also be like the characteristic time for the reorientation of the entire cell. The measurement of four cells is too less for a statistical significant result.

Like the whole cells, the focal adhesions assumed a spheroid shape, after the stretch began. They disassemble and once they orientated themselves, they began to reassemble again and elongate in the direction of the orientation (Fig. 3.7.4).

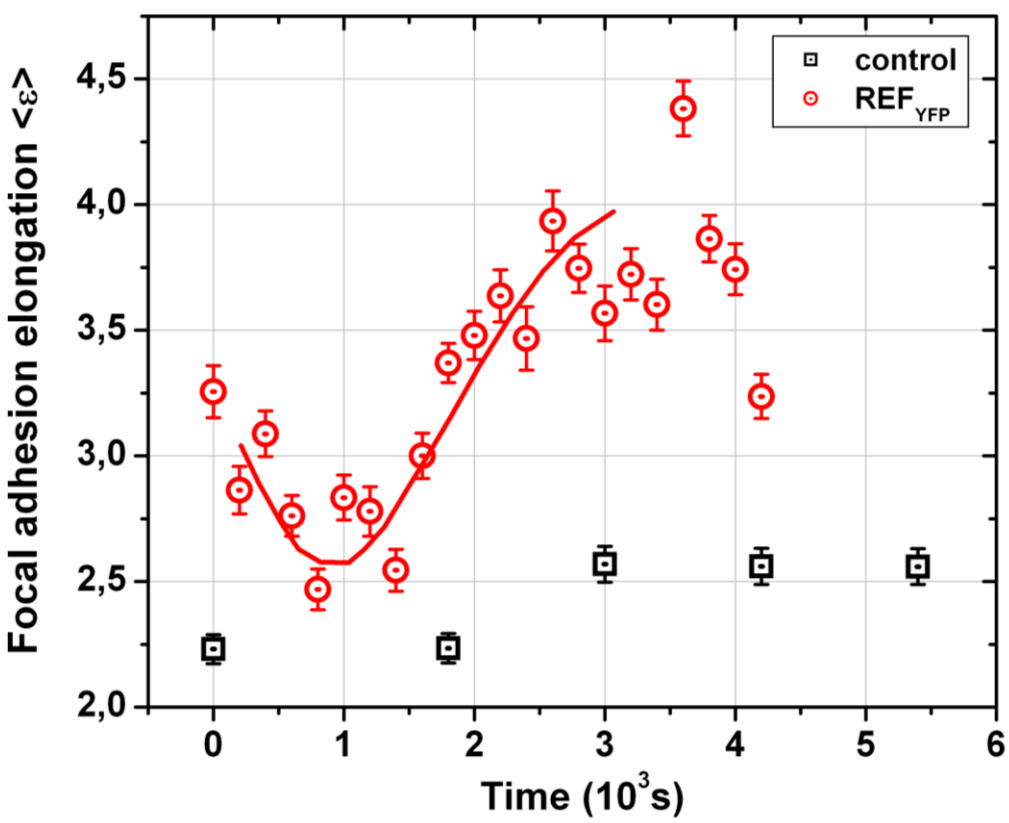


**Fig. 3.7.4: Example of the elongation of a focal adhesion in one cell during cyclical stretch (red), compared with a control cell (black). When the stretch is started the focal adhesions begin to disassemble and round up. Following they are elongating again in the new orientation direction.**

## Discussion

In cell stretching experiments conducted by Riveline (Riveline *et al.* 2001), a single cell was pulled by exerting force through a glass pipette in one direction. The force was applied only for one cycle. These conditions differ from those used in our experiments, in which we used a permanent change of stretch and relaxation.

They observed growth of the focal adhesions in the pulling direction. This finding is in contrast to our results which demonstrated that the focal adhesions shrink and then reorient perpendicular to the stretch direction (Fig. 3.6.4), similar to our findings for the whole cell. Furthermore, we observed that the focal adhesions were initially distributed over the whole cell, whereas during stretch, they arrange themselves at the edge of the cell. The characteristic time of the reorientation process was found to be faster than the characteristic time it took for the reorganization of the whole process, corroborating our assumption that the focal adhesions reorient themselves first, and the rest of the cell then follows. However, this finding has to be corroborated by more measurements to get a higher statistic than for four cells.

Little is known about how cyclical strain affects the reorientation process of the focal adhesions. Some theoretical models arose to describe the results of Riveline *et al.* (Besser and Safran 2006; Bischofs IB 2003; Schwarz *et al.* 2002; Schwarz and Safran 2002; Shemesh *et al.* 2005). One hypothesis suggests that the focal adhesions dispersed by the stretch cause the uptake of more focal adhesion molecules, and a corresponding growth of the focal adhesion in the stretch direction. If that is the case, compression of the focal adhesions would cause them to shrink in size (Shemesh *et al.* 2005). However our results of the studies of the influence of variable stretching rate on the cellular reorientation (Section 3.3.7) showed that the reorientation process is almost independent of the substrate relaxation.

To gain a deeper understanding of the activity and the role of the focal adhesions it is necessary to perform knock-out studies, for example, of vinculin. Vinculin is a focal adhesion protein that is involved in the linkage of integrins to the actin cytoskeleton. A knock-out of this protein would prove if vinculin is involved in the mechanotransduction process (Geiger and Bershadsky 2002; Sawada *et al.* 2006). Furthermore, FRAP measurements could provide additional insight into role of focal adhesions during the cellular response at cyclical stretch.

## 3.8 Cell division during cyclical stretch

In our time-lapse movies of cellular behavior during cyclical stretch, we could also observe the process of cell division. It is obvious, that in some movies, more cells divide, once the cyclical strain had stopped. A quantitatively analysis of cell division in each experiment for both cell types was done, Accordingly, cells undergoing cell division during both the stretching and relaxation periods were counted, and the results plotted in Figs. 3.8.1 and 3.8.2.

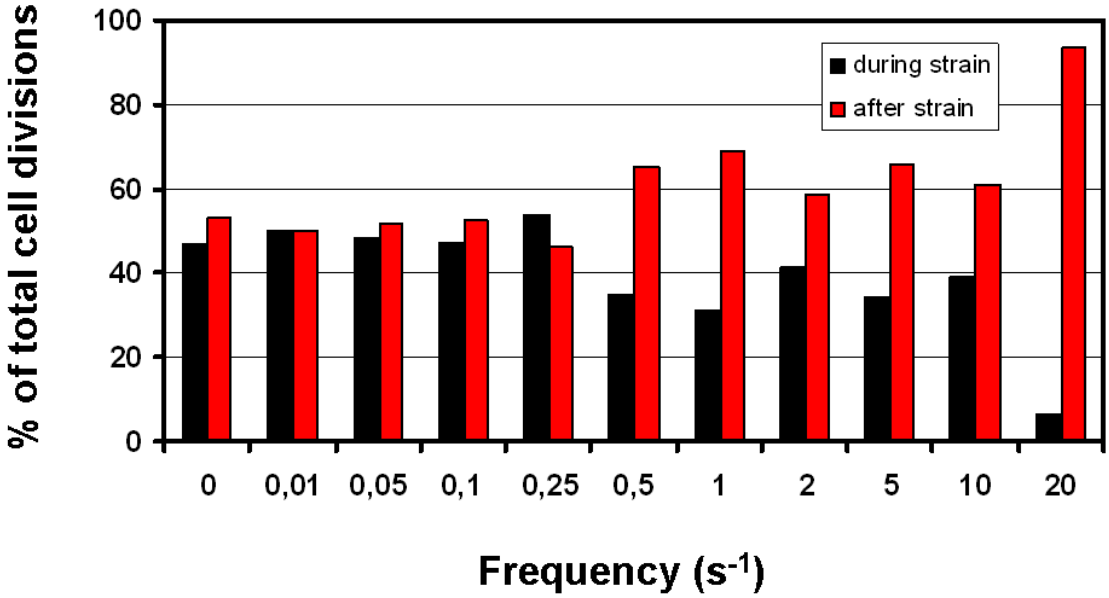


**Fig. 3.8.1: Percentage of cell divisions of REF52 cells during cyclical stretch before (black) and after (red) the cyclical stretch has stopped. The control experiment was performed with no stretch applied (frequency = 0 $s^{-1}$). At a frequency of 0.5 $s^{-1}$, we could observe a decrease in the number of cell divisions during stretch, and an increase in the number of cell divisions, after the stretch had ceased.**

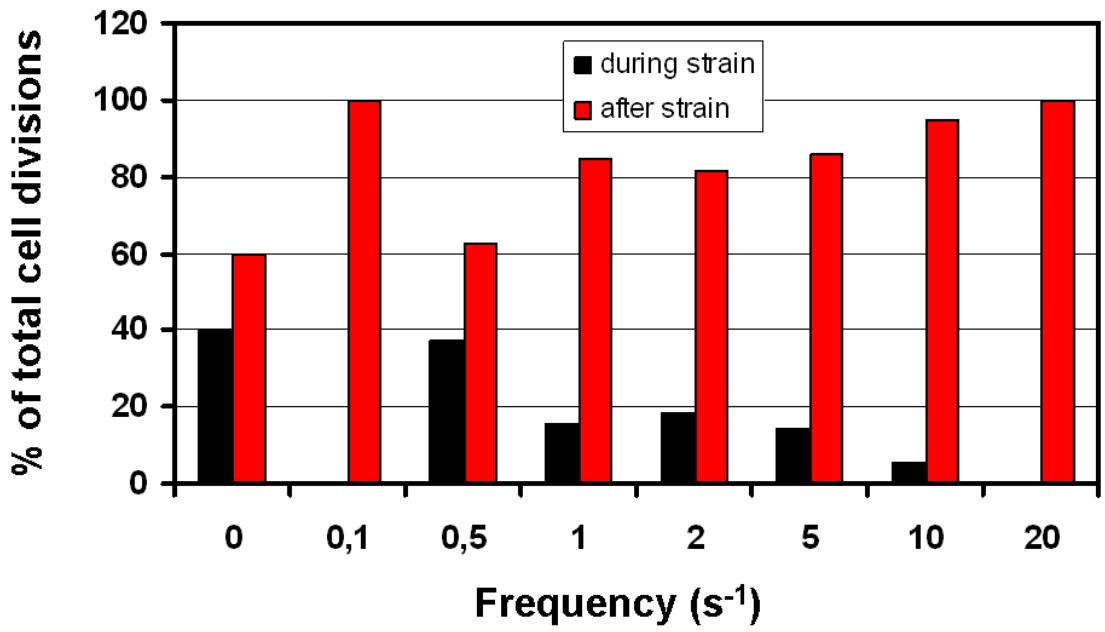


**Fig. 3.8.2: Percentage of cell divisions of HDF1 cells during cyclical stretch before (black) and after (red) the cyclical stretch had stopped. The control experiment was performed with no stretch applied (frequency = 0 $s^{-1}$).**

We counted the cell divisions during the stretch period and during the relaxation period, after the stretch was stopped. The number of cell divisions was uniformly distributed during the control experiments, in which no mechanical stretch was applied ($f$ = 0 $s^{-1}$). We could make the same observation at experiments conducted at a low stretching frequencies up to $f$ = 0.25 $s^{-1}$. However, at a frequency of $f$ = 0.5 $s^{-1}$ and above ( up to $f$ = 20 $s^{-1}$), we could observe a decrease in the total number of cell divisions during the stretching period, and an increase in the total number of cell divisions during the relaxation period, once the stretch was stopped. This behavior could be observed in both cell types. However, for the HDF1 cells the results are not as clear as the results for the REF52 cells (Fig. 3.8.2). This is related to the fact that the proliferation rate of the HDF1 cells is lower compared to the REF52 cells. Therefore, HDF1 cells undergo fewer cell divisions, compared to the REF52 cells and the statistic is very low. For example at the experiment where the HDF cells where stretch with a frequency of $f$ = 1 $s^{-1}$, we could observe only one cell division after the strain is stopped.

## Discussion

Various studies showed that cyclic stretch can influence the proliferation of cells (Guoguang Yang 2004; Kaspar *et al.* 2002; Miller *et al.* 2000; Neidlinger-Wilke *et al.* 1994). In these studies, the dependency of proliferation on the load cycles (time period of cyclical strain) and the stretch amplitude was observed. In our experimental set-up, we could observe single cells during the stretch at different frequencies, and after the stretch is ceased, and quantitatively analyze the cell divisions.

We observed that at a certain frequency of $f = 0.5\ s^{-1}$ the cell division decreased during stretch and increased, once the stretch is stopped. The phenomenon that cell division is influenced by cyclical stretch could be explained with the disturbance of the molecular machinery underlying cell division (e.g., the microtubules and the chromosomal division) by the mechanical strain at higher frequencies. If this is the case, cells might try to build, for example, a mitotic spindle which would be destroyed by the external force, thereby bringing cell division to a halt. During the relaxation period, with no force acting on the cell, it would again be possible for the cell to build up all the necessary constructions and cell division would proceed normally.

To get a deeper insight of the dependence of cell division on cyclical stretch one has to perform experiments by means of fluorescently-labeled proteins such as centrin, or by the uptake of Bromdesoxyuridin (BrdU) at different time points during the cyclical stretch.

Another possible explanation could be that a certain program involving stress genes is switched on during the stretch, thereby halting cell division. When the stretch is switched off, the external stress disappears and the stress program, in turn, is also switched off resulting in renewed cell divisions. This possibly could be evaluated by means of PCR studies.

## 3.9 Summary of the results

- We observed that the time course of the mean orientation <cos2φ> for the reorganization of rat embryonic fibroblasts, human fibroblasts and human mesenchymal stem cells increases exponentially in response to cyclical mechanical stretch. The cells round up and then elongate again in the new direction during the orientation process. Furthermore, the cells decrease the cell area during the reorientation process.

- The characteristic time of the reorientation process demonstrate a general biphasic response characteristic for low cell densities (single cells). The characteristic time decrease with a power law as the frequency increase, up to a certain threshold frequency of $f = 1s^{-1}$. Above this frequency, the characteristic time remain constant. For confluent cells, we could not observe this biphasic behavior. In this case the characteristic time decreases with a power-law in dependency of the frequency.

- The reorientation process was not only dependent on the cell density. We could also observe specific differences between the cell types. The REF52 cells reorient faster, more perpendicular and at lower frequencies, compared to the HDF1 cells

- We found a linear decrease of the characteristic time as the amplitude increase.

- The angle of the maximum orientation increases with an increase of either frequency or amplitude.

- It was demonstrated, that stretch, rather than the relaxation of the substrates, caused the cellular responses.

- We observe a linear decrease in the characteristic time after every change of the stretch direction

- Cyclical stretch can influence cell division. Above a certain frequency, we observed that the number of cell divisions decrease during the stretch, and increase, once the stretch was stopped.

- Studies with old and young cells showed that fibroblasts from young donors oriented themselves slower than fibroblasts from old donors. Furthermore we observed that the old cells were more sensitive to cyclical stretch.

# 4. Conclusions and Outlook

We developed a new stretching apparatus for live-cell imaging which enables us to observe the dynamic behavior of cells during cyclical stretch of their adhesive substrate. Compared to other systems, such as those of Neidlinger-Wilke (Neidlinger-Wilke *et al.* 1994) or the commercially available Flexercell system (Flexcell Int. Corp., Hillsborough, NC, USA), we could observe the behavior of living cells by means of live-cell imaging. Moreover, we could apply a defined strain by varying the stretching amplitude and the stretching frequency. Our entire system is software-controlled by computer programs embedded within the Zeiss AxioVision 4.6 or ImagePro Plus 6.2 software, enabling us to perform automated experiments. This set-up can be routinely used for phase contrast microscopy; improvements in the software were made to enable its use for fluorescence microcopy.
The calibration of the system showed that the strain field is homogenous and highly reproducible, so that experiments under the same stretch conditions can be made.

Previous studies demonstrated that cells oriented themselves perpendicular to the stretch direction, in response to cyclical stretch at various amplitudes (Dartsch *et al.*, Neidlinger-Wilke *et al.*, Wang *et al.*). For example, Dartsch described cellular reorientation at a stretching amplitude of between 2% and 3.5%. However, no studies of the dynamics and the influence of the stretching frequency on cellular orientation during cyclical stretch were previously undertaken. We provided the first detailed, quantitative analysis of the dynamic behavior of cells during cyclical stretch.
Our experiments demonstrated that the time course of the reorientation process of fibroblasts during cyclical stretch has an exponential characteristic. We determined the time, called characteristic time which was needed for the reorientation, with a simple phenomenological model. We could demonstrate that this characteristic time is frequency-dependent; moreover, the dependency has a power-law characteristic until a certain threshold frequency of approximately 1 $s^{-1}$ is reached. Above this threshold frequency, the characteristic time remaines constant as the frequency increases. We observed that this biphasic behavior is a universal characteristic for two different fibroblast types in a sub-confluent cell layer. However, we also observed cell-specific differences in both time course, and strength of the response. REF52 cells were found to be more sensitive to the stretch: they reorient faster than the HDF1 cells at every frequency; moreover, the start frequency, or point at which we could first observe a cellular response, is 10 times lower than the start frequency we obtained for the HDF1 cells ($f_{REF52} = 0.01\ s^{-1}$; $f_{HDF1} = 0.1\ s^{-1}$).
The biphasic nature of the characteristic time of cellular reorientation in dependency of the stretch frequency could be due to the saturation of the molecular mechanotransduction machinery. In order for a cell to sense external forces, a certain period of time is required,

such as the time necessary for a conformational change, or for a protein modification such as by the phosphorylation of a sensor protein.
This hypothesis was corroborated by the differences in orientation response between single cells and cells in a confluent layer. For confluent cell layers, we could not observe such a biphasic characteristic. For confluent cells the characteristic time of reorientation decreases with a power-law characteristic with an increase in frequency; however, we could not observe a constant regime for high frequencies. This finding might be caused by the presence of cell-cell contacts between cells in the confluent layer. In this case, the number of mechanosensory proteins is possibly increased, for example by the activation of cadherins (Ko *et al.* 2001). For single cells the cadherins are lacking and the mechanosensory machinery was mainly consisting of the focal adhesions.

When we compared our results with the biophysical inspired theoretical model of De *et. al* (De Rumi *et al.* 2007) we can see a qualitative agreement in certain observations. De *et. al* also predicted a decrease of the characteristic time at increaseing frequency. However, these researchers expect to see a parallel orientation of the cells at low frequencies, as experimentally shown in studies by Eastwood (Eastwood *et al.* 1998). This effect could not be verified by our experiments. We assume that the cells did not sense the low frequency, because the time involved in the change of signal was too long according to a quasi static state for the cells. If a slow stretch is applied to cells, the cells can change their structure as they are doing during cell migration. For example, a cell can totally reorganize during stretch of $f = 1\ h^{-1}$ if we assume a cell migration speed of 20 µm/h (Maheshwari *et al.* 1999) It is worth mentioning, Eastwood's experiments were performed on collagen matrices which prevented the cells from relaxing and balancing the stretch, what is possible for the cells in our experiments.

Beside the frequency dependence of the response kinetics, we also determined the maximum orientation representing the strength of the cellular response. Previous studies suggested that the maximum orientation is specifically in the direction of the minimum substrate deformation which is dependent on the elongation as well as the transverse compression of the substrate (Wang 2000). Wang *et. al* also observed that the reorientation is independent of the stretching rate after 30 min stretch with two different stretching rates (10%/s and 5%/s) t(Wang *et al.* 2001). However, we could show that the maximum orientation of the cells is also dependent on the stretch frequency.
In the case of the confluent cell layers, we could see a discontinuity in the dose-response curve between $f = 0.25\ s^{-1}$ and $f = 0.5\ s^{-1}$. This finding suggests that at higher frequencies, another cellular sensory pathway is activated, enabling the cells to orient themselves more perpendicular to the stretch direction.
If we compare the two characteristics of cellular reorientation, changes in the characteristic time, and increases in the maximum orientation, we can speak in terms of a model that the

mechnotransduction machinery is in saturation for high frequencies leading to the biphasic characteristic of the characteristic time, while the molecular machinery, responsible for the maximum orientation is not in saturation at high frequencies.
As previously mentioned, we can also argue that above a certain threshold frequency, the time required for cellular reorientation process is too short at high frequencies, while for the process of maximum orientation the number of involved molecules that have not yet reached saturation is crucial.
Knock-out experiments of cadherins or the investigation of GTPases by means of fluorescence resonance energy transfer (FRET) (Katsumi *et al.* 2002)as possible candidates for mechano-induced signaling pathways, could provide more insights into the explanation of our observed effects.

We evaluated, in both REF52 and HDF1 cells, the characteristic time necessary for the reorganization process in dependency on different amplitudes and we could see that the characteristic time was also dependent on the amplitude of the applied stretch. In contrast to the frequency dependence, the characteristic time was dependent on the amplitude in a linear rather than in an power-law characteristic. Furthermore, we observed that the maximum orientation increased, at higher amplitudes.
We would expect that the cellular response can be dependent on the total inserted energy. We expected that this energy was a product of the external signals frequency and amplitude. Our measurements, however, showed a power law behavior for the variation of the frequency, and a linear behavior for the variation of the amplitude. This result shows that the stretching frequency might influence the characteristic time of reorientation more than the amplitude. Therefore, we cannot simply predict that the inserted energy is a product of the external signals, obtained by multiplying the stretching frequency and the stretching amplitude.

The influence of cyclical stretch on cell division has already been investigated (Kaspar *et al.* 2002). However we demonstrated new results concerning the influence of the stretching frequency on cell division. With our experimental set-up, it was possible to follow single cells and observe them as they were dividing, both during stretch, and after the applied stretch was stopped. These measurements demonstrated that the cells divided less, above a certain threshold frequency ($f$ = 0.5 $s^{-1}$). When the cyclical stretch was stopped, the cells began to divide more. The reduction in cell division could be caused by damage to the mitotic spindle at a certain frequency. Experiments with GFP-labeled centrin or the uptake of BrdU at different time points during the stretch could further explain this phenomenon.

Experiments with human fibroblasts from young and old donors showed that cells from both groups responded according to the biphasic time characteristic but old cells respond faster to cyclical stretch than young cells. The differing response to stretch of old and young cells could be attributed to the stiffness of the cells. Previous studies showed that old cells are

stiffer than young cells (Berdyyeva *et al.* 2005; Lieber *et al.* 2004). This relative rigidity could be related to the cytoskeleton, meaning that the cytoskeleton could be damaged more easily than the cytoskeleton of more flexible cells. Moreover, rigid cells could reorient faster, if the cytoskeleton is involved in the mechanoseneory machinery. Higher stiffness could be related to a more complex actin cytoskeleton with more crosslinks and if mechanosensory structures are related to a higher crosslinked cytoskeleton, the cells would sense faster and reorient faster. The stiffness of our cells still must be investigated by means of AFM measurements. Furthermore, the stability and the turn over rate of the focal adhesions may also play a role in the age-related effect. This possibility may be clarified by methods such as total internal reflection (TIRF) or fluorescence recovery after photobleaching (FRAP) measurements. Such measurements could also provide some explanations for the differences between the REF52 and HDF1 cells.

In further studies, we improved our experimental set-up, in order to perform fluorescence microscopy studies. We first observed the actin filaments and the extracellular matrix protein fibronectin in a non-dynamic manner; we obtained antibody-stained images both before stretch, and after eight hours of stretch. Previous studies showed that the actin cytoskeleton also orient itself perpendicular to the stretch direction (Wang *et al.* 2001). We wanted to investigate how the fibronectin is influenced by both the stretch and the cellular orientation. Our studies showed that the cells formed fibronectin fibrils along the actin stress fibers, meaning that the extracellular matrix beneath the cells was also oriented perpendicular to the stretch direction.

In addition, we investigated the dynamics of reorganization of focal adhesions, in response to cyclical stretch. REF52 cells were transfected with yellow fluorescent protein (YFP)-labeled paxillin, enabling us to track the focal adhesions during cyclical stretch. In contrast to Riveline's findings (Riveline *et al.* 2001), indicating that the focal adhesions grow in the direction of a slow stretch, our studies involving cyclical stretch demonstrated that focal adhesion sites also oriented themselves perpendicular to the stretch direction. The focal adhesions were seen to shrink at the beginning of the reorientation process, and elongate once again along the axis of the new orientation direction. In the beginning of the experiment, the focal adhesions were randomly distributed throughout the cell; however, they rearranged themselves at the edge of the cell during the orientation process. The responsible mechanisms responsible underlying this phenomenon are still unknown. The findings of Riveline were described by several models of force dependent focal adhesion growth (Bischofs *et al.* 2004; Nicolas *et al.* 2004; Schwarz *et al.* 2002; Schwarz and Safran 2002; Shemesh *et al.* 2005). Even less is known about the influence of cyclic strain on the focal adhesion reorganization. One hypothesis predicts that the focal adhesions would grow when they are stretched. When the stretched substrate relaxes back during one stretching cycle, the focal adhesions are compressed and their growth is stopped (Shemesh *et al.* 2005). Our results however showed

that the focal adhesions are reorganizing and orienting perpendicular to the stretch direction; moreover, in Section 3.2.7 we demonstrated that the relaxation of the substrate does not affect the cellular response

Knock-out measurements of focal adhesion proteins, such as vinculin or other proteins involved in the mechanosensation by the cytoskeleton [p130CAS (Sawada *et al.* 2006)], or detailed FRET measurements of such proteins, could provide further details into the mechanosensory process.

In short, this project raises a number of questions requiring further exploration. The molecular mechanisms underlying cellular reorganization, mechnosensing, or mechanotransduction are still not fully understood. In this study we attempt to get a deeper insight in the mechanisms behind the reorientation of cells during cyclical stretch and the results of the present study may aid in the tissue engineering of artificial tendons or other tissues under mechanical strain. Furthermore, some of our results provide new insights into the influence of external forces and cyclical stretch on cells.

# Bibliography

184 S. http://www.dowcorning.com/applications/search/default.aspx?R=131EN.

Athanasiou KA, Thoma BS, Lanctot DR, Shin D, Agrawal CM, LeBaron RG. 1999. Development of the cytodetachment technique to quantify mechanical adhesiveness of the single cell. Biomaterials 20(23-24):2405-15.

Augat P, Simon U, Liedert A, Claes L. 2005. Mechanics and mechano-biology of fracture healing in normal and osteoporotic bone. Osteoporos Int 16 Suppl 2:S36-43.

Balaban NQ, Schwarz US, Riveline D, Goichberg P, Tzur G, Sabanay I, Mahalu D, Safran S, Bershadsky A, Addadi L and others. 2001. Force and focal adhesion assembly: a close relationship studied using elastic micropatterned substrates. Nat Cell Biol 3(5):466-72.

Banes AJ, Gilbert J, Taylor D, Monbureau O. 1985. A new vacuum-operated stress-providing instrument that applies static or variable duration cyclic tension or compression to cells in vitro. J Cell Sci 75:35-42.

Bao G, Suresh S. 2003. Cell and molecular mechanics of biological materials. Nat Mater 2(11):715-25.

Bausch AR, Ziemann F, Boulbitch AA, Jacobson K, Sackmann E. 1998. Local measurements of viscoelastic parameters of adherent cell surfaces by magnetic bead microrheometry. Biophys J 75(4):2038-49.

Beningo KA, Wang YL. 2002. Flexible substrata for the detection of cellular traction forces. Trends Cell Biol 12(2):79-84.

Benoit M. 2002. Cell adhesion measured by force spectroscopy on living cells. Methods Cell Biol 68:91-114.

Berdyyeva TK, Woodworth CD, Sokolov I. 2005. Human epithelial cells increase their rigidity with ageing in vitro: direct measurements. Phys Med Biol 50(1):81-92.

Besser A, Safran SA. 2006. Force-induced adsorption and anisotropic growth of focal adhesions. Biophys J 90(10):3469-84.

Bischofs IB, Safran SA, Schwarz US. 2004. Elastic interactions of active cells with soft materials. Phys Rev E Stat Nonlin Soft Matter Phys 69(2 Pt 1):021911.

Bischofs IB SU. 2003. Cell organization in soft media due to active mechanosensing. Proc Natl Acad Sci U S A 100(16):9274–9279.

Blough ER, Rice KM, Desai DH, Wehner P, Wright GL. 2007. Aging alters mechanical and contractile properties of the Fisher 344/Nnia X Norway/Binia rat aorta. Biogerontology 8(3):303-13.

Brown RA, Prajapati R, McGrouther DA, Yannas IV, Eastwood M. 1998. Tensional homeostasis in dermal fibroblasts: mechanical responses to mechanical loading in three-dimensional substrates. J Cell Physiol 175(3):323-32.

Brown TD. 2000. Techniques for mechanical stimulation of cells in vitro: a review. J Biomech 33(1):3-14.

Bursac P, Lenormand G, Fabry B, Oliver M, Weitz DA, Viasnoff V, Butler JP, Fredberg JJ. 2005. Cytoskeletal remodelling and slow dynamics in the living cell. Nat Mater 4(7):557-61.

Calve S, Dennis RG, Kosnik PE, 2nd, Baar K, Grosh K, Arruda EM. 2004. Engineering of functional tendon. Tissue Eng 10(5-6):755-61.

Campbell BH, Clark WW, Wang JH. 2003. A multi-station culture force monitor system to study cellular contractility. J Biomech 36(1):137-40.

Carrillo F, Gupta, S., Balooch, M., Marshall, S. J., Marshall, G. W., Pruitt,, L. & Puttlitz CM. 2005. Nanoindentation of polydimethylsiloxane elastomers: Effect of crosslinking, work of adhesion, and fluid environment on elastic modulus. J. Mater. Res. 20:2820-2830.

Chen CS, Ingber DE. 1999. Tensegrity and mechanoregulation: from skeleton to cytoskeleton. Osteoarthritis Cartilage 7(1):81-94.

Chen CS, Mrksich M, Huang S, Whitesides GM, Ingber DE. 1997. Geometric control of cell life and death. Science 276(5317):1425-8.

Chen CS, Mrksich M, Huang S, Whitesides GM, Ingber DE. 1998. Micropatterned surfaces for control of cell shape, position, and function. Biotechnol Prog 14(3):356-63.

Chen CS, Tan J, Tien J. 2004. Mechanotransduction at cell-matrix and cell-cell contacts. Annu Rev Biomed Eng 6:275-302.

Chen J, Fabry B, Schiffrin EL, Wang N. 2001. Twisting integrin receptors increases endothelin-1 gene expression in endothelial cells. Am J Physiol Cell Physiol 280(6):C1475-84.

Chen S, and Huajian, Gao. 2006. Non-slipping adhesive contact of an elastic cylinder on stretched substrates. Proc. R. Soc. A (Proceedings of the Royal Society A) 462:211-228.

Cogoli A, Tschopp A, Fuchs-Bislin P. 1984. Cell sensitivity to gravity. Science 225(4658):228-30.

Costa KD, Hucker WJ, Yin FC. 2002. Buckling of actin stress fibers: a new wrinkle in the cytoskeletal tapestry. Cell Motil Cytoskeleton 52(4):266-74.

Curtis A, Riehle M. 2001. Tissue engineering: the biophysical background. Phys Med Biol 46(4):R47-65.

Dartsch PC, Betz E. 1989. Response of cultured endothelial cells to mechanical stimulation. Basic Res Cardiol 84(3):268-81.

Dartsch PC, Hammerle H, Betz E. 1986. Orientation of cultured arterial smooth muscle cells growing on cyclically stretched substrates. Acta Anat (Basel) 125(2):108-13.

De Rumi, Zemel Assaf , Safran SA. 2007. Dynamics of cell orientation. Nature Physics 3:655-659.

De Rumi , Zemel Assaf , Safran SA. 2007. Dynamics of cell orientation. Nature Physics 3:655-659.

DeMali KA, Wennerberg K, Burridge K. 2003. Integrin signaling to the actin cytoskeleton. Curr Opin Cell Biol 15(5):572-82.

Dembo M, Wang YL. 1999. Stresses at the cell-to-substrate interface during locomotion of fibroblasts. Biophys J 76(4):2307-16.

Dewey CF, Jr., Bussolari SR, Gimbrone MA, Jr., Davies PF. 1981. The dynamic response of vascular endothelial cells to fluid shear stress. J Biomech Eng 103(3):177-85.

Discher DE, Janmey P, Wang YL. 2005. Tissue cells feel and respond to the stiffness of their substrate. Science 310(5751):1139-43.

Dobereiner HG, Dubin-Thaler B, Giannone G, Xenias HS, Sheetz MP. 2004. Dynamic phase transitions in cell spreading. Phys Rev Lett 93(10):108105.

du Roure O, Saez A, Buguin A, Austin RH, Chavrier P, Silberzan P, Ladoux B. 2005. Force mapping in epithelial cell migration. Proc Natl Acad Sci U S A 102(7):2390-5.

Eastwood M, Mudera VC, McGrouther DA, Brown RA. 1998. Effect of precise mechanical loading on fibroblast populated collagen lattices: morphological changes. Cell Motil Cytoskeleton 40(1):13-21.

Engler AJ, Sen S, Sweeney HL, Discher DE. 2006. Matrix elasticity directs stem cell lineage specification. Cell 126(4):677-89.

Evans E, Yeung A. 1989. Apparent viscosity and cortical tension of blood granulocytes determined by micropipet aspiration. Biophys J 56(1):151-60.

Even-Ram S, Artym V, Yamada KM. 2006. Matrix control of stem cell fate. Cell 126(4):645-7.

Felder S, Elson EL. 1990. Mechanics of fibroblast locomotion: quantitative analysis of forces and motions at the leading lamellas of fibroblasts. J Cell Biol 111(6 Pt 1):2513-26.

Finkel T, Serrano M, Blasco MA. 2007. The common biology of cancer and ageing. Nature 448(7155):767-74.

Franza BR, Jr., Maruyama K, Garrels JI, Ruley HE. 1986. In vitro establishment is not a sufficient prerequisite for transformation by activated ras oncogenes. Cell 44(3):409-18.

Fukuda S, Schmid-Schonbein GW. 2003. Regulation of CD18 expression on neutrophils in response to fluid shear stress. Proc Natl Acad Sci U S A 100(23):13152-7.

Galbraith CG, Sheetz MP. 1998. Forces on adhesive contacts affect cell function. Curr Opin Cell Biol 10(5):566-71.

Galbraith CG, Yamada KM, Sheetz MP. 2002. The relationship between force and focal complex development. J Cell Biol 159(4):695-705.

Gao M, Craig D, Vogel V, Schulten K. 2002. Identifying unfolding intermediates of FN-III(10) by steered molecular dynamics. J Mol Biol 323(5):939-50.

Gasteier P, Reska A, Schulte P, Salber J, Offenhausser A, Moeller M, Groll J. 2007. Surface Grafting of PEO-Based Star-Shaped Molecules for Bioanalytical and Biomedical Applications. Macromol Biosci 7(8):1010-23.

Geiger B, Bershadsky A. 2002. Exploring the neighborhood: adhesion-coupled cell mechanosensors. Cell 110(2):139-42.

Geiger B, Bershadsky A, Pankov R, Yamada KM. 2001. Transmembrane crosstalk between the extracellular matrix--cytoskeleton crosstalk. Nat Rev Mol Cell Biol 2(11):793-805.

Geng WD, Boskovic G, Fultz ME, Li C, Niles RM, Ohno S, AND, Wright GL. 2001. Regulation of Expression and Activity of Four PKC Isozymes in Con¯uent and Mechanically Stimulated UMR-108 Osteoblastic Cells. Journal of Cellular Physiology 189(-):216-228.

Grabner B. 2000. A new stretching apparatus for applying anisotropic mechanical strain to bone cells in-vitro. REVIEW OF SCIENTIFIC INSTRUMENTS 71(9):3522-3529.

Guck J, Ananthakrishnan R, Moon TJ, Cunningham CC, Kas J. 2000. Optical deformability of soft biological dielectrics. Phys Rev Lett 84(23):5451-4.

Guoguang Yang RCC, James H-C. Wang. 2004. Proliferation and collagen production of human patellar tendon
fibroblasts in response to cyclic uniaxial stretching
in serum-free conditions. Journal of Biomechanics 37(-):1543–1550.

Hall A. 1998. Rho GTPases and the actin cytoskeleton. Science 279(5350):509-14.

Hasegawa S, Sato S, Saito S, Suzuki Y, Brunette DM. 1985. Mechanical stretching increases the number of cultured bone cells synthesizing DNA and alters their pattern of protein synthesis. Calcif Tissue Int 37(4):431-6.

Hayakawa K, Sato N, Obinata T. 2001. Dynamic reorientation of cultured cells and stress fibers under mechanical stress from periodic stretching. Exp Cell Res 268(1):104-14.

Heidemann SR, Buxbaum RE. 1994. Mechanical tension as a regulator of axonal development. Neurotoxicology 15(1):95-107.

Iba T, Sumpio BE. 1991. Morphological response of human endothelial cells subjected to cyclic strain in vitro. Microvasc Res 42(3):245-54.

Ignatius A, Blessing H, Liedert A, Schmidt C, Neidlinger-Wilke C, Kaspar D, Friemert B, Claes L. 2005. Tissue engineering of bone: effects of mechanical strain on osteoblastic cells in type I collagen matrices. Biomaterials 26(3):311-8.

Ingber DE. 2003. Mechanobiology and diseases of mechanotransduction. Ann Med 35(8):564-77.

Janmey PA, McCulloch CA. 2007. Cell mechanics: integrating cell responses to mechanical stimuli. Annu Rev Biomed Eng 9:1-34.

Janmey PA, Weitz DA. 2004. Dealing with mechanics: mechanisms of force transduction in cells. Trends Biochem Sci 29(7):364-70.

Jungbauer S, Kemkemer R, Gruler H, Kaufmann D, Spatz JP. 2004. Cell shape normalization, dendrite orientation, and melanin production of normal and genetically altered (haploinsufficient NF1)-melanocytes by microstructured substrate interactions. Chemphyschem 5(1):85-92.

K.J. Van Vliet GB, S. Suresh. 2003. The biomechanics toolbox: experimental approaches for living cells and biomolecules. Acta Materialia 51:5881–5905.

Kakisis JD, Liapis CD, Sumpio BE. 2004. Effects of cyclic strain on vascular cells. Endothelium 11(1):17-28.

Kaspar D, Seidl W, Neidlinger-Wilke C, Beck A, Claes L, Ignatius A. 2002. Proliferation of human-derived osteoblast-like cells depends on the cycle number and frequency of uniaxial strain. J Biomech 35(7):873-80.

Katsumi A, Milanini J, Kiosses WB, del Pozo MA, Kaunas R, Chien S, Hahn KM, Schwartz MA. 2002. Effects of cell tension on the small GTPase Rac. J Cell Biol 158(1):153-64.

Kaufmann D, Muller R, Bartelt B, Wolf M, Kunzi-Rapp K, Hanemann CO, Fahsold R, Hein C, Vogel W, Assum G. 2001. Spinal neurofibromatosis without cafe-au-lait macules in two families with null mutations of the NF1 gene. Am J Hum Genet 69(6):1395-400.

Kaunas R, Nguyen P, Usami S, Chien S. 2005. Cooperative effects of Rho and mechanical stretch on stress fiber organization. Proc Natl Acad Sci U S A 102(44):15895-900.

Kaunas R, Usami S, Chien S. 2006. Regulation of stretch-induced JNK activation by stress fiber orientation. Cell Signal 18(11):1924-31.

Keller H, Niggli V, Zimmermann A. 1991. Diversity in motile responses of human neutrophil granulocytes: functional meaning and cytoskeletal basis. Adv Exp Med Biol 297:23-37.

Kemkemer R, Jungbauer S, Kaufmann D, Gruler H. 2006. Cell orientation by a microgrooved substrate can be predicted by automatic control theory. Biophys J 90(12):4701-11.

Kemkemer R, Neidlinger-Wilke C, Claes L, Gruler H. 1999. Cell orientation induced by extracellular signals. Cell Biochem Biophys 30(2):167-92.

Kemkemer R, Schrank S, Vogel W, Gruler H, Kaufmann D. 2002. Increased noise as an effect of haploinsufficiency of the tumor-suppressor gene neurofibromatosis type 1 in vitro. Proc Natl Acad Sci U S A 99(21):13783-8.

Ko KS, Arora PD, McCulloch CA. 2001. Cadherins mediate intercellular mechanical signaling in fibroblasts by activation of stretch-sensitive calcium-permeable channels. J Biol Chem 276(38):35967-77.

Ko KS, McCulloch CA. 2001. Intercellular mechanotransduction: cellular circuits that coordinate tissue responses to mechanical loading. Biochem Biophys Res Commun 285(5):1077-83.

Kurpinski K, Chu J, Hashi C, Li S. 2006a. Anisotropic mechanosensing by mesenchymal stem cells. Proc Natl Acad Sci U S A 103(44):16095-100.

Kurpinski K, Park J, Thakar RG, Li S. 2006b. Regulation of vascular smooth muscle cells and mesenchymal stem cells by mechanical strain. Mol Cell Biomech 3(1):21-34.

Lazopoulos KA, Stamenovic D. 2006. A mathematical model of cell reorientation in response to substrate stretching. Mol Cell Biomech 3(1):43-8.

Lee JN, Jiang X, Ryan D, Whitesides GM. 2004. Compatibility of mammalian cells on surfaces of poly(dimethylsiloxane). Langmuir 20(26):11684-91.

Lehnert D, Wehrle-Haller B, David C, Weiland U, Ballestrem C, Imhof BA, Bastmeyer M. 2004. Cell behaviour on micropatterned substrata: limits of extracellular matrix geometry for spreading and adhesion. J Cell Sci 117(Pt 1):41-52.

Leung LY, Tian D, Brangwynne CP, Weitz DA, Tschumperlin DJ. 2007. A new microrheometric approach reveals individual and cooperative roles for TGF-beta1 and IL-1beta in fibroblast-mediated stiffening of collagen gels. Faseb J 21(9):2064-73.

Lieber SC, Aubry N, Pain J, Diaz G, Kim SJ, Vatner SF. 2004. Aging increases stiffness of cardiac myocytes measured by atomic force microscopy nanoindentation. Am J Physiol Heart Circ Physiol 287(2):H645-51.

Liu B, Qu MJ, Qin KR, Li H, Li ZK, Shen BR, Jiang ZL. 2007. Role of cyclic strain frequency in regulating the Alignment of Vascular Smooth Muscle Cells in vitro. Biophys J.

Lu T, Pan Y, Kao SY, Li C, Kohane I, Chan J, Yankner BA. 2004. Gene regulation and DNA damage in the ageing human brain. Nature 429(6994):883-91.

Maheshwari G, Wells A, Griffith LG, Lauffenburger DA. 1999. Biophysical integration of effects of epidermal growth factor and fibronectin on fibroblast migration. Biophys J 76(5):2814-23.

Mathur AB, Collinsworth AM, Reichert WM, Kraus WE, Truskey GA. 2001. Endothelial, cardiac muscle and skeletal muscle exhibit different viscous and elastic properties as determined by atomic force microscopy. J Biomech 34(12):1545-53.

Micoulet A, Spatz JP, Ott A. 2005. Mechanical response analysis and power generation by single-cell stretching. Chemphyschem 6(4):663-70.

Miller CE, Donlon KJ, Toia L, Wong CL, Chess PR. 2000. Cyclic strain induces proliferation of cultured embryonic heart cells. In Vitro Cell Dev Biol Anim 36(10):633-9.

Minguell JJ, Erices A, Conget P. 2001. Mesenchymal stem cells. Exp Biol Med (Maywood) 226(6):507-20.

Na S, Meininger GA, Humphrey JD. 2007. A theoretical model for F-actin remodeling in vascular smooth muscle cells subjected to cyclic stretch. J Theor Biol 246(1):87-99.

Neidlinger-Wilke C, Grood E, Claes L, Brand R. 2002. Fibroblast orientation to stretch begins within three hours. J Orthop Res 20(5):953-6.

Neidlinger-Wilke C, Grood ES, Wang J-C, Brand RA, Claes L. 2001. Cell alignment is induced by cyclic changes in cell length: studies of cells grown in cyclically stretched substrates. J Orthop Res 19(2):286-93.

Neidlinger-Wilke C, Wilke HJ, Claes L. 1994. Cyclic stretching of human osteoblasts affects proliferation and metabolism: a new experimental method and its application. J Orthop Res 12(1):70-8.

Nelson CM, Jean RP, Tan JL, Liu WF, Sniadecki NJ, Spector AA, Chen CS. 2005. Emergent patterns of growth controlled by multicellular form and mechanics. Proc Natl Acad Sci U S A 102(33):11594-9.

Nicolas A, Geiger B, Safran SA. 2004. Cell mechanosensitivity controls the anisotropy of focal adhesions. Proc Natl Acad Sci U S A 101(34):12520-5.

Ning Wang EO, George M. Whitesides and, Ingber DE. 2002. Micropatterning Tractional Forces
in Living Cells. Cell Motility and the Cytoskeleton 52(-):97–106.

Oberhauser AF, Badilla-Fernandez C, Carrion-Vazquez M, Fernandez JM. 2002. The mechanical hierarchies of fibronectin observed with single-molecule AFM. J Mol Biol 319(2):433-47.

Ostuni Emanuele , Ravi Kane, Christopher S. Chen, Donald E. Ingber, and, Whitesides GM. 2000. Patterning Mammalian Cells Using Elastomeric
Membranes. Langmuir 16(20):7811-7819.

Passerini AG, Polacek DC, Shi C, Francesco NM, Manduchi E, Grant GR, Pritchard WF, Powell S, Chang GY, Stoeckert CJ, Jr. and others. 2004. Coexisting proinflammatory and antioxidative endothelial transcription profiles in a disturbed flow region of the adult porcine aorta. Proc Natl Acad Sci U S A 101(8):2482-7.

Pelham RJ, Jr., Wang Y. 1997. Cell locomotion and focal adhesions are regulated by substrate flexibility. Proc Natl Acad Sci U S A 94(25):13661-5.

Pender N, McCulloch CA. 1991. Quantitation of actin polymerization in two human fibroblast sub-types responding to mechanical stretching. J Cell Sci 100 ( Pt 1):187-93.

Poole K, Khairy K, Friedrichs J, Franz C, Cisneros DA, Howard J, Mueller D. 2005. Molecular-scale topographic cues induce the orientation and directional movement of fibroblasts on two-dimensional collagen surfaces. J Mol Biol 349(2):380-6.

Puig-De-Morales M, Grabulosa M, Alcaraz J, Mullol J, Maksym GN, Fredberg JJ, Navajas D. 2001. Measurement of cell microrheology by magnetic twisting cytometry with frequency domain demodulation. J Appl Physiol 91(3):1152-9.

Radmacher M. 2002. Measuring the elastic properties of living cells by the atomic force microscope. Methods Cell Biol 68:67-90.

Rehfeldt F, Discher DE. 2007. Cell dipoles feel their way. Nature Physics 3:592-593.

Ridley AJ, Hall A. 1992. The small GTP-binding protein rho regulates the assembly of focal adhesions and actin stress fibers in response to growth factors. Cell 70(3):389-99.

Riveline D, Zamir E, Balaban NQ, Schwarz US, Ishizaki T, Narumiya S, Kam Z, Geiger B, Bershadsky AD. 2001. Focal contacts as mechanosensors: externally applied local mechanical force induces growth of focal contacts by an mDia1-dependent and ROCK-independent mechanism. J Cell Biol 153(6):1175-86.

Safran S. *personal communication*.

Sawada Y, Sheetz MP. 2002. Force transduction by Triton cytoskeletons. J Cell Biol 156(4):609-15.

Sawada Y, Tamada M, Dubin-Thaler BJ, Cherniavskaya O, Sakai R, Tanaka S, Sheetz MP. 2006. Force sensing by mechanical extension of the Src family kinase substrate p130Cas. Cell 127(5):1015-26.

Schwarz US, Balaban NQ, Riveline D, Bershadsky A, Geiger B, Safran SA. 2002. Calculation of forces at focal adhesions from elastic substrate data: the effect of localized force and the need for regularization. Biophys J 83(3):1380-94.

Schwarz US, Safran SA. 2002. Elastic interactions of cells. Phys Rev Lett 88(4):048102.

Shemesh T, Geiger B, Bershadsky AD, Kozlov MM. 2005. Focal adhesions as mechanosensors: a physical mechanism. Proc Natl Acad Sci U S A 102(35):12383-8.

Shirinsky VP, Antonov AS, Birukov KG, Sobolevsky AV, Romanov YA, Kabaeva NV, Antonova GN, Smirnov VN. 1989. Mechano-chemical control of human endothelium orientation and size. J Cell Biol 109(1):331-9.

Shraiman BI. 2005. Mechanical feedback as a possible regulator of tissue growth. Proc Natl Acad Sci U S A 102(9):3318-23.

Silver FH, DeVore D, Siperko LM. 2003. Invited Review: Role of mechanophysiology in aging of ECM: effects of changes in mechanochemical transduction. J Appl Physiol 95(5):2134-41.

Sleep J, Wilson D, Simmons R, Gratzer W. 1999. Elasticity of the red cell membrane and its relation to hemolytic disorders: an optical tweezers study. Biophys J 77(6):3085-95.

Smith DH, Wolf JA, Meaney DF. 2001. A new strategy to produce sustained growth of central nervous system axons: continuous mechanical tension. Tissue Eng 7(2):131-9.

Somjen D, Binderman I, Berger E, Harell A. 1980. Bone remodelling induced by physical stress is prostaglandin E2 mediated. Biochim Biophys Acta 627(1):91-100.

Stamenovic D. 2005. Contractile torque as a steering mechanism for orientation of adherent cells. Mech Chem Biosyst 2(2):69-76.

Stamenovic D. 2006. Cell mechanics: two regimes, maybe three? Nat Mater 5(8):597-8.

Sukharev S, Anishkin A. 2004. Mechanosensitive channels: what can we learn from 'simple' model systems? Trends Neurosci 27(6):345-51.

Svoboda K, Block SM. 1994. Biological applications of optical forces. Annu Rev Biophys Biomol Struct 23:247-85.

Takemasa T, Sugimoto K, Yamashita K. 1997. Amplitude-dependent stress fiber reorientation in early response to cyclic strain. Exp Cell Res 230(2):407-10.

Takemasa T, Yamaguchi T, Yamamoto Y, Sugimoto K, Yamashita K. 1998. Oblique alignment of stress fibers in cells reduces the mechanical stress in cyclically deforming fields. Eur J Cell Biol 77(2):91-9.

Tamada M, Sheetz MP, Sawada Y. 2004. Activation of a signaling cascade by cytoskeleton stretch. Dev Cell 7(5):709-18.

Tan JL, Tien J, Pirone DM, Gray DS, Bhadriraju K, Chen CS. 2003. Cells lying on a bed of microneedles: an approach to isolate mechanical force. Proc Natl Acad Sci U S A 100(4):1484-9.

Thompson DAW. 1992. On growth and form. Dover publications:0-1116.

Tschumperlin DJ, Dai G, Maly IV, Kikuchi T, Laiho LH, McVittie AK, Haley KJ, Lilly CM, So PT, Lauffenburger DA and others. 2004. Mechanotransduction through growth-factor shedding into the extracellular space. Nature 429(6987):83-6.

Uhthoff HK, Jaworski ZF. 1978. Bone loss in response to long-term immobilisation. J Bone Joint Surg Br 60-B(3):420-9.

Usami S, Chen HH, Zhao Y, Chien S, Skalak R. 1993. Design and construction of a linear shear stress flow chamber. Ann Biomed Eng 21(1):77-83.

Vogel V. 2006. Mechanotransduction involving multimodular proteins: converting force into biochemical signals. Annu Rev Biophys Biomol Struct 35:459-88.

Vogel V, Sheetz M. 2006. Local force and geometry sensing regulate cell functions. Nat Rev Mol Cell Biol 7(4):265-75.

Wang DL, Wung BS, Shyy YJ, Lin CF, Chao YJ, Usami S, Chien S. 1995a. Mechanical strain induces monocyte chemotactic protein-1 gene expression in endothelial cells. Effects of mechanical strain on monocyte adhesion to endothelial cells. Circ Res 77(2):294-302.

Wang H, Ip W, Boissy R, Grood ES. 1995b. Cell orientation response to cyclically deformed substrates: experimental validation of a cell model. J Biomech 28(12):1543-52.

Wang J., Su M, Fan J, Seth A, McCulloch CA. 2002. Transcriptional regulation of a contractile gene by mechanical forces applied through integrins in osteoblasts. J Biol Chem 277(25):22889-95.

Wang J. H.-C. PG-C, and FRANK C.-P. YIN. 2000. Contractility Affects Stress Fiber Remodeling and Reorientation
of Endothelial Cells Subjected to Cyclic Mechanical Stretching. Annals of Biomedical Engineering 28(-):1165–1171.

Wang JH. 2000. Substrate deformation determines actin cytoskeleton reorganization: A mathematical modeling and experimental study. J Theor Biol 202(1):33-41.

Wang JH, Goldschmidt-Clermont P, Wille J, Yin FC. 2001. Specificity of endothelial cell reorientation in response to cyclic mechanical stretching. J Biomech 34(12):1563-72.

Wang JH, Yang G, Li Z, Shen W. 2004. Fibroblast responses to cyclic mechanical stretching depend on cell orientation to the stretching direction. J Biomech 37(4):573-6.

Wang YL, Pelham RJ, Jr. 1998. Preparation of a flexible, porous polyacrylamide substrate for mechanical studies of cultured cells. Methods Enzymol 298:489-96.

Wei Z, Deshpande Vikram S., M. MR, G. EA. to appear in ASME Journal of Biomechanical Engineering, Vol. 130, 2008.

Weibel DB, Diluzio WR, Whitesides GM. 2007. Microfabrication meets microbiology. Nat Rev Microbiol 5(3):209-18.

Wolff J. 1892. Das Gesetz der Transformation der Knochen. Berlin, A. Hirschwald.

Xia Y, Whitesides GM. 1998. Soft Lithography. Annu. Rev. Mater.Sci 28:153-84.

Yano Y, Saito Y, Narumiya S, Sumpio BE. 1996. Involvement of rho p21 in cyclic strain-induced tyrosine phosphorylation of focal adhesion kinase (pp125FAK), morphological changes and migration of endothelial cells. Biochem Biophys Res Commun 224(2):508-15.

Yeung A, Evans E. 1989. Cortical shell-liquid core model for passive flow of liquid-like spherical cells into micropipets. Biophys J 56(1):139-49.

Yeung T, Georges PC, Flanagan LA, Marg B, Ortiz M, Funaki M, Zahir N, Ming W, Weaver V, Janmey PA. 2005. Effects of substrate stiffness on cell morphology, cytoskeletal structure, and adhesion. Cell Motil Cytoskeleton 60(1):24-34.

Yin HL, Janmey PA. 2003. Phosphoinositide regulation of the actin cytoskeleton. Annu Rev Physiol 65:761-89.

Yoshigi M, Hoffman LM, Jensen CC, Yost HJ, Beckerle MC. 2005. Mechanical force mobilizes zyxin from focal adhesions to actin filaments and regulates cytoskeletal reinforcement. J Cell Biol 171(2):209-15.

Zamir E, Katz BZ, Aota S, Yamada KM, Geiger B, Kam Z. 1999. Molecular diversity of cell-matrix adhesions. J Cell Sci 112 ( Pt 11):1655-69.

# Appendix : Additional experiments

## A.1. Dynamic behavior of human mesenchymal stem cells during cyclical stretch

In addition, we observed how commercially available human mesenchymal stem cells reacted to cyclical stretching. The stretching experiments were performed in a manner similar to the phase contrast experiments (Section 3.3). The stretching frequencies were 0.01 $s^{-1}$, 0.1 $s^{-1}$, 0.5 $s^{-1}$ and 1 $s^{-1}$, and the stretching amplitudes were 8% and 15% (Fig. A.1.1). The control experiment was performed without applying any stretch. We did not investigate differentiated mesenchymal stem cells. Therefore, the cells were cultivated with the standard medium (see Section 2.2.5) for stem cells without any additions for differentiation.

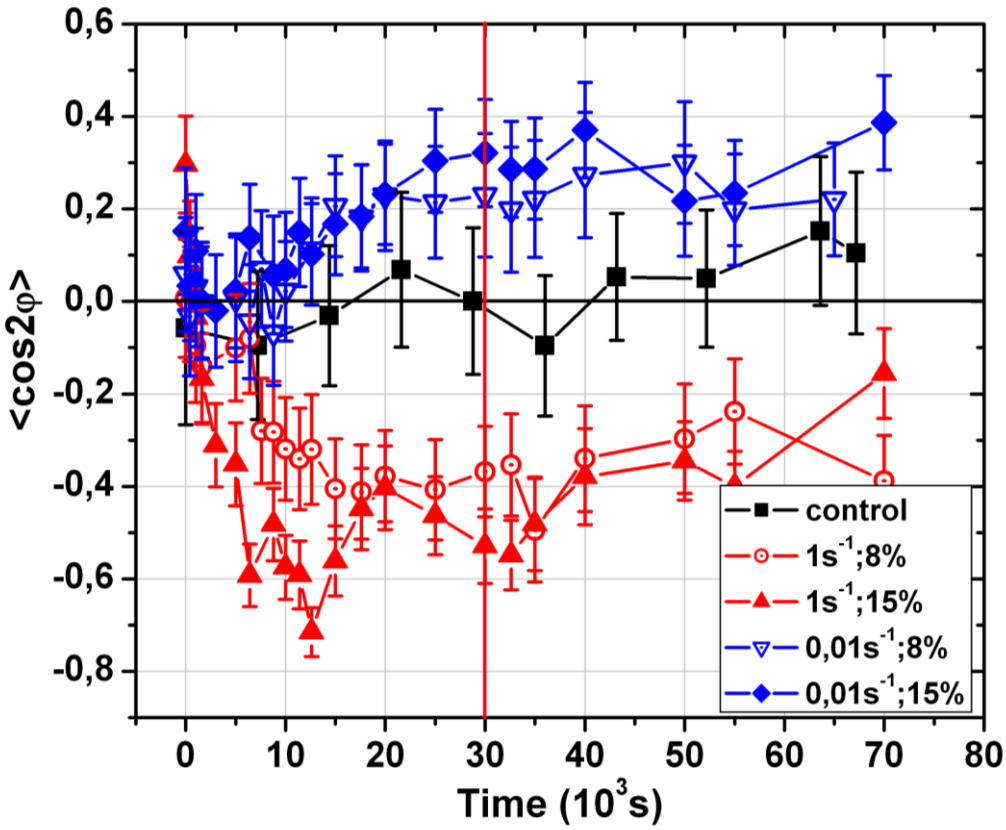


**Fig. A1.1: Reorientation of human mesenchymal stem cells during cyclical stretch at two different frequencies (0.01 $s^{-1}$ and 1 $s^{-1}$) and two different amplitudes (8% and 15%). The control experiment was performed without applying any stretch.**

The characteristic times for the reorientation of the hMSC cells were determined at two different frequencies, and compared to the characteristic time of reorientation of the human fibroblasts. At a frequency of $f = 0.5\ s^{-1}$, the characteristic time was 10624.05 s (±1230.17 s),

and at $f = 1\ s^{-1}$, it was 8131.43 s (±1030.5 s). These times were within the range observed for the human fibroblasts (for $f = 0.5\ s^{-1} \approx 10000$ s; for $f = 1\ s^{-1} \approx 7000$ s).
The time course of the reorientation process in hMSC cells also has an exponential characteristic, up to a maximum orientation which is close to the values we obtained for the human fibroblasts. The hMSC cells also remain in an orientation perpendicular to the stretch direction after we stopped the cyclical stretch. A major difference between the hMSC cells and the human fibroblasts was our finding that the hMSC cells began to orient themselves slightly parallel to the stretch direction, once the threshold frequency of $f_{t2} = 0.1\ s^{-1}$ dropped to a frequency of $f = 0.01\ s^{-1}$. We could observe this behavior at amplitudes of both 8% and 15%.

## Discussion

Our first experiments with hMSC cells demonstrated that they reacted in a manner similar to the human fibroblasts; however, they reacted differently at low frequencies compared to the human fibroblasts. Eastwood *et al.* (Eastwood *et al.* 1998) previously demonstrated that cells aligned parallel to the stretch direction at low frequencies of cyclical stretch. We also tried to corroborate this behavior (Section 3.3.3), but could not observe alignment that was parallel to the stretch direction in fibroblasts, at the lowest possible frequency.
In the case of the hMSC cells, we could already observe parallel alignment to the stretch direction at a frequency of $f = 0.01\ s^{-1}$. It seemed that between $f = 1\ s^{-1}$ and $f = 0.01\ s^{-1}$, cells start to respond differently to cyclical stretch. Instead of orienting themselves perpendicular to the stretch direction, they align themselves parallel to the stretch direction. It would be interesting to investigate if this change in response has any influence on the differentiation of hMSC cells. Further studies should help to address this issue. For example, experiments must be performed with PCR and qRTPCR analytic techniques to investigate, if the mechanical stimulation enables the hMSC cells to differentiate into particular types of cells; e.g., osteoblasts or chondrocytes. These experiments should be designed in a manner similar to the studies of Engler *et al.*, in which the influence of the substrate stiffness on cell differentiation was investigated or those of Kurpinski *et al.*, in which cyclical stretch was applied to cells forced to orient themselves in a given direction by means of microgroove substrates (Engler *et al.* 2006; Even-Ram *et al.* 2006; Kurpinski *et al.* 2006a).

## A.2 Influence of the surrounding temperature on cellular reorientation during cyclical stretch

We were interested in learning whether cellular behavior is more a biological or more a physical phenomenon. The biological response is dependent on the surrounding temperature: the enzymes and the biochemical processes function more slowly as the temperatures decrease. Therefore, we reduced the surrounding temperatures from 37°C to 17°C for the experiments with REF52 and HDF1 cells. Afterwards, we evaluated the characteristic times of the dynamic reorientation of the cells at two different frequencies (Fig. A2.1). If the reorientation were a fully passive process, we would not observe any difference in the characteristic times, between the two temperatures.

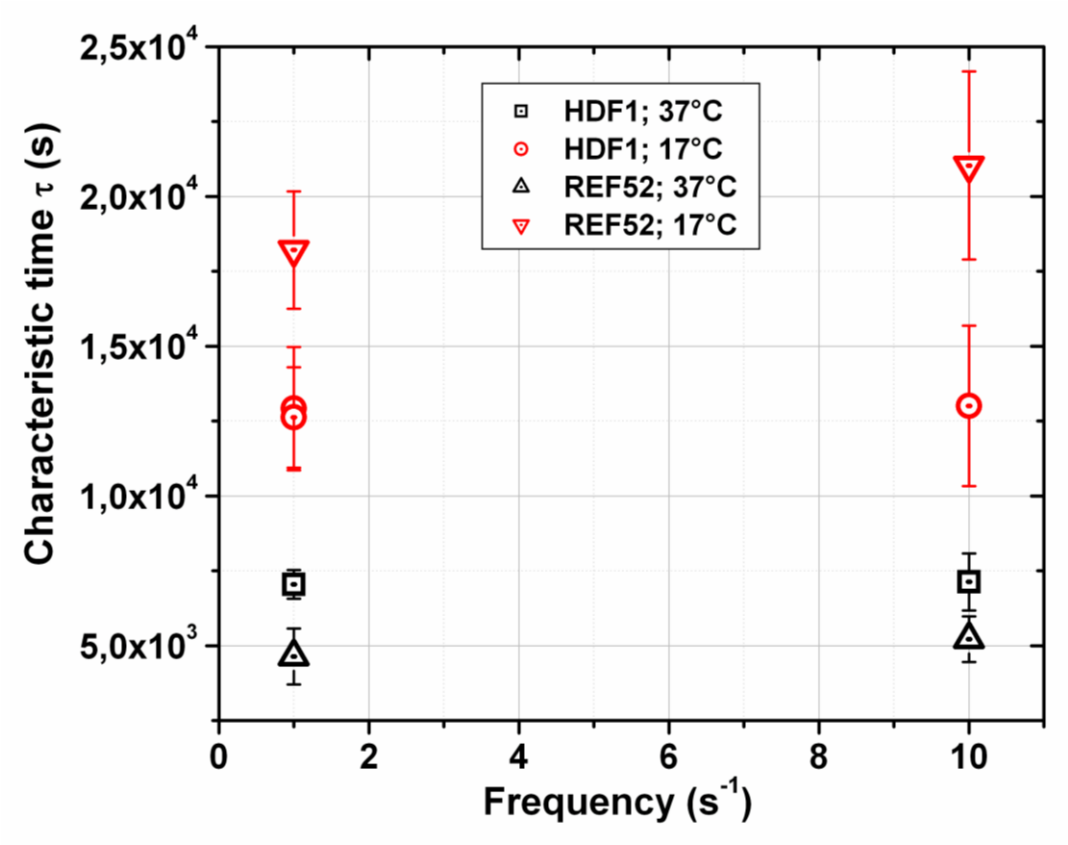


**Fig. A2.1: Characteristic time for REF52 and HDF1 cell reorientation during cyclical stretch, at two different temperatures (17°C and 37°C), and at two different frequencies (1 $s^{-1}$ and 10 $s^{-1}$). The cells react more slowly at lower temperatures, indicating that the reorientation process involves an active biological mechanism.**

Furthermore, we observed that the characteristic time increases along with a decrease in temperature: the cells reoriented themselves more slowly at 17°C compared with cells examined in experiments performed at 37°C. These results were as we would have expected. If the underlying biological processes are slowed down, the dynamic of the cellular response also becomes slower. Notably, the reorientation of REF52 cells is slower at low temperature

than the reorientation of the HDF1 cells. This is in contrast to the behavior of these cells at 37°C where it is the other way round (Section 3.3.3).

## Discussion

As we expected, the surrounding temperature influenced the cellular response. If the reorientation process was a totally passive mechanical process, the characteristic times would not be influenced by changes in temperature.

However, our experimental results showed that the characteristic time decreases at low temperatures for both cell types. We assumed that the temperature decrease also caused a decrease in metabolic rate, slowing the reaction of the cells. We therefore hypothesize that the reorientation process is an active, cell driven process, or at least it is not solely due to a passive mechanical effect.

Surprisingly, the REF52wt cells displayed lower characteristic times than the human fibroblasts. We would have expected that the cells at 17°C would behave similar to those examined at 37°C, in which the REF52wt cells responded faster than the human fibroblasts. Why the characteristic time for REF52 cells is at 17°C suddenly lower than the characteristic time for the HDF1 cells is not clear and may lie in the specific metabolism of the cells. It could be the case that the metabolism of the REF52wt cells is more temperature-sensitive.

## A.3 Stretching of human fibroblasts on micropatterned substrates

We investigate the behavior of cells which are only allowed to adhere on certain adhering islands on the stretching substrate. Therefore, we printed adhesive lines on a non-adhesive starPEG layer on the stretching chambers, as described in Section 2.5.

First, we had to prove that we had obtained well-printed fibronectin lines on the surface of the stretching chamber (Fig. A3.1) and then, if the cells adhered to these lines, and not to the space in between. We then had to prove that the non-adhesive layer with the printed fibronectin lines resisted the cyclical stretch for more than 30000 s the length of our experiment.

Once we had verified our experimental set-up, we performed stretching experiments at a stretching frequency of 1 $s^{-1}$, and a stretching amplitude of 8%. For the stretching experiments, we used HDF1 cells; the experiments were carried out with two different patterns. The lines were printed at different angles with respect to the stretching direction.

The experimental procedure used was the same as in our previous experiments (Sections 3.2 and 3.3). The cells were stretched along the x-axis and the stretch was stopped after 30000 s. Afterwards, the cells were observed for a further 35000 s.

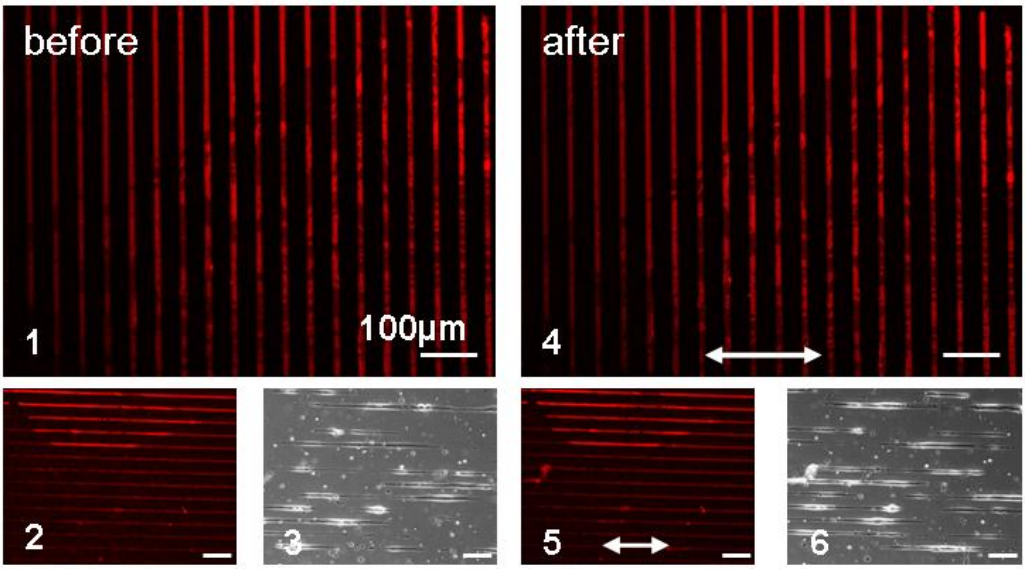


**Fig. A3.1: Microcontact printing of fibronectin on a non-adhesive star-PEG layer on the stretching chambers. Before stretch: 1: Alexa568 fibronectin lines, printed perpendicular to the stretch direction on a starPEG layer; 2: Alexa568 fibronectin lines, printed parallel to the stretching direction on a starPEG layer; 3: HDF1 cells on the fibronectin lines with 40 µm spacing in between; After stretch: Panels 4,5 and 6 as in Panels 1,2, and 3, but after 30000 s stretch. White bars: 100 µm.**

We observed that both passivation and the printing of the substrates worked very well. The non-adhesive starPEG layer and the printed fibronectin were not damaged after more than 30000 s of stretching (Figs. A.3.1 and A3.2).

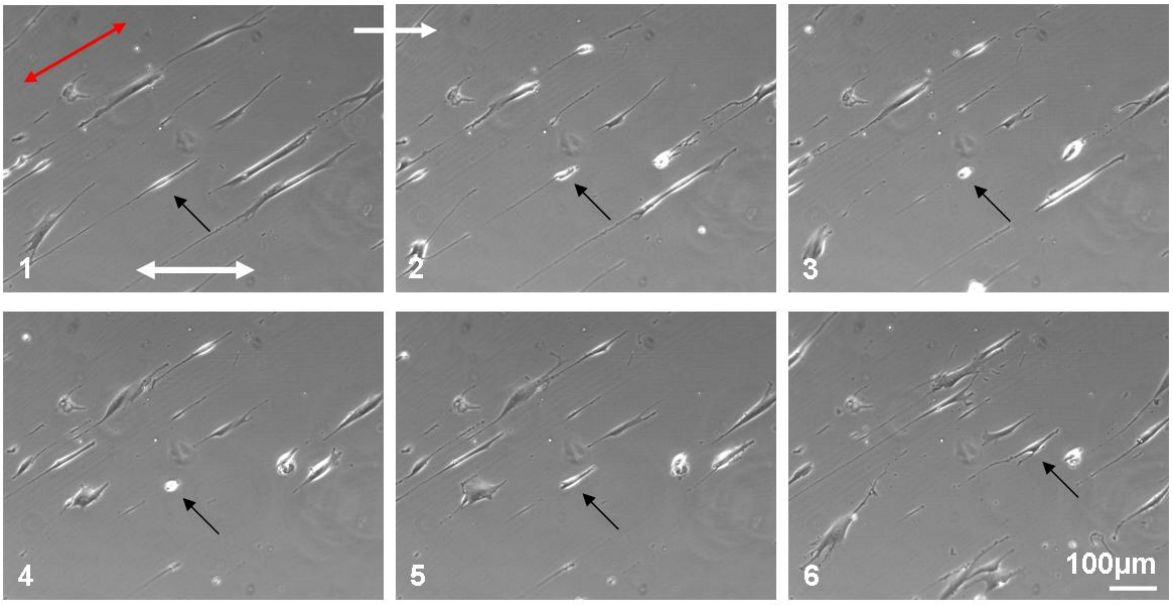


**Fig. A3.2: Sequence of phase contrast images of HDF1 cells on micropatterned substrates (10 µm lines; 40 µm spacing in between; 30° in respect to the stretch direction) during cyclical stretch (stretch in x-direction; 1 $s^{-1}$, 8%). 1: 0 s; 2: 1000 s; 2: 5000 s; 3: 30000 s; 4: 32500 s; 5: 65000 s. Stretch was stopped at 30000 s. Black arrows indicate a cell assuming a spherical shape during cyclical stretch, and relaxing back once the stretch was stopped.**

We investigated substrates with 10 µm adhesive lines and 40 µm non-adhesive spaces, oriented parallel, perpendicular and at an angle of 30° to the stretch direction. In each instance, the cells behaved differently. In the case of the perpendicular lines, we could not observe any cellular reaction. Similar results we observed if we had preoriented the cells to be parallel to the direction of stretch. In the case of a 30° angle with respect to the stretching direction, the cells began to round up during the stretching period, but began spread again along the fibronectin lines, once the stretch had been stopped (Fig. A3.2).

The same experiments were then performed with 10 µm adhesive lines and 5 µm non-adhesive spacing (Fig.A3.3). In this case, we observed a perpendicular orientation of the cells. And once the stretch was stopped, the cells again realigned themselves along the printed lines.

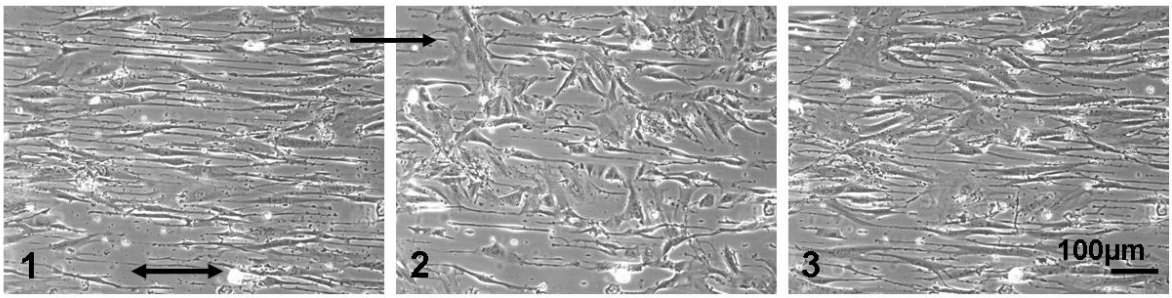


**Fig. A3.3: HDF1 cells on microstructured substrates (10 µm lines with 5 µm distance in between) during cyclical stretch (1 $s^{-1}$; 8%). 1: 0 s; 2: 30000 s; 3: 60000 s.**

## Discussion

The micro-contact printing of the substrates served as a very useful method to microstructure the substrates. The transfer of the passivation layer and the micro-contact printing of the lines were carried out in a routine manner and we subsequently proved the transfer by measuring the adhesion of the cells on the passivation layer and by fluorescence microscopy of the micro-printed lines. The question of whether the layer and the lines also resisted cyclical stretch for more than 8 hours was also proven. Images show that the cyclical stretch had no effect on the passivation layer or the fibronectin lines. The cells also did not adhere to the spaces between the lines after stretching, indicating that the passivation still worked after 8 hours. Furthermore, the passivation layer and the printed fibronectin adhered to the surface of the stretching chamber in a stable manner.

Previous measurements taken by Kurpinski *et al.* (Kurpinski *et al.* 2006a) have shown that forcing the cells to adhere to the surface at a certain angle to the stretch, influences cellular behavior; in this case cellular differentiation. In our experiments, we observed that the cells attempted to avoid the mechanical stress by means of cytoskeletal reorientation, and perpendicular alignment to the stretch direction. Cells adhering to the micro-patterned surface, however, could not orient themselves in a perpendicular manner because of the non-adhesive layer lying between the adhesive fibronectin lines. Therefore, the cells remained in the same orientation (parallel or perpendicular) as the printed lines. In the case of the lines printed at a 30° angle, the cells reacted by rounding up. Once the stretch was stopped, the cells were no longer stressed, and they could begin to align themselves once again along the fibronectin lines.

We varied the spacing between the lines, and separated them by a non-adhesive layer of 5 µm. It seems that this space is narrow enough so that the cells could bridge the non-adhesive layer. The cells could turn again, and begin to reorient themselves perpendicular to the stretch direction

## A.4 Actin filaments and the extracellular matrix staining

To clarify the reasons for the cellular reactions described above, it was necessary to explore these processes at the molecular level. The driving force behind cellular movement originates in the cytoskeleton. Therefore, we attempt to view the cytoskeleton and the extracellular matrix with fluorescence microscopy.

To visualize changes in the cytoskeleton, we performed phalloidin staining of the actin filaments of the REF52 and the HDF1 cells, both without stretch and after 8 hours cyclical stretch.

Besides the cytoskeleton, we were also interested in the influence of cyclical stretch on the extracellular matrix. Therefore, we performed a second antibody staining, this time of the extracellular matrix protein fibronectin (Fig. A4.1, A4.2 and A4.3). The actin is shown in green. The actin filaments are marked by green arrows. The fibronectin is depicted in red; red arrows indicate the fibronectin fibrils. The reason for the red background is the coating of the stretching chamber surfaces with fibronectin, in order to make the surface adhesive, and the fibronectin itself which is also produced by the cells.

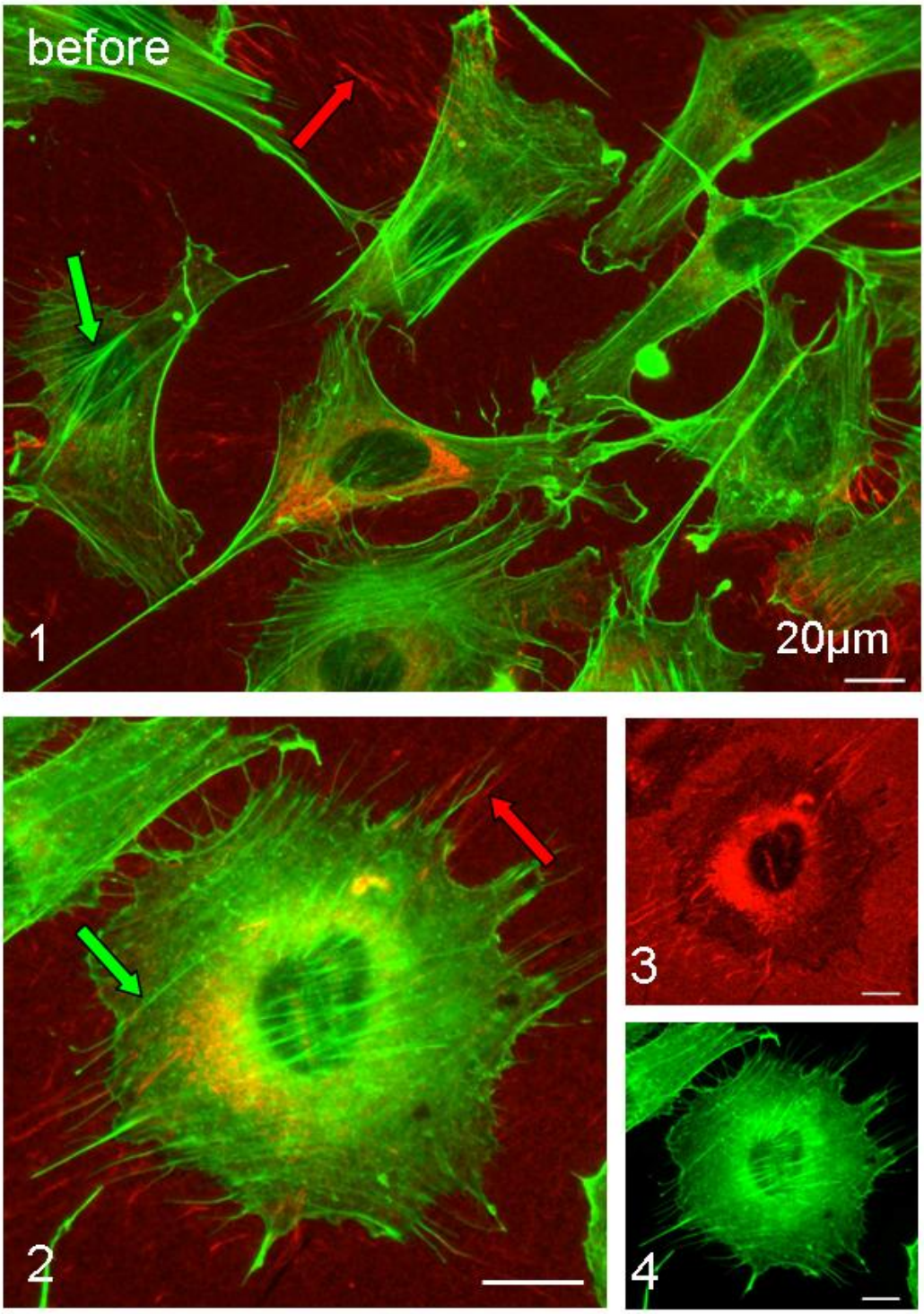


**Fig. A4.1: Antibody and phalloidin staining of fibronectin (red; red arrows) and actin filaments (green; green arrows) of REF52 cells before stretch. 1: Merged overview of randomly orientated REF52 cells. 2: Merged view of a single REF52 cell; 3: Fibronectin staining of the extracellular matrix surrounding the cell; 4: Actin filaments of REF52 cells without fibronectin. Bars: 20 µm**.

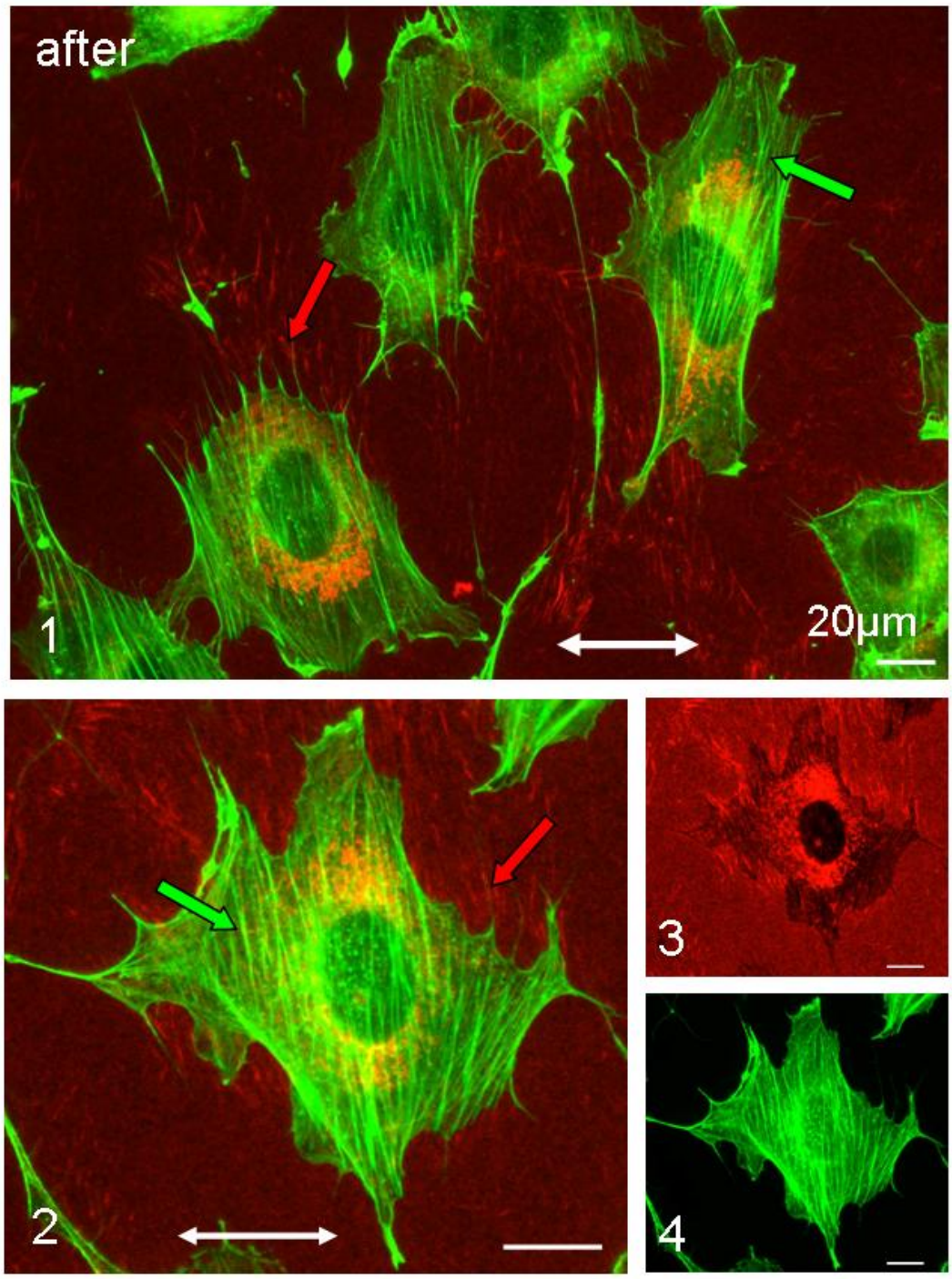


**Fig. A4.2: Antibody and phalloidin staining of fibronectin (red; red arrows) and actin filaments (green; green arrows) of REF52 cells after stretch. 1: Merged overview of random orientated REF52 cells. 2: Merged view of a single REF52 cell; 3: Fibronectin staining of the extracellular matrix surrounding the cell; 4: Actin filaments of REF52 cells without fibronectin. Bars: 20 µm. The white double arrow indicates the stretch direction.**

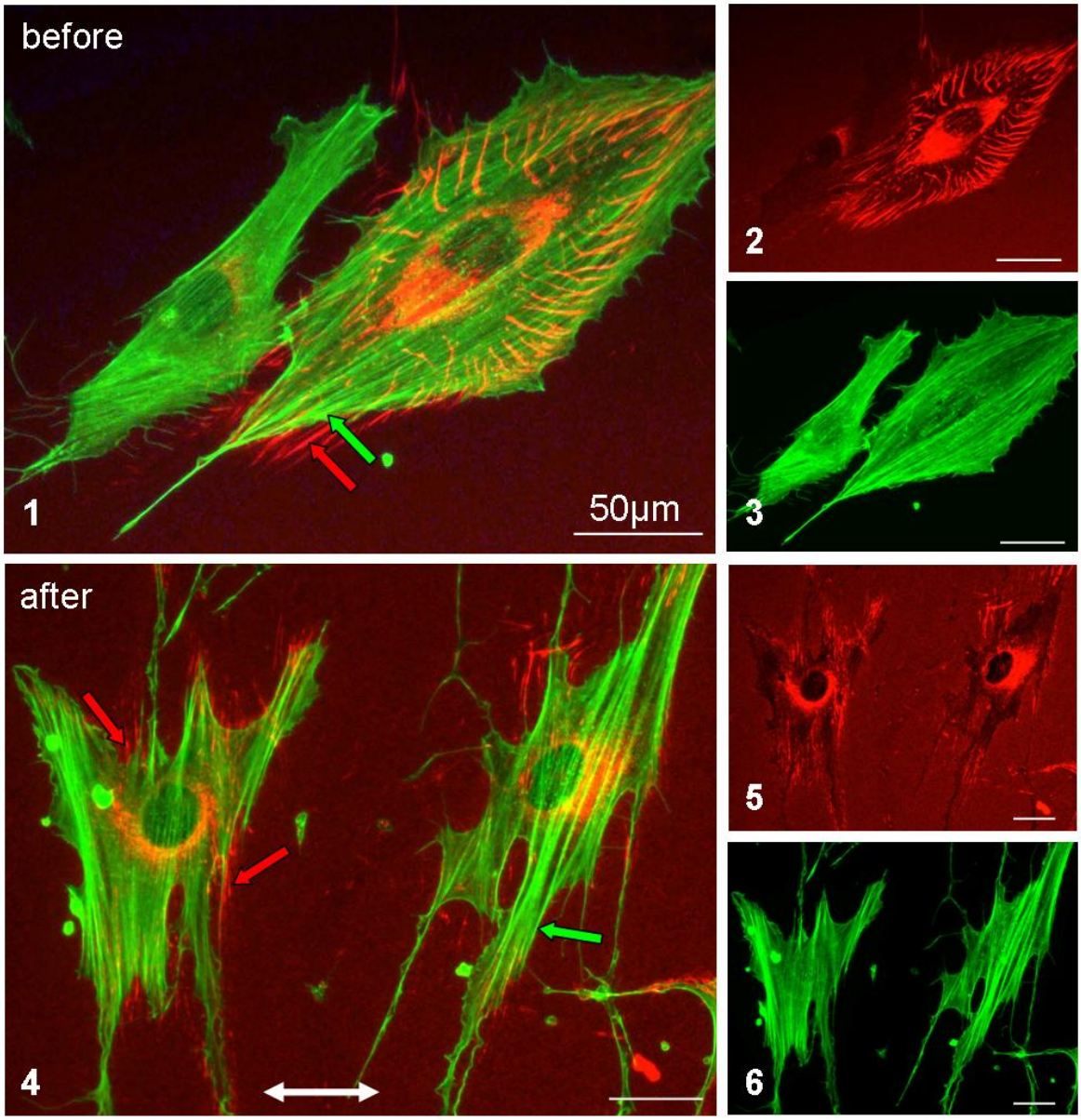


**Fig. A4.3: Antibody and phalloidin staining of fibronectin (red; red arrows) and actin filaments (green; green arrows) of HDF1 cells before (Panels 1, 2, and 3) and after stretch (Panels 4, 5, and 6). 1: HDF1cells with randomly orientated actin filaments and fibronectin fibrils. 2: Fibronectin without cell. 3: Actin cytoskeleton. 4: HDF1 cells after stretch. 5: Fibronectin orientated perpendicular to the stretch direction. 6: Actin filaments alone. Bars: 50 µm. The white double arrow indicates the stretch direction.**

## Discussion

The fluorescence images for both cell types indicated that the actin filaments oriented themselves randomly if they were not stretched.
The cells produced fibronectin and together with the fibronectin from the coating, they formed fibrils at the bottom of the cell. The fibronectin in the direct surrounding from the cell was not affected. Only the fibronectin on which the cells migrated formed fibrils.
The fibrils also oriented themselves randomly if the cells were not subjected to an external force.
After stretching the cells for 30000 s, the actin fibers oriented itself perpendicular to the stretch direction, as did the entire cell. This finding indicated that cytoskeletal orientation was responsible for the orientation of the entire cell, as shown by previous studies (Dartsch *et al.* 1986; Wang *et al.* 2001).
If we focused on the fibronectin orientation, we could see that the cells formed fibronectin fibrils. These fibrils which lay underneath the cell, oriented themselves in the same direction as the actin filaments, because of the linkage between the cytoskeleton and the extracellular matrix (Geiger and Bershadsky 2002). This observation suggested that during the cyclical stretch the entire extracellular matrix orients itself nearly perpendicular to the stretch direction, in the same way as the cell did. This orientation of the extracellular matrix could be an explanation for fact that the HDF1 cells remain perpendicular after the stretch is switched off.

# Abbreviations

| | |
|---|---|
| µCP | micro contact printing |
| AFM | atomic force microscope |
| BSA | bovine serum albumin |
| $CO_2$ | carbon dioxide |
| DMEM | dulbeccos's modified eagle medium |
| ECM | extracellular matrix |
| EDTA | ethylenediamine tetraacetic acid |
| EGF | epidermal growth factor |
| F-actin | filamentous actin |
| FBS | fetal bovine serum |
| Fig. | figure |
| FRAP | fluorescence recovery after photobleaching |
| FRET | fluorescence resonance energy transfer |
| GFP | green fluorescent protein |
| GTP | guanosintriphosphate |
| HDF | human dermal fibroblasts |
| hMSC | human mesenchymal stem cells |
| MLCK | myosin light chain kinase |
| MTC | magnetic twisting cytometry |
| PBS | phosphate buffered saline |
| PCR | polymerase chain reaction |
| PDMS | polydimethylsiloxane |
| PEG | polyethylene glycol |
| PFA | paraformaldehyde |
| qRT-PCR | quantitative-real-time polymerase chain reaction |
| ROI | region of interest |
| TIRF | total internal reflection fluorescence microscopy |
| SEM | scanning electron microscopy |
| YFP | yellow fluorescent protein |

# Supplementary Materials

- **Supplementary movie 1.** REF52 cells adhering to a cyclically stretched substrate at strain amplitude *A*=8% and strain frequency *f*=10 $s^{-1}$. The stretch was applied in x-direction and stopped after 30000 s (STOP sign). The total duration of the experiment was 65000 s.

- **Supplementary movie 2.** HDF1 cells adhering to a cyclically stretched substrate at strain amplitude *A*=8% and strain frequency *f*=10 $s^{-1}$. The stretch was applied in x-direction and stopped after 30000 s (STOP sign). The total duration of the experiment was 65000 s.

- **Supplementary movie 3.** REF52-YFPpaxillin-labeled cell adhering to a cyclically stretched substrate at strain amplitude *A*=8% and strain frequency *f*=1 $s^{-1}$. The stretch was applied in x- direction for 70 min.

- **Supplementary movie 4.** Confluent REF52 cells adhering to a cyclically stretched substrate at strain amplitude *A*=8% and strain frequency *f*=10 $s^{-1}$. The stretch was applied in x- direction and stopped after 30000 s (STOP sign). The total duration of the experiment was 65000 s.

- **Supplementary movie 5.** HDF1 cell on micro patterned substrates (10 µm lines; 40 µm spacing in between). During cyclical stretch (stretch in x-direction, 1 $s^{-1}$, 8%). The lines were printed in a angle of 30° to the stretch direction. The stretch was applied in x- direction and stopped after 30000 s (STOP sign). The total duration of the experiment was 65000 s.

# Acknowledgements

It is nearly impossible to write a thesis without the support of a lot of people. That's why I want to take the opportunity to thank the people who supported me during the past three years, either in connection with my research, or on a personal level.

First, I want to thank Prof. Dr. G.E. Pollerberg for enabling me to do my Ph.D. degree at the University of Heidelberg.

I want to thank Prof. Dr. J.P. Spatz, who has also accompanied me on my academic journey during the past several years. Thank you for your support of my ideas, our discussions, the freedom you gave me, and the financial support of my work.

Furthermore, I want to thank Prof. H. Gao, who gave me the opportunity to work in his department for two years, and initially suggested the idea for this project. We had wonderful discussions as he shared with me his theoretical and engineering view of biology.

I am grateful to my mentor, Dr. Ralf Kemkemer and his family, for their friendship, and for his excellent supervision, and the chance to learn as much as I possibly could from him.

For assistance with the micro-contact printing, I want to thank Peter Gasteier and Dr. Jürgen Groll in Prof. Dr. M. Moeller's department at the DWI Aachen.

I want to thank the following scientists for fruitful discussions:
From the physical side : Prof. H. Gruler, University of Ulm; Prof. Samuel Safran and Dr. Rumi De, Weizmann Institute of Science; and Prof. Krishnakumar Garikipati, University of Michigan.

From the biological side: Dr. Dieter Kaufmann,University of Ulm; Prof. Benny Geiger and Prof. Alexander Bershadsky, Weizmann Institute of Science, and Dr. Christoph Ballestrem, University of Manchester

A big thank-you to Mr. Bulling and Markus in the tool shop of the Max-Planck-Institute. They always tried to do their best to translate my technical ideas into reality, and they did a great job.

Furthermore, I want to thank the people from Zeiss for their guidance, when we had problems with the microscope or the software.

Together with Nils Brödling, I had a great time in the "Chinese" department, where I met a lot of interesting and lovely people.

I also want to thank the Prof. Spatz's research group, with whom I had a lot of fun, and many fruitful discussions.

My special thanks to the "subgroup" led by Ralf Kemkemer: Alexandra Goldyn, Sarah Biela, Borja Aragues Melih Kalafat, Marc Gronle and Su Yi.

Furthermore, I thoroughly enjoyed the great times and great discussions with Christian Greiner from the Arzt Department, even if he is a Schwabe. I also thank Peter Kaiser for forcing me to go running which kept my body in shape during the writing period.

A dissertation can never be realized without the support of people in private life.
Here, I want to take the opportunity to thank the "Eppingen guys," Markus Elsinger, Thomas Lang, Michael Preusch, Wolf and Jörg Edelmann, Ulrich Waechter and Sabine Weiss.
I want to thank my friends Jens Thiele, Hans Mathee, Denis Scholz and Marco Straus for their support, and for making it possible to have a look beyond one's own nose.

Furthermore, I thank Kajori Lahiri, Jessica Araya Contreras and Betiel Wasihun for our discussions during my time in Stuttgart.

Thanks to Shelley Gunness for her great friendship, and her help in improving my English.

Thanks to Petra Salame for everything.

In closing, I want to thank my family for supporting me in all my ideas and endeavors.

*"I am enough of an artist to draw freely upon my imagination. Imagination is more important than knowledge. Knowledge is limited. Imagination encircles the world."*

*Albert Einstein*